NASA CONTRACTOR REPORT 177395

Phase 4 Static Tests of the J-97 Powered, External Augmentor V/STOL Model at the NASA, Ames Research Center, November 1983

D. B. Garland

CONTRACT NASW-2797

December 1985

NASA

NASA CONTRACTOR REPORT 177395

Phase 4 Static Tests of the J-97 Powered, External Augmentor V/STOL Model at the NASA, Ames Research Center, November 1983

D. B. Garland

The de Havilland Aircraft of Canada, Limited

Prepared for
Ames Research Center
under Grant NASW-2797

December 1985

National Aeronautics and
Space Administration

Ames Research Center
Moffett Field, California 94035

1. Report No.	2. Government Accession No.	3. Recipient's Catalog No.
NASA CR 177395		

4. Title and Subtitle	5. Report Date
Phase 4 Static Tests of the J-97 Powered, External Augmentor V/STOL Model at the NASA, Ames Research Center, November 1983	December 1985
	6. Performing Organization Code
7. Author(s)	8. Performing Organization Report No.
D. B. Garland	
	10. Work Unit No.
	T-7526
9. Performing Organization Name and Address	11. Contract or Grant No.
The de Havilland Aircraft of Canada, Limited Downsview, Ontario M3K 1Y5 Canada	NASW 2797
	13. Type of Report and Period Covered
	Contractor Report
12. Sponsoring Agency Name and Address	14. Sponsoring Agency Code
National Aeronautics and Space Administration Washington, D.C. 20546	505-43-01

15. Supplementary Notes

Point of Contact: Technical Monitor, Kiyoshi Aoyagi, M.S. 247-1
Ames Research Center, Moffett Field, CA 94035
(415) 694-5047 or FTS 464-5047

16. Abstract

A large scale, ejector-lift V/STOL Model, powered by a J-97 engine, was tested at the NASA Ames Research Center Outdoor Aerodynamics Research Facility. The model incorporated the external augmentor concept developed by DHC. Since the first test at Ames in 1979, the fuselage augmentor nozzle array has been redesigned with a larger pitch and notched nozzles instead of plain slot nozzles.

Thrust augmentation of the ejector as measured at Ames Research Center was lower than that measured in the DHC laboratory. It is believed that this difference is due to the high temperature of the primary jet flow as compared to the DHC blown-down rig.

An ejector-lift/vectored thrust configuration was also included in the recent tests. This is an arrangement where the fuselage augmentor is shortened in the chordwise direction and the extra thrust is generated with a vectorable, ventral nozzle. In free-air the shortened fuselage augmentor produced the same augmentation as the long augmentor. In ground proximity, at a height of 27", and with zero pitch angle, a negative ground effect was measured equal to 6-1/2% of the free-air lift.

17. Key Words (Suggested by Author(s))	18. Distribution Statement
Augmentor Ground effect V/STOL Ejector Model	Unclassified - Unlimited STAR Category 02

19. Security Classif. (of this report)	20. Security Classif. (of this page)	21. No. of Pages	22. Price*
Unclassified	Unclassified	84	

*For sale by the National Technical Information Service, Springfield, Virginia 22161

1.0 SUMMARY

A large scale, ejector-lift V/STOL model, powered by a J-97 engine, was tested for a second time on the Outdoor Aerodynamics Research Facility (OARF) at the Ames Research Center, NASA, in October/November 1983. The model incorporated the external augmentor concept developed by DHC. Since the first test at Ames in 1979, the fuselage augmentor nozzle array has been redesigned with a larger pitch and notched nozzles instead of plain slot nozzles.

Thrust augmentation of the ejector as measured at Ames Research Center was lower than that measured in the DHC laboratory. It is believed that this difference is due to the high temperature of the primary jet flow as compared to the DHC blow-down rig.

An ejector-lift/vectored thrust configuration was also included in the recent tests. This is an arrangement where the fuselage augmentor is shortened in the chordwise direction and the extra thrust is generated with a vectorable, ventral nozzle. In free-air the shortened fuselage augmentor produced the same augmentation as the long augmentor. In ground proximity, at a height of 27", and with zero pitch angle, a negative ground effect was measured equal to 6½% of the free-air lift. At 10° of pitch angle, this effect was reduced to 3.3%.

2.0 CONTENTS PAGE NO.

2.0 CONTENTS (CONT'D)

3.0 INTRODUCTION

A large-scale model of the de Havilland Aircraft of Canada (DHC) external augmentor V/STOL concept was tested statically on the outdoor test facility at the Ames Research Center, NASA. Powered by a J-97 engine, the conceptual model applies ejector-type thrust augmentor principles to both chordwise fuselage augmentors and the wing flap augmentors as shown in **Figure 1**. The basic model had previously undergone static tests in the outdoor test site and forward speed tests in the NASA Ames 40 x 80 foot wind tunnel, following initial static test at DHC, (References 1-6).

The present static tests were confined to evaluation of an improved fuselage augmentor plus an initial study of the EL/VT (ejector lift/vectored thrust) concept as outlined in Proposal DHC P80-1, (Reference 7). In the latter configuration, shown in **Figure 2**, roughly one half of the fuselage augmentor nozzles are blanked-off and the remainder of the engine exhaust flow is diverted through a conical ventral nozzle aft of the fuselage augmentor. In future tests, this nozzle will be vectorable, but at present, only the 90° (straight down) angle was tested. This arrangement gives a 37%/63% thrust split between the fuselage augmentor and the ventral nozzle, simulating the fan/core thrust split of the GE-F101 DFE, a candidate engine for future use in the EL/VT research program.

The major objectives of the present static test program were:

(i) To demonstrate the structural integrity of the new duct/nozzle assembly.

(ii) To determine lifting performance and the optimum hovering configuration of the new fuselage augmentor.

(iii) To measure the performance with the ventral nozzle operating (at 90° only) and fuselage augmentor reduced to 7 nozzles per side, both in and out of ground effect.

A complete run history is given in **Table 1**. The research work described here was conducted in cooperation with the Ames Research Center, NASA; funding for the program was provided by NASA and the Canadian Department of National Defence.

4.0 MODEL DESCRIPTION

The de Havilland large scale G.E. J-97 powered model has proven to be quite adaptable to fairly quick conceptual changes as was shown in the present static test series, where two DHC concepts were investigated. Firstly, the External Augmentor configuration with an improved primary "notched" nozzle design, based on the work of Reference 8, was tested in free air. Its general arrangement is shown in **Figure 1**. A similar arrangement with "slot" type primary nozzles was tested both statically and at forward speed previously and is reported in the references cited.

Secondly, the Ejector Lift/Vectored Thrust STOVL concept, was examined in both free air and in ground effect. Its general arrangement is shown in **Figure 2**.

The model has a double-delta planform layout and the major geometric parameters are listed in **Table 2**.

The moment arms of the various thrust-producing components are shown in **Figure 3**.

4.1 External Augmentor V/STOL Concept

Referring to **Figure 1**, the external augmentor arrangement features twin chordwise ejector slots located adjacent to the fuselage sides. These ejectors augment 80% of the installed engine thrust and provide a positive ground effect on lift due to the formation of a positive pressure on the fuselage base between the augmentors. The remaining 20% of the engine thrust is ducted to spanwise wing ejectors or augmentor flaps. The flaps are used for lift generation to lower the transition speed, for thrust deflection to assist in longitudinal acceleration and for generating a nose-down pitching moment during transition to help off-set the nose-up moment of the fuselage augmentor inlet flow.

4.1.1 Fuselage Augmentor

The significant difference of this augmentor over the one previously tested, is the design of the primary nozzles. A notched exit design, as shown in **Figure 4**, has permitted a reduction in the number of nozzles required by 50%, i.e. from 27 nozzles to 13 nozzles per side. The notches allow the primary flow to expand in the chordwise direction thereby promoting greater primary/secondary mixing per nozzle than with the previous slot design. The fuselage augmentor geometry is given in **Table 3**. Another important quality of the new nozzles, since the pitch in the nozzle array had doubled, is the circular inlet to the nozzle. This greatly facilitates nozzle vectoring and flow shut-off valve installation, both of which may be used in the transition regime. Cold flow lab tests also showed a reduction in duct/nozzle inlet flow losses for the circular inlet compared with the previous slot/type inlet.

The effective area for the new primary notched nozzle arrays in the fuselage augmentors remained as before to provide 80% of the installed engine thrust.

A cross section of the fuselage augmentor system is shown in **Figure 5**. As previously, the augmentor fuselage wall was fixed, but the augmentor doors were hinged to allow for variation in diffuser area ratio (DAR).

The fuselage augmentor end-plates, (both front and rear), were split at the fuselage baseline to allow the lower portion to be removed for shortened end-plate investigation, (see **Figure 5**). Shorter end-plates would be easier to stow in the cruise configuration and may be considered if their performance penalty were small.

Inlet fairing plates were provided for the fuselage augmentors so the inlet profile for the new notched nozzle

array would be similar to the previous one, (see **Figure 6**). These fairing plates were removable and their effect on augmentor performance was determined.

4.1.2 Wing Augmentor

Details of the wing augmentor geometry are given in **Table 4** and a cross section of the augmentor is shown in **Figure 7**. The augmentor design remained unchanged from the previous static test series. The complete augmentor flap and duct/nozzle assembly rotates as a unit. A flap deflection of 0° only, was tested power-on during the present static tests on the V/STOL concept.

4.1.3 Fuselage Base

The external augmentor concept includes provision for a significant base area between the fuselage augmentors as can be seen in **Figure 5**. In ground effect, a positive pressure acting on this base gives a favourable lift force which off-sets the augmentor thrust loss due to back pressure and "suck-on" forces due to entrainment into the jet efflux. Base end-plates (**Figure 5**) were available to reduce base cavity ventilation when in ground proximity, hence increasing the positive base effect on lift, but these were not tested on this configuration during this test.

4.2 The Ejector Lift/Vectored Thrust STOVL Concept

The Ejector Lift/Vectored Thrust (EL/VT) concept tested statically uses shortened twin chordwise ejector slots located adjacent to the fuselage sides in combination with a ventral propulsion nozzle installed just aft of the wing hinge line. The general arrangement is shown in **Figure 2** and provides an approximate 37%/63% installed engine thrust split between the fuselage augmentors and ventral nozzle. The exhaust flow to

the wing augmentor flap system was blanked off for testing of this concept, which would normally rely on a simple blown flap for high lift in transition.

4.2.1 Fuselage Augmentor

The shorter fuselage augmentor lengths required for the EL/VT concept were obtained by inserting blanking plates in the rearmost 6 nozzles on each side. New, short augmentor doors were installed and were hinged to again provide for diffuser area ratio changes. New rear end-plates were fitted just aft of nozzle number 7 to give an augmentor length of 51.5 inches. The fuselage augmentor cross section was unchanged, (Refer to **Figure 5**). The augmentor geometry is shown in **Table 3**. Cover plates were installed over the blanked-off augmentor section, (Refer to **Figure 8**). The fuselage side extension plates (that portion which protrudes below the fuselage base) were removed aft of the new shortened augmentor to provide a more representative lower fuselage contour between the fuselage augmentors and the ventral nozzle.

Base end-plates were available to reduce base cavity ventilation and their effect was determined at the low ground beight.

4.2.2 Wing Augmentors

Blanking plates were installed in the wing ducts to shut-off flow to the wing augmentors. The wing flap system was still rotatable and flap angles of 0° and 60° were tested (unblown) while in ground effect.

4.2.3 Aft Ventral Nozzle (AVN)

The rear fuselage duct was modified for this test series to include a vertical off-take to provide flow to a ventral nozzle. This is shown in **Figure 9**. Nozzles could be

installed at this location to provide various nozzle flow angles (vectorable). For the present tests however, only a 90° deflection nozzle with an I.D. of 9.48" was used.

A blanking plate was available instead of the nozzle when operating without the AVN.

4.3 Trim Nozzles

A variety of rear trim nozzles, listed in **Table 5**, was available to adjust engine exit area with configuration change. However, the 9.46" diameter calibration type nozzle also provided accurate thrust and mass flow data. It provided the link between the reduced length fuselage-augmentor-only configuration and addition of the aft ventral nozzle, enabling the thrust and mass flow of the ventral nozzle to be more accurately determined.

4.4 Instrumentation

4.4.1 G.E. J-97 Engine

The following engine parameters were monitored during the test:

(a) Exhaust Gas Temperature
(b) % Engine RPM
(c) Oil Pressure
(d) Oil Temperature
(e) Fuel Pressure
(f) Fuel Flow
(g) Engine Bay Temperatures - 3 Locations
(h) Engine Vibration - 2 Locations
(i) Engine Inlet Temperature - 4 Locations as shown in **Figure 10**
(j) Engine Inlet Static Pressure (see **Figure 10**)

4.4.2 Engine Exhaust Duct

Static pressures were recorded at various duct locations as shown in **Figure 11**.

4.4.3 Fuselage Augmentors

Fuselage augmentor nozzle reference static pressures (PSN, **Figure 4**) were measured in 5 nozzle array locations as shown in **Figure 11**. The pressure ratio obtained from nozzle number 6 in the left fuselage augmentor was used to set the engine thrust level.

A rake containing total and static pressure taps as well as thermocouples was used to determine the flow conditions at the exit plane of the left fuselage augmentor for some configurations while the model was at the free-air height, **Figure 12**).

Static pressures were measured in the throat area at various locations in the left fuselage augmentor as shown in **Figure 13**).

4.4.4 Wing Augmentors

A wing duct entry static and a duct end stagnation pressure for each wing were measured. The wing augmentor exit flow was monitored by a total pressure rake at one location on the left wing, (see **Figure 7**).

4.4.5 Aft Ventral Nozzle

Two total pressure probes were located at the exit plane of the ventral nozzle, **Figure 9**.

4.4.6 Fuselage Base

Static pressure and temperature were measured over most of

the model's fuselage base area as shown in **Figure 14**.

4.4.7 Ground Plane

The ground plane contained several longitudinal and lateral rows of static pressure taps and thermocouples (**Figure 15**.) Measurements were recorded with the model at the low strut height in ground effect.

Two 30 inch high rakes, (**Figure 16**), containing total pressure probes and thermocouples were used to measure flow over the ground plane. The location of these rakes is shown in **Figure 15**.

5.0 TEST FACILITY

A photograph of the model in position at the OARF - Outdoor Aerodynamics Research Facility, Ames Research Center, NASA, is shown in **Figure 17**.

Model height above ground was varied by interchanging support struts of appropriate lengths. Model pitch attitude was variable by means of an adjustable nose strut. Load cells, positioned between the model and strut tips measured normal and axial force components. A ground plane surface, raised a few feet above ground level, contained surface pressure taps and temperature probes and stand-off rakes as required. Wind data monitoring equipment were located at the site.

A computer based acquisition system provided all data recording, real time display of required parameters and full output computing facilities.

6.0 PRESENTATION OF FORCE DATA

The measured lift force on the model was normalized with respect to ambient pressure and is presented as (L/δ) versus PRF. For the general case, the total lift force can be assumed to be composed of:

(i) fuselage augmentor thrust

(ii) wing augmentor thrust

(iii) ventral nozzle thrust

(iv) fuselage base thrust

(v) induced lift on the wing

In free air (represented by height of 227" or 148") and with zero flap angle, the induced lift on the model is believed to be negligible. The fuselage augmentor performance, ϕ_G, was determined primarily from configurations without the ventral nozzle in operation. Hence, gross thrust augmentation was calculated from:

$$\phi_{G_F} = \frac{L - XB}{XNF}$$

where L = measured lift on the model

XB = base thrust integrated from pressure data

and XNF = the sum of individual nozzle thrusts for the fuselage augmentor array

The "total" thrust augmentation ratio is sometimes used - this quantity includes the base thrust, i.e.

$$\phi_{GTOT} = \frac{L}{XNF}$$

With the ventral nozzle on, thrust augmentation ratio was determined to a lesser degree of accuracy by first subtracting the ventral nozzle thrust from the model lift force.

The values used for the fuselage augmentor nozzle thrust, XNF, and mass flow, $W\sqrt{T}$, were based on the summation of single nozzle test data from cold flow tests conducted in the

DHC Aerodynamics Research Laboratory. These tests are described in **Appendix "A"**.

Similarly, the wing augmentor nozzle assemblies were blown cold in the DHC lab to provide the basis for thrust and mass flow. These tests are described in **Appendix "B"**. Flap angle of δ_F = 0° only, was blown during the present tests. While wing augmentor thrust was available from the static tests of Reference 6, some small wing ducting changes necessitated re-evaluation by axial force differences.

The ventral nozzle thrust was determined through off/on tests in conjunction with the reduced length fuselage augmentor and appropriate trim nozzles.

A condensed log of configuration tests is given in **Table 6**. Four basic configurations were tested:

"A" - 13 fuselage augmentor nozzles/side (i.e. FAUG = 1.0) + wing augmentor blowing + 4.8" diameter trim nozzle
"B" - Same as **"A"** except with 2.8" diameter trim nozzle
"C" - 7 fuselage augmentor nozzles/side (i.e. FAUG = 0.538) + 9.46" diameter trim nozzle
"D" - 7 fuselage augmentor nozzles/side (i.e. FAUG = 0.538) + 2.8" diameter trim nozzle + 9.48" diameter ventral nozzle

The static tests of Reference 6, evaluated fuselage augmentor performance in ground effect. It was not expected to be significantly different with the notched nozzle array. Therefore, the present tests were primarily aimed at free air augmentor performance of the new augmentor and ground effect tests were reserved for the short augmentor configuration including the addition of the ventral nozzle.

7.0 DISCUSSION OF RESULTS

7.1 Free-Air Performance of the Full-Length Augmentor

Initial tests were done at 18.9 feet above the ground plane. The fuselage augmentor exit rake was installed on the left-hand augmentor to determine the degree of flow attachment to the diffuser walls and augmentor end-plates. The stepped augmentor inlet was used, i.e., the 20° fairing was not installed. The diffuser area ratio was 1.7.

Results are shown in **Figure 18**, together with DHC cold flow (same scale) laboratory tests for comparison (Reference 9). Lower values of augmentation for the present test, at least in part, reflect the higher core nozzle temperature and the presence of the exit rake. With inlet fairing installed, thrust augmentation showed no significant change.

DAR was increased from 1.7 to 1.8 and 1.9 with a small increase in ϕ_G as shown in **Figure 19**.

Some oscillation of the test rig was noticed, and the model height was reduced to 12.3 ft. It was shown that performance was unchanged, which enabled testing to continue at this height, (**Figure 20**).

The augmentor exit rake was than removed and a small increase in lift force was evident, (see **Figure 21**).

As a result of these tests, it was concluded that the fuselage augmentor was operating up to its capability, i.e. there were no separated flow regions and the optimum DAR had been bracketed. The throat Mach number was lower than that measured during the cold-flow laboratory tests at DHC (see **Figure 22**) and it was concluded that the difference in

performance was in fact due to primary gas temperature effects. These might affect primary nozzle thrust or thrust augmentation, or both. Since a knowledge of nozzle thrust is crucial to determination of ϕ_G, this subject was explored further. First, the augmentor doors were removed and the performance compared with the equivalent cold-flow test data, (see **Figure 23**). The hot result was about 2 points below the cold result of ϕ_G = 1.16 at NPR = 2.5, indicating that the nozzle thrust was probably not much affected by temperature. The augmentation with doors-off is attributed to the remaining structural elements surrounding the nozzle array.

An alternative approach to determine nozzle thrust was by way of comparisons of engine running line. The effective area of the fuselage ejector nozzles was measured, cold, in the laboratory, as were also the smaller areas of the wing augmentor nozzles and rear fuselage trim nozzles. From comparisons of the running lines (ETR vs $N/\sqrt{\theta}$ of the configurations with and without the large rear calibration nozzle, whose hot-effective area was well defined, it was estimated that the effective area of the fuselage ejector nozzles was several percent larger during hot test than during cold flow laboratory tests. (See **Figure 24**).

A third estimate of ejector nozzle area was available from the engine inlet static pressure tap. On the assumption that the inlet flow was uniform at the static tap location, the calculated ratio of inlet flow to total exit flow (fuselage nozzles, wing nozzles and trim nozzle) was determined to be 0.96. Taken at face value, this would imply that fuselage nozzle effective area was 6% less than the cold measurement in the laboratory. This might mean 6% less thrust. Within the range of experimental accuracy, therefore, no strong conclusion could be made concerning the likely hot, notched nozzle effective area.

It is suspected that the effective area of a notched nozzle may be affected by temperature and/or that the plume development may be different from that of a cold flow nozzle. An experimental program to investigate these effects would seem to be needed.

7.2 Effect of Reduction in Length of Augmentor End Plates

The vertical length of the augmentor end plates was reduced by 30% for one test. The measured reduction in augmentation ratio was about 6 points, (see **Figure 25**). The trade-off between end plate length and augmentation will affect the eventual design of end plates for an actual aircraft installation.

7.3 Performance of Augmentor with Reduced Chordwise Length

The shortened augmentor, used with the EL/VT configuration, was tested in free-air at DAR = 1.6 and 1.7. **Figure 26** shows a comparison between the standard length and shortened augmentors, with DAR = 1.7. There was essentially no difference.

7.4 Performance of EL/VT Configuration in Free-Air

As noted above, the short augmentor performance in free-air was as expected. The ventral nozzle thrust performance in free-air was obtained by difference between "with" and "without" configurations, (**Figure 27**). Its thrust efficiency was determined to be 0.92 and discharge coefficient was 0.95. The low thrust may be attributed to internal losses, caused by the rod which carries nozzle thrust back to the structure, but may also include some external jet mixing drag loss. The latter is not expected to be large in free-air though.

7.5 Ground Effect on EL/VT Configuration

The effect of ground proximity was measured only at h = 27". Previous tests, (Reference 6), with the full length augmentor and plain slot nozzles had been at h = 28" and 16", the latter being an approximate undercarriage height. In these previous tests, ground effect had been insignificant at 28" but 6½% positive on lift force at 16" (base end plates off; δ_F = 0°).

The present tests with the short augmentor and no ventral nozzle showed a reduction in lift at 27" amounting to 10% of the free-air lift, (**Figure 28**), or 16% of the augmentor nozzle thrust, (**Figure 29**). The difference between the performance of the full and short augmentors appears to be due to the magnitude of base thrust generated in the two cases. For the full augmentor, a positive base thrust was generated which off-set reductions in augmentor thrust due to back-pressure and suck-down interference, if any. For the short augmentor, the base thrust was insignificant. This is believed to be due to the more effective ventilation of the base cavity. The effect of base end plates was not determined with this configuration until the ventral nozzle was in operation.

There was a small increase in lift force when the (unblown) flaps were deflected to 60°, presumably due to a strengthening of fountain effect, (see **Figure 30**).

Addition of the ventral nozzle to the short augmentor configuration in ground effect produced a slightly more adverse result best displayed in the table following:

HEIGHT (INS)	VENTRAL NOZZLE	RUN NO.	NOZZLE THRUST (PRF=2.5)	LIFT (LB)	ϕ_G TOT	X_{B_2} LB
148	OFF	35	1270	2007	1.58	-11
27	OFF	48	1270	1803	1.42	-5
			ΔL =	-204	ΔX_{B_2}	= + 6
					$\Delta L/L$	= -10.2%
148	ON	38	1270+ 1990	4026	1.235	-13
27	ON	45	=3260	3765	1.155	+48
			ΔL =	-261	ΔX_{B_2}	= + 61
					$\Delta L/L$	= -6.5%

This table shows a more favourable base thrust increment due to ground proximity when the ventral nozzle was operating. It is believed to be due to an effective reduction in ground height as the radial ground flow from the ventral nozzle passes under the augmentor flow or perhaps forms a fountain in the base cavity. Despite this favourable effect, there was virtually no change in the overall increment of lift loss in the two cases.

Two likely reasons for this, are as follows:

(a) reduction in augmentor thrust due to increased back-pressure and,

(b) suck-down effect induced by the ventral nozzle jet.

Positive angle of attack (nose-up rotation of the model) in ground effect caused the lift force to increase, as a result of increasing the ground height of the fuselage augmentor, (see **Figure 31**).

Base end plates were fitted with the EL/VT configuration at h = 27" and produced the expected increase in base thrust,

(Figure 32), but the overall lift force decreased. The table following gives details:

HEIGHT (INS)	VENTRAL NOZZLE	RUN NO.	BASE END PLATES	LIFT (LB)	$\phi_{G_{TOT}}$	X_{B2} (LB)
27	ON	45	OFF	3765	1.155	+48
27	ON	44	ON	3668	1.125	+93

$\Delta L = -97 \quad \Delta X_{B_2} = +45$

$\Delta L/_L = -2.6\%$

This was an unexpected result and may be due to experimental error associated with obtaining the difference between two large measured quantities.

7.6 Pitching Moment Data

In free air the measured full-length augmentor pitching moment arm about the moment reference centre agreed with the augmentor geometric location, i.e., 1.21 ft. (Figure 33).

Similar results were obtained for the reduced length fuselage augmentor, i.e. the pitching moment arm agreed with the geometric arm of 3.39 ft., (Figure 34).

Addition of the ventral nozzle in conjunction with the short augmentor, i.e. the EL/VT configuration, showed a pitch moment arm length of about -0.85 ft. in free air, increasing to -1.15 ft. at a ground height of 27 inches, compared with a geometric arm of -.72 ft. in free-air. This is an indication that the low derived thrust efficiency of the ventral nozzle may be due to "suck-down" interference effects in free-air operating ahead of the nozzle location.

Repositioning the flaps to 60° from 0° provided a "fence"

only, since wing augmentors were unblown, and produced little change in pitching moment. Increasing angle of attack to 10° with δ_F = 60° produced a positive pitching moment as a result of increased fuselage augmentor performance with increased effective ground height. The pitching moment arm increased positively to about -1.0 ft., (**Figure 35**).

The addition of fuselage base end-plates gave an insignificant pitching moment change,(see **Figure 36**).

7.7 Description of Flow Over the Ground Plane

The basic ground plane flow pattern around the model with full length fuselage augmentors was described in Reference 6. The present tests in ground effect were limited to the EL/VT configuration, i.e. reduced length fuselage augmentor and addition of the ventral nozzle.

Ground plane instrumentation provided a fairly extensive coverage of ground plane static and total pressures and temperatures as shown in **Figures 15 and 16**. Unfortunately, the hot ventral nozzle flow took its toll of instrumentation, limiting the amount of available data.

Some of these data are shown in **Figures 37(a) to 37(d)**, illustrating the effect of adding ventral nozzle, base end-plates, flap angle (unblown) and angle of attack.

Augmentor exit temperatures were noticeably reduced with the new augmentor nozzles, **Figure 38**, indicating increased secondary flow over the previous slot nozzle augmentor of Reference 6.

Ground plane temperatures are given in **Figure 39**, for the reduced length fuselage augmentor. It includes the effects of adding ventral nozzle and of flap angle. The ventral nozzle flow can be seen penetrating the full length of the fuselage augmentor region.

8.0 CONCLUSIONS

8.1 Full Length Ejector

(i) Ejector performance, in terms of $\emptyset$, was determined as follows:

PRF	1.6	2.0	2.6
$\emptyset_{G_F}$	1.69	1.66	1.57

These values relate to DAR = 1.9 and compare to DHC cold flow test results at the same scale of 1.81, 1.80 and 1.74 respectively. Both sets represent "best" performance at this DAR.

(ii) It is believed that the lower values of $\emptyset_G$ measured at Ames Research Center, largely reflect the higher exhaust temperature of the J-97 model as compared to the de Havilland "cold" blow-down rig.

(iii) Exit pressure surveys of the augmentor indicated that flow distribution and wall control was good.

(iv) A 30% reduction in length of the fuselage augmentor end plate resulted in a 4% thrust loss.

(v) Determination of $\emptyset_G$ is critically dependent upon a sound knowledge of primary nozzle thrust which, at present, is based on "cold" flow tests. Special tests are recommended to determine the effect of temperature on notch nozzle thrust performance.

(vi) Structural integrity of the new vectorable nozzle array was validated.

8.2 Short Ejector With or Without Ventral Nozzle

(i) With the model at "free air" height, performance of the short ejector was essentially the same as that of the long ejector.

(ii) At a height of 27" above the ground, the model suffered a 10% loss in lift, compared to the "free-air" value (ventral nozzle inoperative).

(iii) At a height of 27" and with the ventral nozzle operative, the overall loss in lift (relative to the free air value) was 6½%.

(iv) At a height of 27", there was a substantial restoration in augmentor thrust with increase in pitch angle largely due to a corresponding effective increase in height above the ground.

9.0 REFERENCES

1. Garland, D.B. — Static Tests of the J-97 Powered, External Augmentor V/STOL Wind Tunnel Model at DHC. DHC-DND 77-4, February 1978 (also as NASA CR 152403, February 1978).

2. Aoyagi, K. Aiken, T.N. — Wind-Tunnel Investigation of a Large-Scale VTOL Aircraft Model with Wing Root and Wing Thrust Augmentors. NASA TM 78589, September 1979.

3. Garland, D.B. — Phase I Wind Tunnel Tests of the J-97 Powered, External Augmentor V/STOL Model. DHC-DND 79-4, September 1979 (also as NASA CR 152255 September 1979).

4. Garland, D,B. Harris, J.L. — Phase 2 and 3 Wind Tunnel Tests of the J-97 Powered, External Augmentor V/STOL Model. DHC-DND 80-1, April 1980 (also as NASA CR 152380, October 1980).

5. Whittley, D.C. — Large-Scale Model Tests of a New Technology V/STOL Concept. AIAA Paper No. 80-0233, January 1980.

6. Gilbertson, F.L. Garland, D.B. — Static Tests of the J-97 Powered, External Augmentor V/STOL Model at the Ames Research Center, NASA. DHC-DND 80-2, January 1982.

7. Whittley, D.C. — Thrust Vectoring of Ejector Systems for High Performance V/STOL Aircraft. DHC-P80-1, Janaury 1980.

8. Garland, D.B. Gilbertson, F.L. — Final Report on Further Development of a New Nozzle Concept for V/STOL Aircraft. DHC-DND 82-4, November 1982.

9. Gilbertson, F.L. Garland, D.B. — Cold Flow, Outdoor Tests of a Large-Scale Thrust Augmentor with Notched Nozzles (Model ST-CF). DHC-DND 83-1, February 1986.

10.0 NOTATION

AVN	=	aft ventral nozzle
BLC	=	boundary layer control
c.g.	=	centre of gravity
DAR	=	diffuser area ratio
EGT	=	exhaust gas temperature
EL/VT	=	Ejector Lift/Vectored Thrust
E/P	=	end plate
ETR	=	engine exhaust temperature ratio, EGT/Ti
F/A	=	free air
FN	=	normal force
FAUG	=	fuselage augmentor chord ratio; 13 nozzles/side = 1.0; 7 nozzles/side = 0.538
H	=	height above ground, measured to lower end (trailing edge) of augmentor doors, $\alpha = 0°$
H'	=	average value of H when $\alpha \neq 0$
L	=	lift force
L_I	=	interference lift force
mac	=	mean aerodynamic chord
N	=	engine r.p.m. %
Pa	=	ambient pressure
PAV1,PAV2	=	aft ventral nozzle exit total pressure
PF1,PF2	=	fuselage duct upstream static pressures
PM	=	pitching moment
PNT	=	trim nozzle rear duct static pressure
PRF	=	fuselage augmentor nozzle pressure ratio = (PSN + Pa)/Pa
PRTN	=	trim nozzle reference pressure ratio = (PNT + Pa)/Pa
PRW	=	wing augmentor reference pressure ratio
PRVN	=	aft ventral nozzle pressure ratio
PS	=	static pressure
PS_B	=	fuselage base static pressure
PS_{IN}	=	engine inlet static pressure
PSN	=	fuselage augmentor nozzle reference static pressure

PT	=	total pressure
PW	=	fuselage duct static pressure at wing duct entry
PWDL, PWDR	=	wing augmentor duct end static pressure
RPR	=	fuselage duct reference static pressure ratio = (PF1 + Pa)/Pa
T	=	temperature
T_a	=	ambient temperature
T_{AUG}	=	augmentor exit temperature
T_{GP}	=	ground plane temperature
T_i	=	engine inlet temperature
W_{IN}	=	engine intake mass flow, lb./sec. = f (PS_{IN} , Pa)
W_{EXIT}	=	model exit mass flow, lb./sec. = $W_F + W_w$ + WTN + WVN
W_F	=	fuselage augmentor nozzle mass flow, lb./sec.
W_{TN}	=	trim nozzle mass flow, lb./sec.
W_w	=	wing augmentor mass flow, lb./sec.
WVN	=	aft ventral nozzle mass flow, lb./sec.
X_B	=	total fuselage base thrust
X_{B_2}	=	fuselage base thrust, area confined by fuselage augmentors
X_F	=	fuselage augmentor thrust
X_{INTEG}	=	fuselage augmentor exit integrated thrust obtained when exit rake "on"
X_{NF}	=	fuselage augmentor nozzle thrust
X_{NTN}	=	trim nozzle thrust
X_{NV}	=	aft ventral nozzle thrust
X_{NW}	=	wing augmentor nozzle thrust
X_W	=	wing augmentor thrust
α	=	model pitch attitude, degs.
δ	=	ambient pressure/standard day pressure at sea level
δ_F	=	wing augmentor flap deflection
η_∞	=	fuselage augmentor nozzle efficiency (based on single nozzle cold flow tests)

θ = engine inlet temperature ratio,
T /standard day temperature (288°K)

μ = fuselage augmentor secondary/primary mass flow ratio $(W\sqrt{T})$ sec/$(W\sqrt{T})$ prim.

$\phi_{G_F} = \frac{L - XB}{XNF}$ (or $\frac{L - XB - XNV}{XNF}$ if $\delta_{VN} = 90°$)

$\phi_{G_{TOT}} = \frac{L}{XNF}$ (or $\frac{L - XNV}{XNF}$ if $\delta_{VN} = 90°$)

$\phi_{G_{MODEL}} = \frac{L}{XNF + XNV}$ when $\delta_{VN} = 90°$

NOTE: All pressures are gauge, not absolute.

TABLE 1: RUN HISTORY OF VTOL4 STATIC TEST, NASA AMES RESEARCH CENTER
DHC EXTERNAL AUGMENTOR AND EJECTOR LIFT/VECTORED THRUST MODEL

RUN NO.	HEIGHT h INCHES	DAR	MAIN EXIT RAKE	20° INLET FAIRING	AUG'R END PLATES	BASE END PLATES	δ F°	TRIM NOZZLE DIA.	AFT VENTRAL NOZZLE	REMARKS
1	227	1.7	ON	OFF	FULL	OFF	0°	4.8"	OFF	Initial Check Runs
2										
3										
4										
5										Axial Check Loads
6										
7										
8										Full Augmentor
9								2.8"		13 nozzle/side
10										Axial Check Loads
11										
12				ON						
13		1.8								
14		1.9								
15										Axial Check Loads
16										
17										
18										
19										
20										δ Tare Run
21										

TABLE 1 (CONT'D): RUN HISTORY OF VTOL4 STATIC TESTS, NASA AMES RESEARCH CENTER
DHC EXTERNAL AUGMENTOR AND EJECTOR LIFT/VECTORED THRUST MODEL

RUN NO.	HEIGHT h INCHES	DAR	MAIN EXIT RAKE	20° INLET FAIRING	AUG'R END PLATES	BASE END PLATES	δ_F°	TRIM NOZZLE DIA.	AFT VENTRAL NOZZLE	REMARKS
22	227	1.9	ON	ON	FULL	OFF	0°	2.8"	OFF	Normal Check Loads
23										
24	148									
25			OFF							
26		1.7								
27					SHORT					
28					FULL					
29										Normal Check Loads
30										
31										Normal Check Loads
32										Repeat of Runs 26,28,30
33										Aug. doors off
34		1.6								
35		1.7					0°BLANKED	9.46"		Short Augmentor (7 Nozzles/side)
36										
37								2.8"	ON	
38										
39										
40	27									Data Checks
41										
42										

TABLE 1 (CONT'D): RUN HISTORY OF VTOL4 STATIC TEST, NASA AMES RESEARCH CENTER
DHC EXTERNAL AUGMENTOR AND EJECTOR LIFT/VECTORED THRUST MODEL

RUN NO.	HEIGHT h INCHES	DAR	MAIN EXIT RAKE	20° INLET FAIRING	AUG'R END PLATES	BASE END PLATES	δ_F°	TRIM NOZZLE DIA.	AFT VENTRAL NOZZLE	REMARKS
43	27	1.7	OFF	ON	FULL	OFF	0°BLANKED	2.8	ON	
44						ON				
45						OFF				
46							60°BLANKED			
47										
48							0°BLANKED	9.46	OFF	
49		—								Fuselage Augmentor Doors Off
50		1.7					60°BLANKED	2.8	ON	α Tare Run
51										α = 10°
52										
53										α = 5°
54										
55										α = 10°
56		—					0° OPEN	2.8	OFF	Fuselage Augmentor Doors Off

TABLE 2

GEOMETRY OF J-97 POWERED, EXTERNAL AUGMENTOR V/STOL MODEL

WING			
Area, gross		141	$ft.^2$
Area, net		97	$ft.^2$
Span		15.25	ft.
Aspect ratio		1.65	
t/c		8%	
m.a.c.		12.68	ft.
Chord on fuselage C_L		16.92	ft.
FUSELAGE			
Overall length	Approx.	28	ft.

MOMENT REFERENCE CENTRE – (Wing leading edge joint, on wing chord datum)

Distance ahead of rear strut location $\bar{x}$ = 44.0" (also equal to 47.2% of m.a.c.).

TABLE 3

GEOMETRY OF FUSELAGE AUGMENTORS

	EXTERNAL AUGMENTOR V/STOL	EL/VT STOVL
AUGMENTOR		
Chordwise Length	97.5 in.	51.5 in.
Throat Width (LT)	10.5 in.	10.5 in.
Exit Width (LE) } nominal	17.85 in.	17.85 in.
Diffuser Area Ratio (DAR) } nominal	1.7	1.7
Length (min) (L)	34 in.	34 in.
Mean Nozzle Width ($\bar{t}$)	0.414 in.	0.414 in.
Augmentor Length Ratio ($L/\bar{t}$)	77	77
NOZZLES (4 NOTCHES/NOZZLE)		
Geometric Exit Area Per Nozzle	8.58 $in.^2$	8.58 $in.^2$
Total Geometric Exit Area (per side)	111.5 $in.^2$	60.1 $in.^2$
Notch Area/Total Nozzle Area (geometric)	0.62	0.62
Number of Nozzles (per side)	13	7
Effective Exit Area (per nozzle) } HOT	3.179 $in.^2$	3.179 $in.^2$
Total Effective Area (per side) } HOT	41.33 $in.^2$	22.25 $in.^2$
Effective Aspect Ratio $(AR)_e$	32	32
Nozzle Exit Span (L_N)	10.12 in.	10.12 in.
Basic Thickness at Exit (to)	0.125 in.	0.125 in.
Pitch (p)	7.68 in.	7.68 in.
Pitch Ratio ($p/\bar{t}$)	18.5	18.5

NOTE: 1. Clearance between end nozzles and augmentor end plates was 0.35 p when hot.

2. Effective area and $\bar{t}$ are shown for PR = 2.5.

TABLE 4

GEOMETRY OF WING AUGMENTOR

Span (per wing)			= 69.5 in.
Total nozzle area (per wing)			= 11.5 $in.^2$
Bay Spans	24.25	22.75	22.5 in.
Nozzle area/bay	4.88	3.73	2.88 $in.^2$
$\bar{t}$	0.201	0.164	0.128 in.
Number of nozzles (N)	15	17	22
Area per nozzle (A_N)	0.325	0.219	0.131 $in.^2$
Pitch (p)	1.60	1.32	1.01 in.
Nozzle span (b)	3.61	2.96	2.29 in.
Nozzle thickness (t)	.090	.074	.057
Nozzle aspect ratio (AR)	40	40	40
Throat (mid span) (L_T)	4.17	3.40	2.65
Exit (mid span) (L_E)	6.67	5.44	4.24
Diffuser area ratio L_E/L_T	1.60	1.60	1.60
Nozzle inlet area/exit area	5.0	5.0	5.0
Augmentor length (mid span) (L)	17.3	14.7	12.1
$L/\bar{t}$	86	90	95

NOTE: Measured effective exit area at PR = 2.5. (HOT)

L.H. Wing	12.5 $in.^2$
R.H. Wing	12.4 $in.^2$
Total	24.9 $in.^2$

TABLE 5

REAR TRIM NOZZLES

AFT TRIM NOZZLES	ORIFICE TYPE				
Nozzle dia. (in.) (Cold)	2.8	4.8	6.2	7.5	8.75
Nozzle geometric area (in.^{2}) (Hot)	6.22	18.3	30.5	44.6	60.7
Approximate effective exit area (in.^{2}); PR = 2.5 (Hot)	5.1	14.9	24.9	36.4	49.6

AFT TRIM NOZZLES	CONICAL TYPE	
Nozzle dia. (in.) (Cold)	11.3	12.4
Nozzle geometric area (in.^{2}) (Hot)	101.29	121.97
Approximate effective exit area (in.^{2}); PR = 2.5 (Hot)	100.2	120.5

AFT TRIM NOZZLES	CALIBRATION TYPE
Nozzle dia. (in.) (Cold)	9.46
Nozzle geometric area (in.^{2}) (Hot)	70.99
Approximate effective exit area (in.^{2}); PR = 2.5 (Hot)	70.29

TABLE 6: TEST CONFIGURATIONS

CONFIGURATION "A": 13 FUSELAGE AUGMENTOR NOZZLES/SIDE 4.8" DIA. TRIM NOZZLE, VENTRAL NOZZLE "OFF", WING DUCTS "OPEN"

CONFIG#	HEIGHT H	INLET FAIRING	DAR	AUG. END PLATES	AUG. EXIT RAKE	BASE END PLATES	δ_F °	α	RUNS
A-1	227	OFF	1.7	FULL	ON	OFF	0	0	4, 8

CONFIGURATION "B": 13 FUSELAGE AUGMENTOR NOZZLES/SIDE 2.8" DIA. TRIM NOZZLE, VENTRAL NOZZLE "OFF"; WING DUCTS "OPEN"

B-1	227	OFF	1.7	FULL	ON	OFF	0	0	9, 11
B-2	↓	ON	1.7	↓	↓	↓	↓	↓	12
B-3	↓	↓	1.8	↓	↓	↓	↓	↓	13
B-4	↓	↓	1.9	↓	↓	↓	↓	↓	14, 19, 21
B-5	148	↓	1.9	↓	↓	↓	↓	↓	24
B-6	↓	↓	1.9	↓	OFF	↓	↓	↓	25
B-7	↓	↓	1.7	↓	↓	↓	↓	↓	26, 29, 30, 32
B-8	↓	↓	1.7	SHORT	↓	↓	↓	↓	27
B-9	↓	↓	DOORS OFF	FULL	↓	↓	↓	↓	33
B-10	27	↓	DOORS OFF	FULL	↓	↓	↓	↓	56

CONFIGURATION "C": 7 FUSELAGE AUGMENTOR NOZZLES/SIDE 9.46" DIA. TRIM NOZZLE, VENTRAL NOZZLE "OFF"; WING DUCTS "BLANKED"

C-1	148	ON	1.6	FULL	OFF	OFF	0 PRW=1.0	0	34
C-2	148	↓	1.7	↓	↓	↓	↓	↓	35
C-3	27	↓	1.7	↓	↓	↓	↓	↓	48
C-4	27	↓	DOORS OFF	↓	↓	↓	↓	↓	49

CONFIGURATION "D": 7 FUSELAGE NOZZLES PER SIDE 2.8" DIA. TRIM NOZZLE; VENTRAL NOZZLE "ON"; WING DUCTS "BLANKED"

D-1	148	ON	1.7	FULL	OFF	OFF	0 PRW=1.0		36, 37, 38, 39
D-2	27	↓	↓	↓	↓	↓	↓		42, 43, 45
D-3	↓	↓	↓	↓	↓	ON	↓		44
D-4	↓	↓	↓	↓	↓	OFF	60 PRW=1.0	0	46, 47, 54
D-5	↓	↓	↓	↓	↓	↓	↓	5	53
D-6	↓	↓	↓	↓	↓	↓	↓	10	51, 52, 55

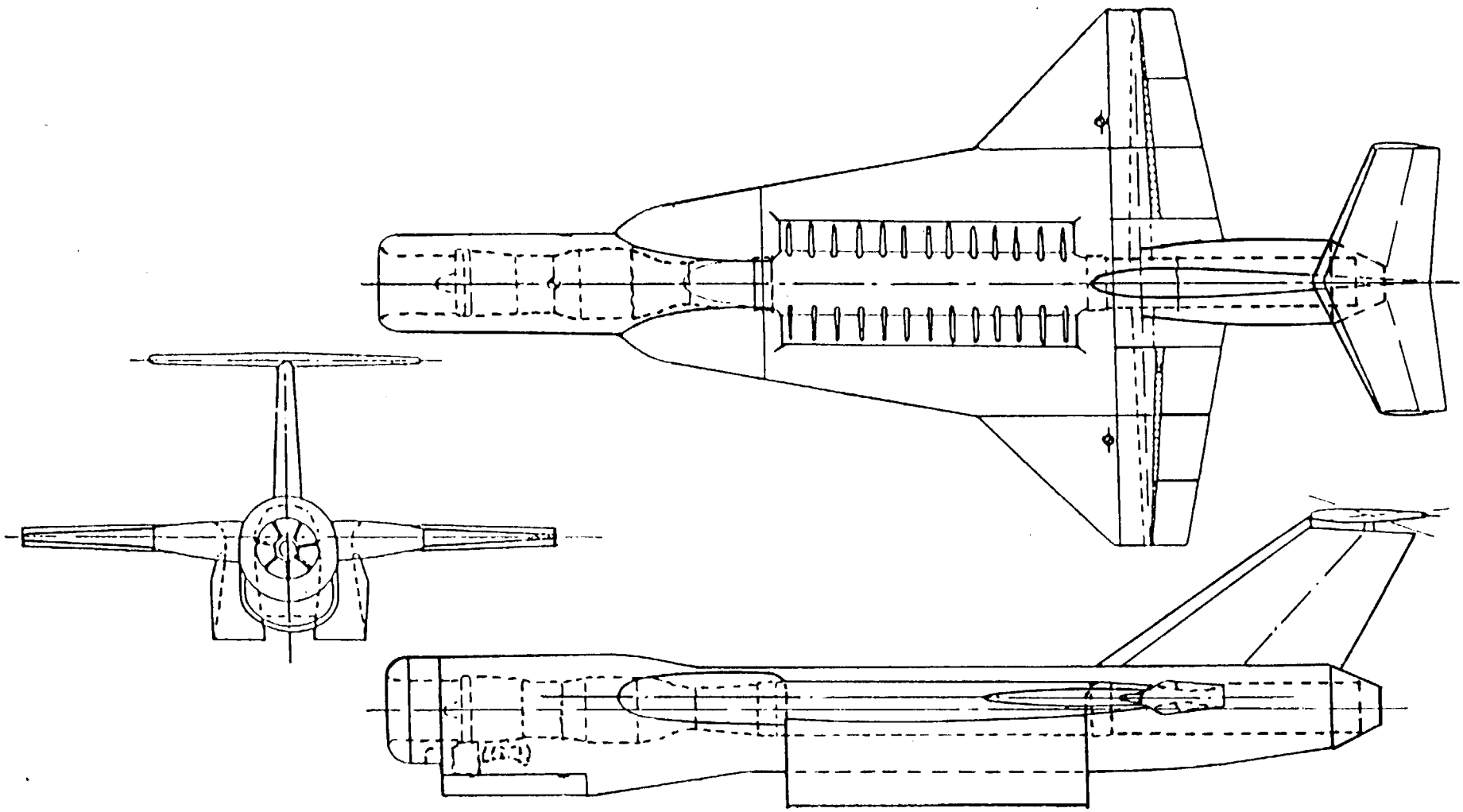

DHC EXTERNAL AUGMENTOR V/STOL CONCEPT

G.A. OF J-97 POWERED MODEL

Fig. 1

Fig. 2

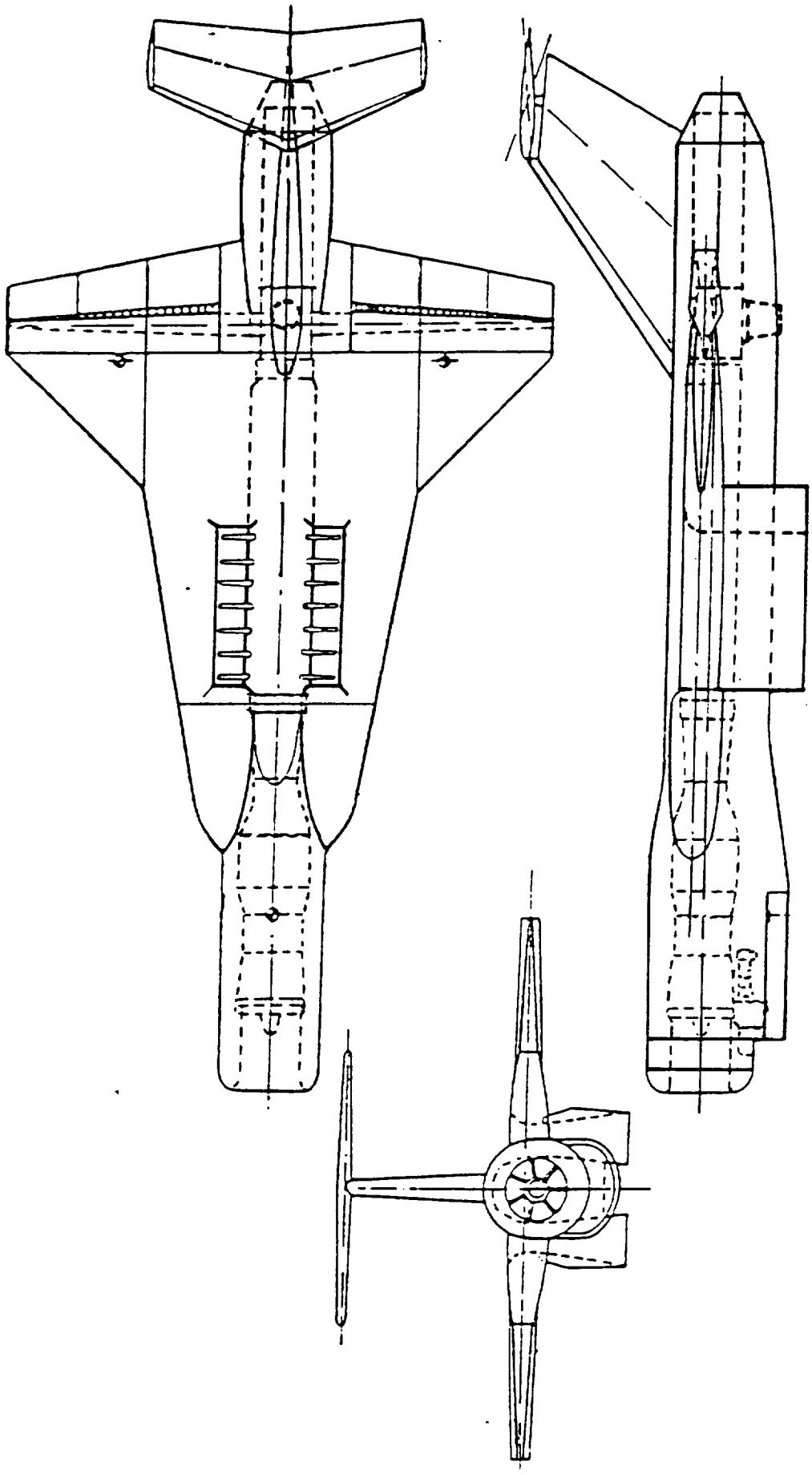

DHC EJECTOR LIFT/VECTORED THRUST STOVL CONCEPT

G.A. OF J-97 POWERED MODEL

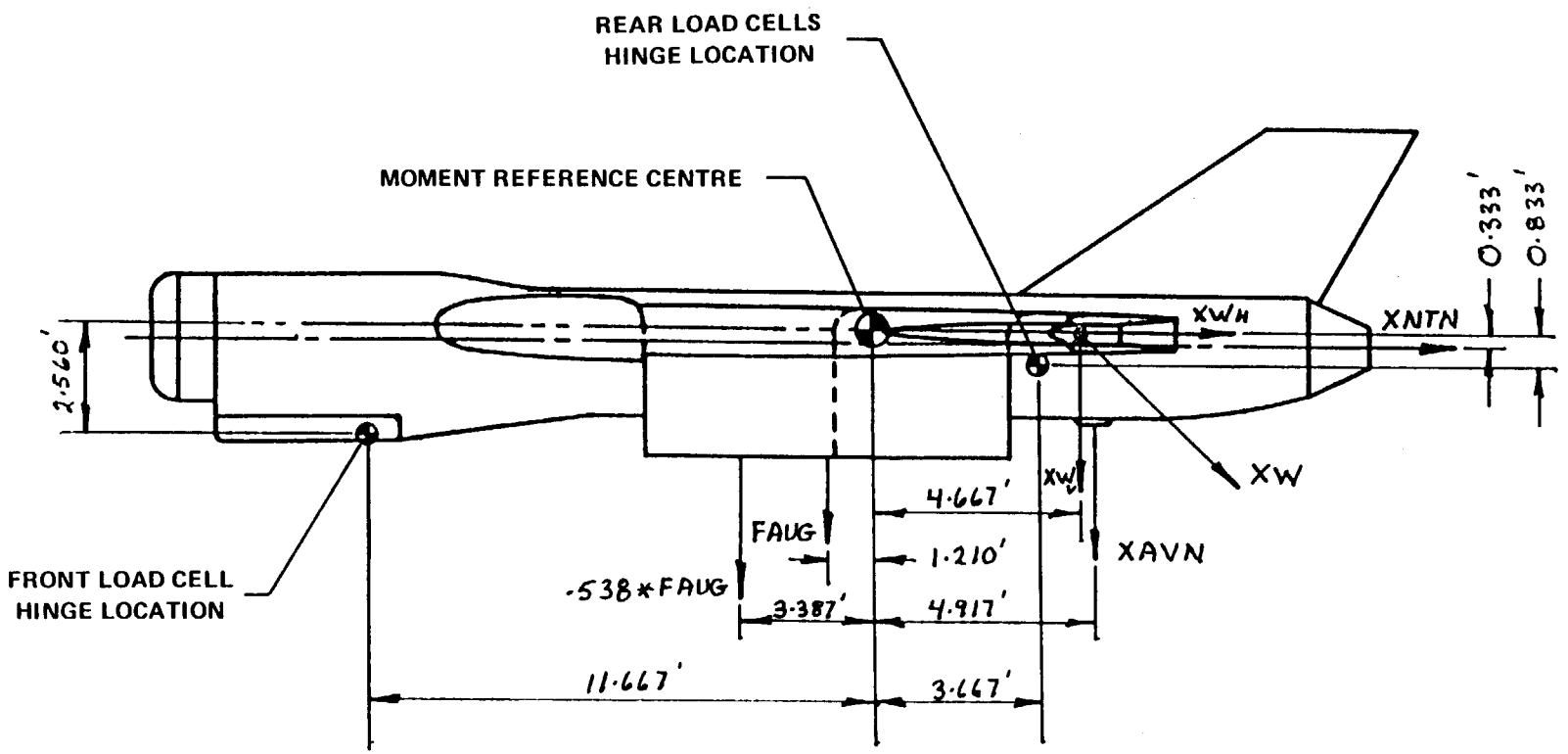

MODEL FORCE LOCATIONS

Fig. 3

Fig. 4

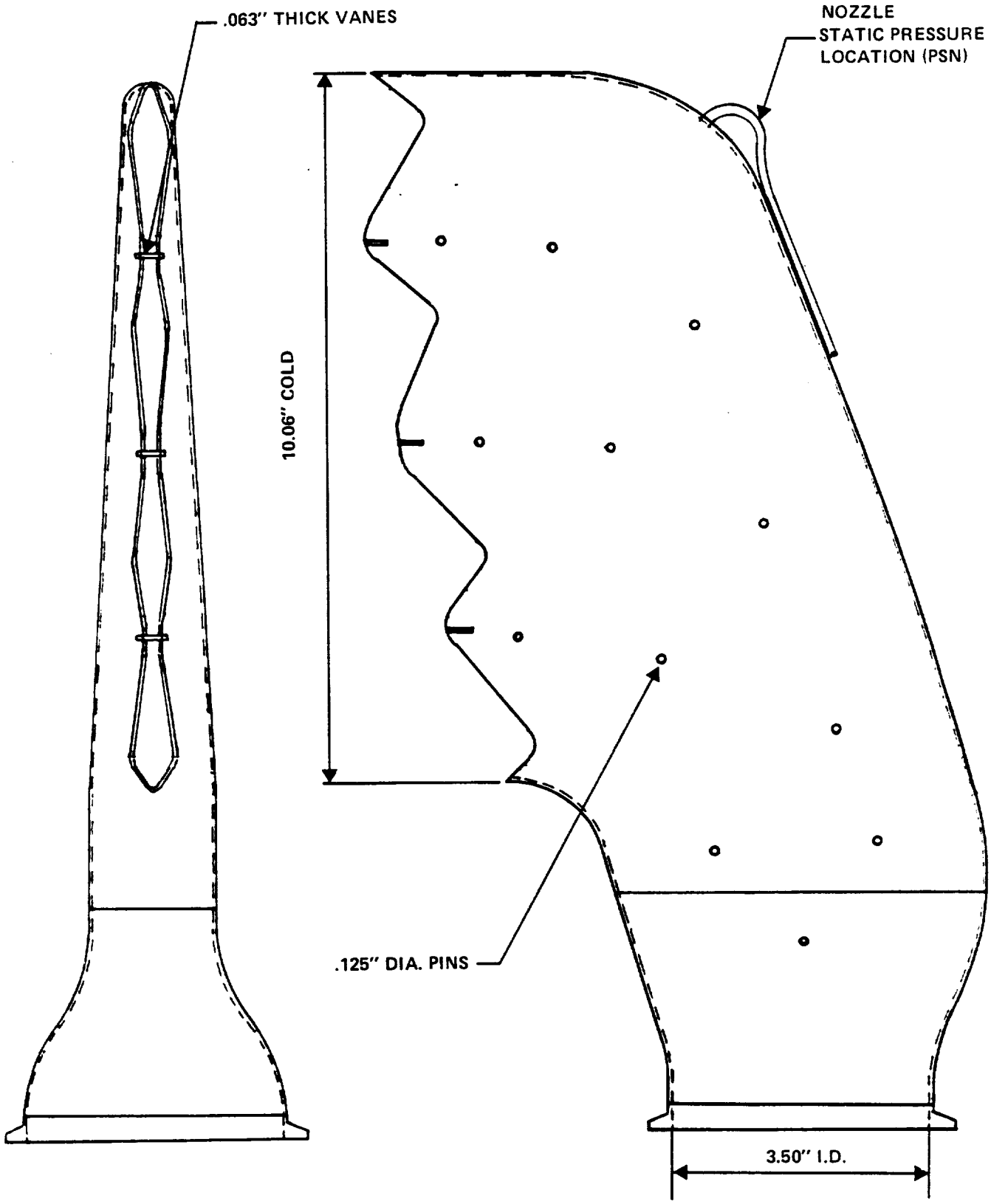

FUSELAGE AUGMENTOR NOTCHED NOZZLE

Fig. 5

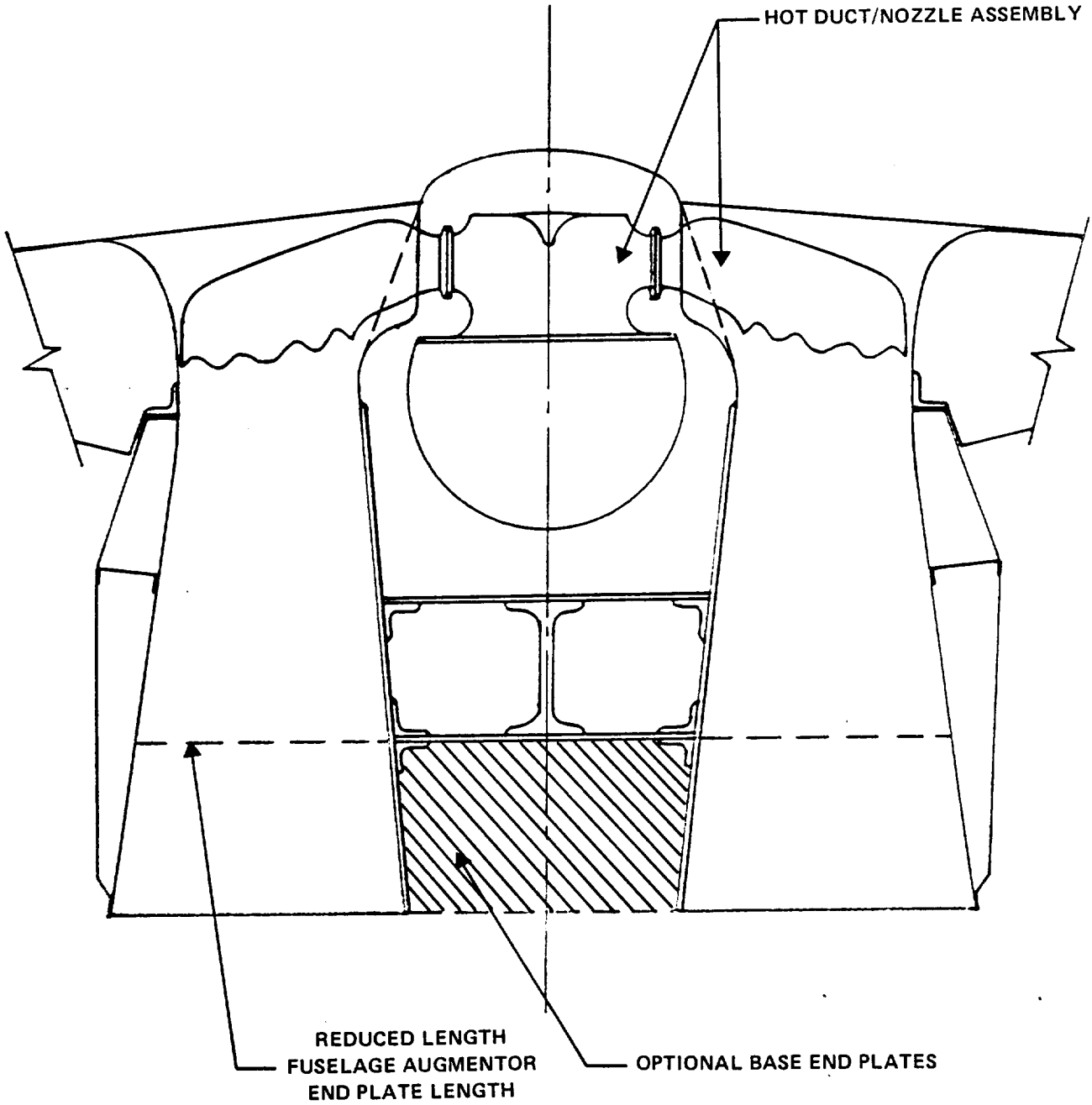

SECTION THROUGH FUSELAGE AUGMENTOR

Fig. 6

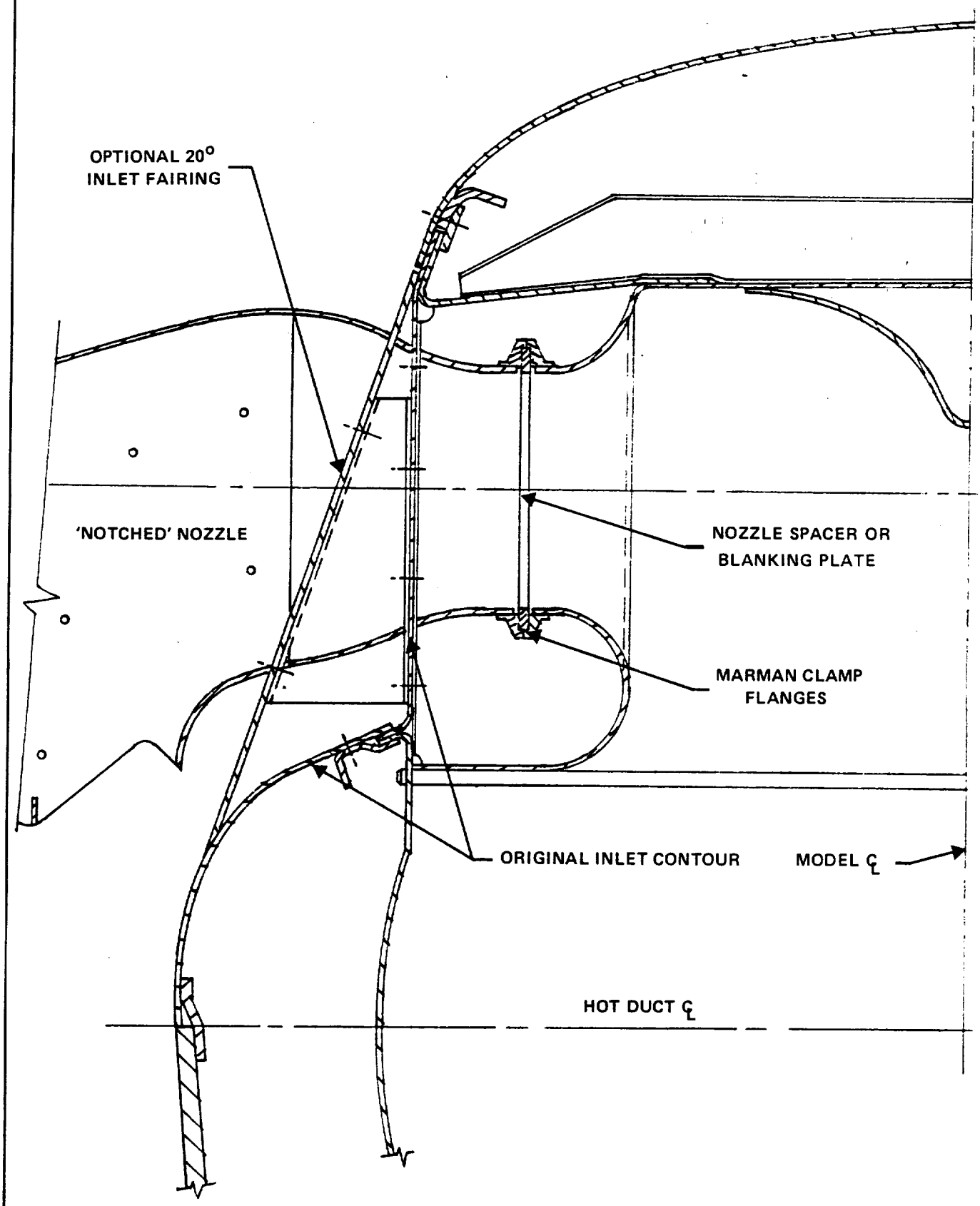

SECTION THROUGH FUSELAGE AUGMENTOR SHOWING 20° INLET FAIRING AND NOTCHED NOZZLE ATTACHMENT

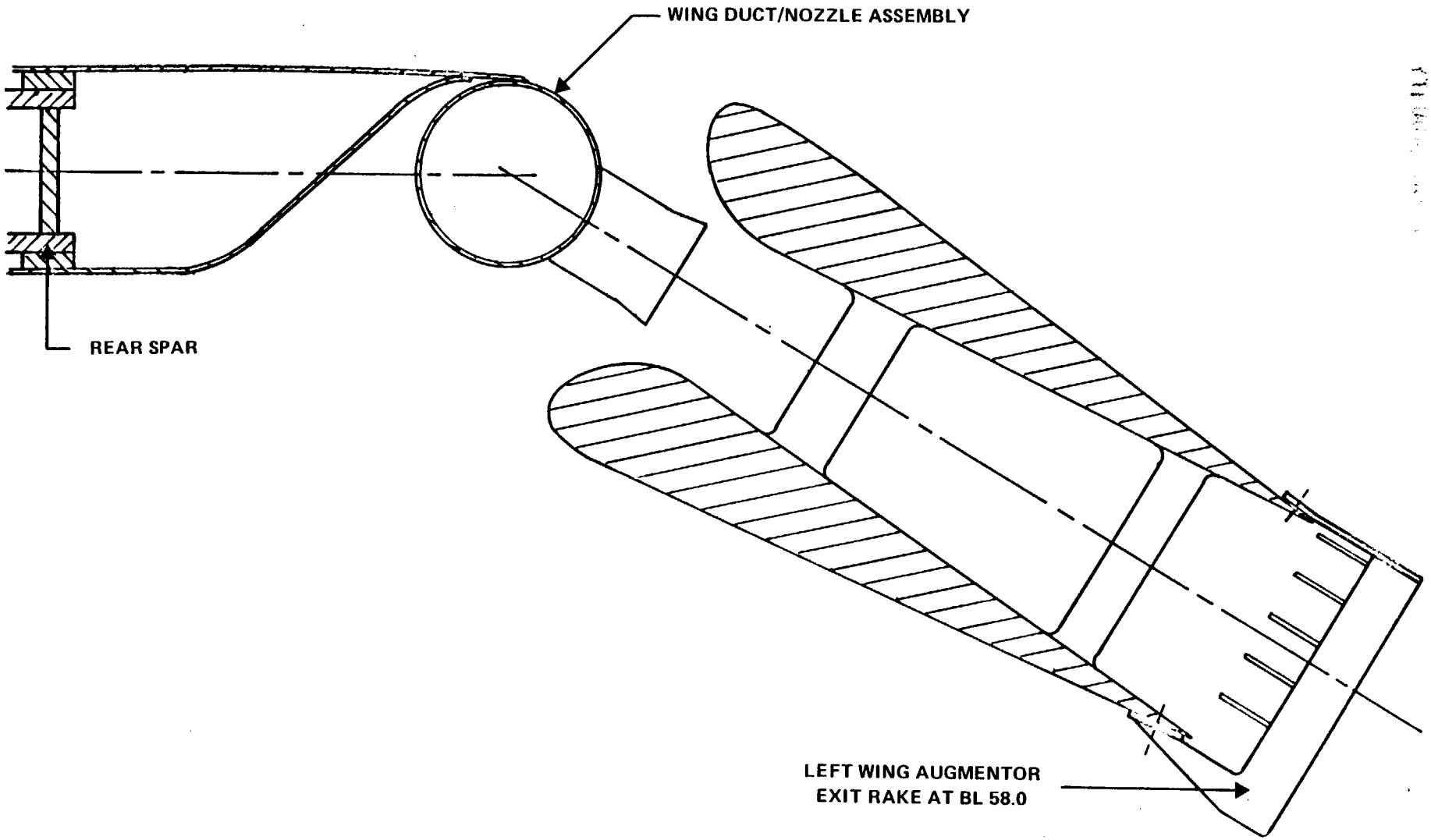

SECTION THROUGH WING AUGMENTOR FLAP

Fig. 7

Fig. 8

VIEW OF AUGMENTOR INLET WITH COVER PLATES INSTALLED OVER REAR SECTION

Fig. 9

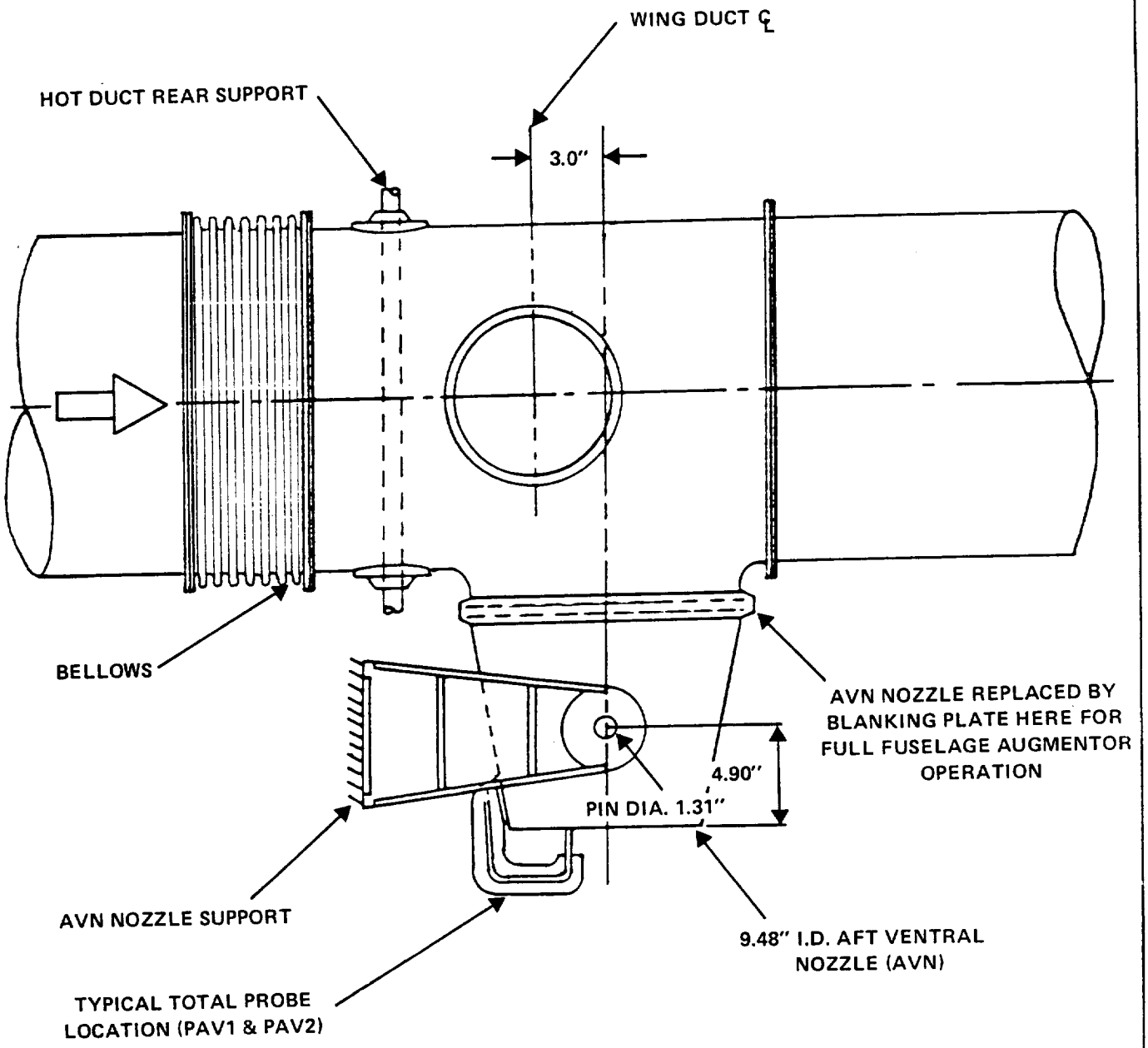

AFT VENTRAL NOZZLE INSTALLATION

Fig. 10

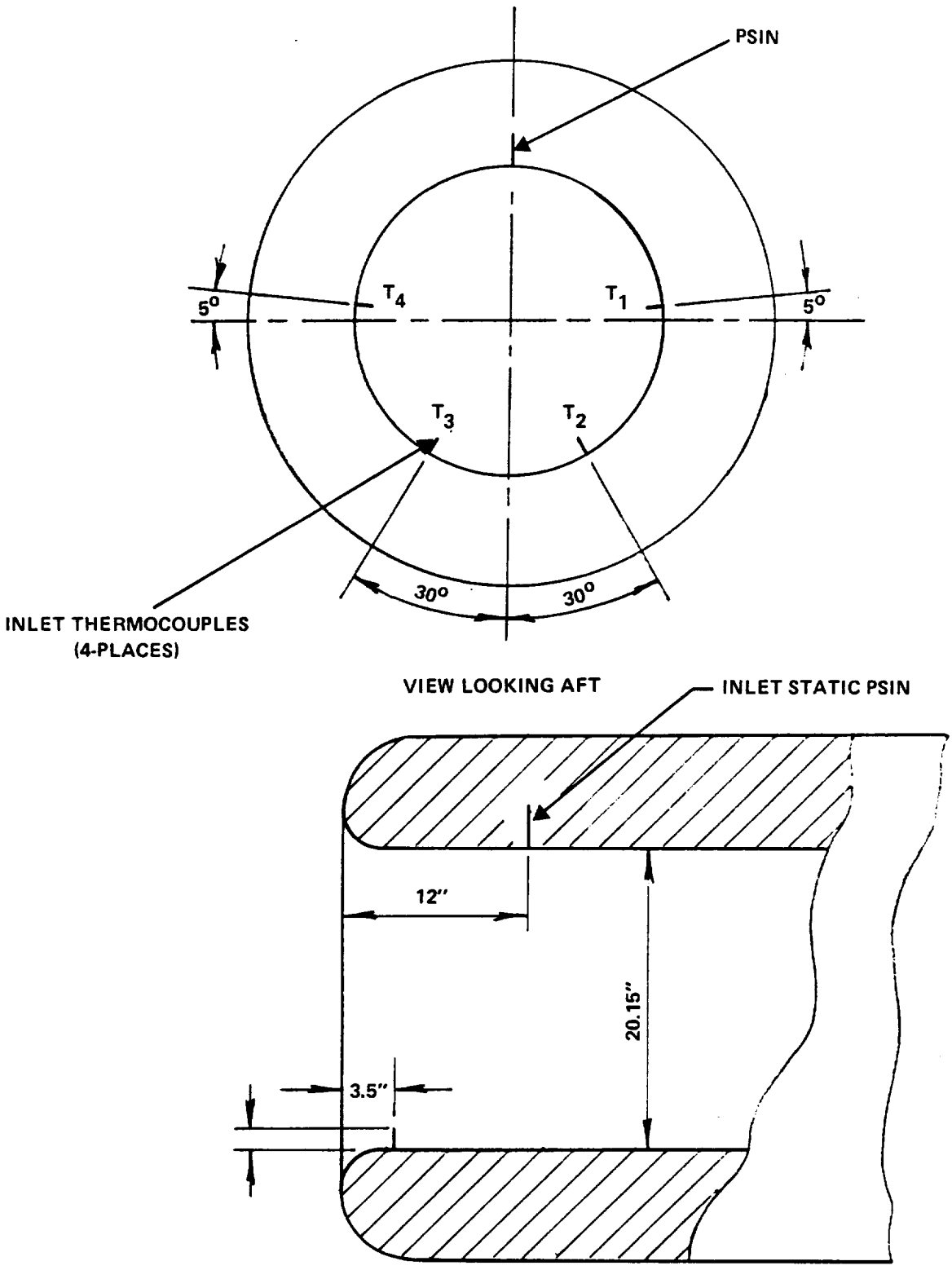

J-97 INLET INSTRUMENTATION LOCATIONS

Fig. 11

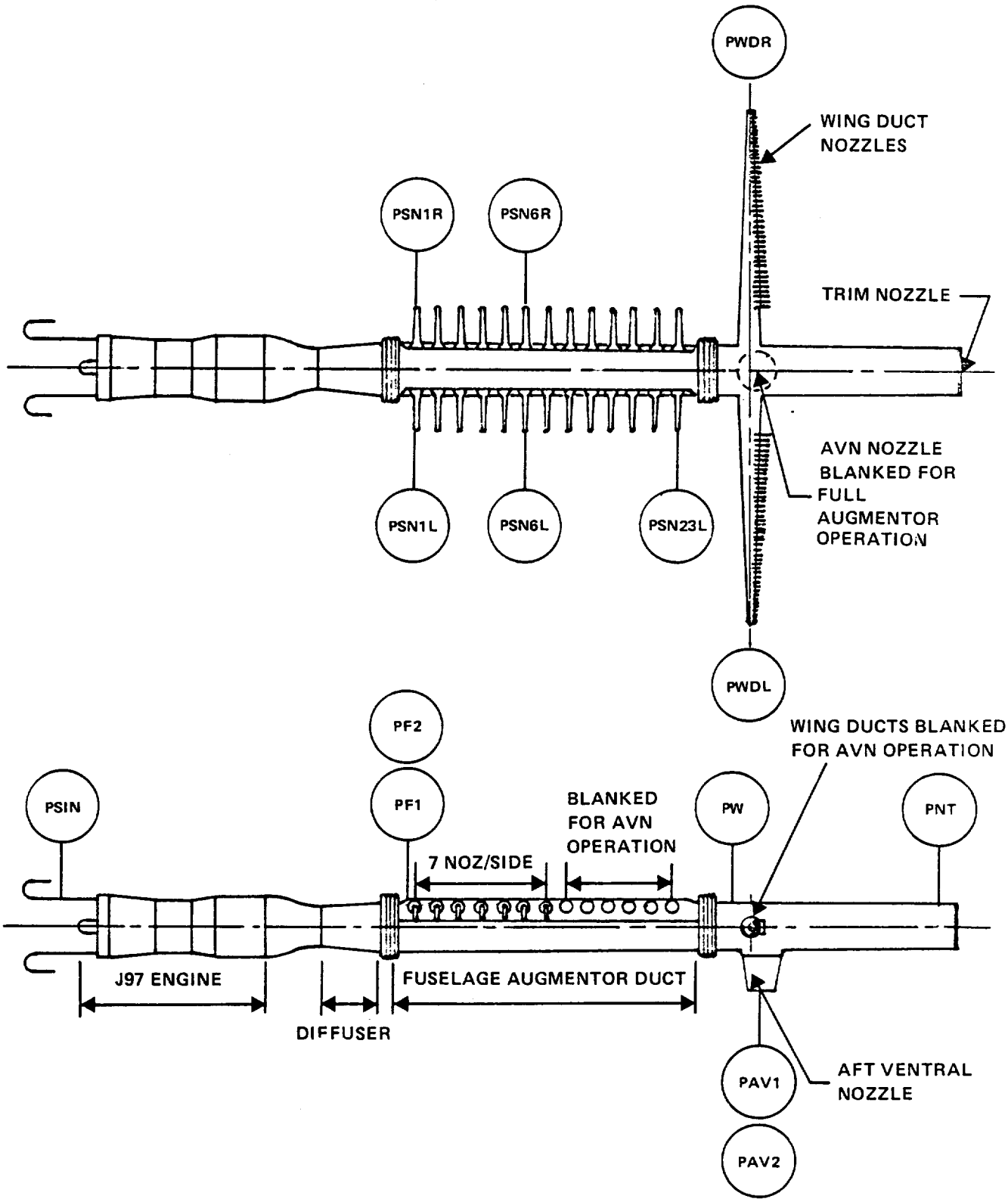

DUCT STATIC AND TOTAL PRESSURE LOCATIONS

Fig. 12

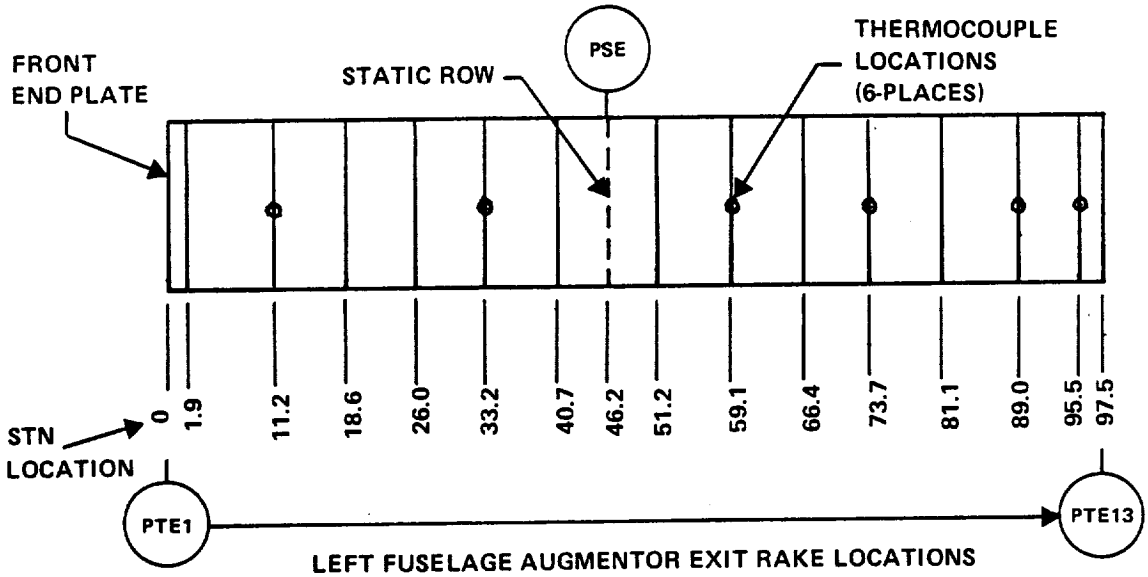

LEFT FUSELAGE AUGMENTOR EXIT RAKE LOCATIONS

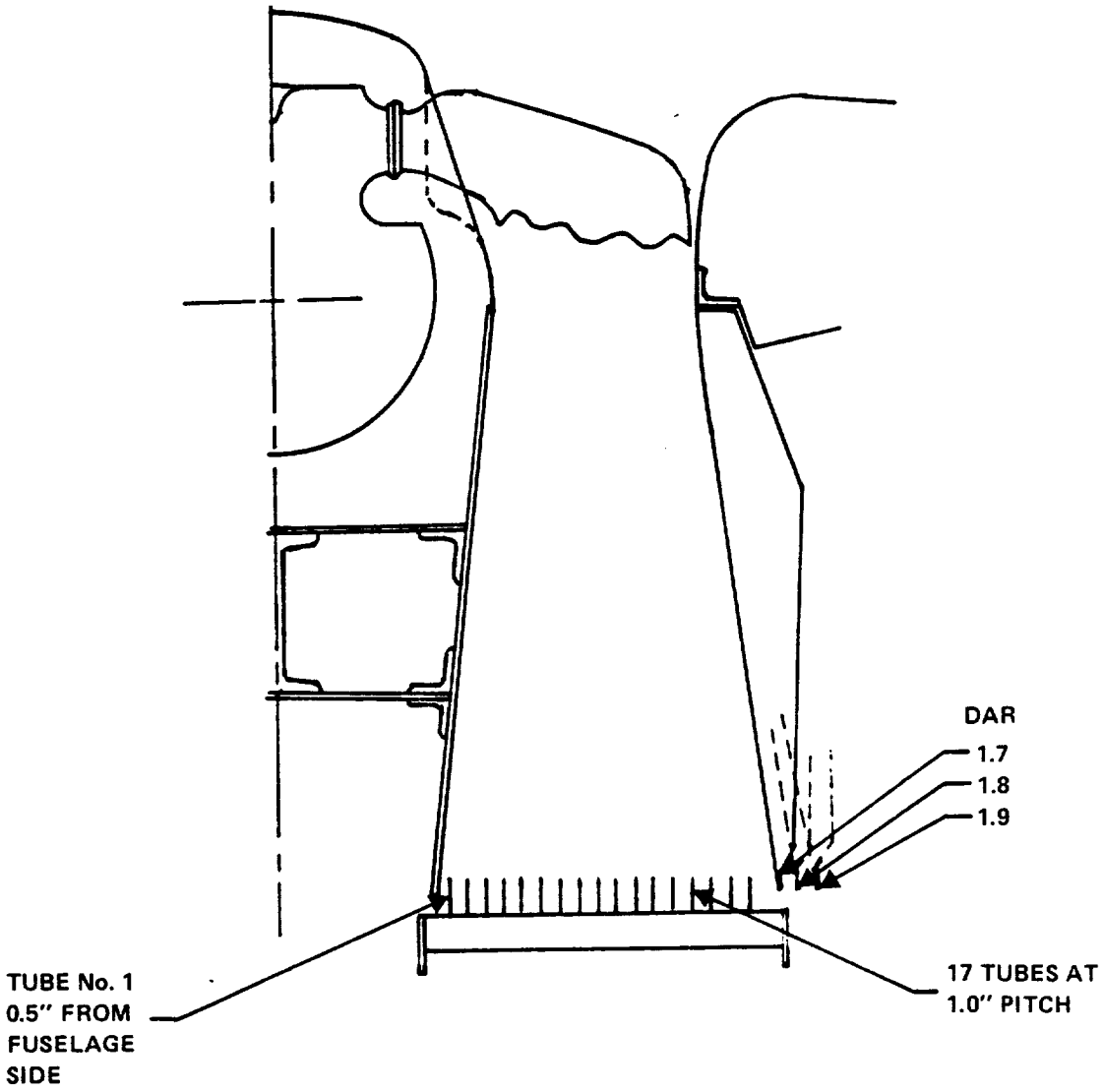

SECTION SHOWING AUGMENTOR EXIT RAKE

Fig. 13

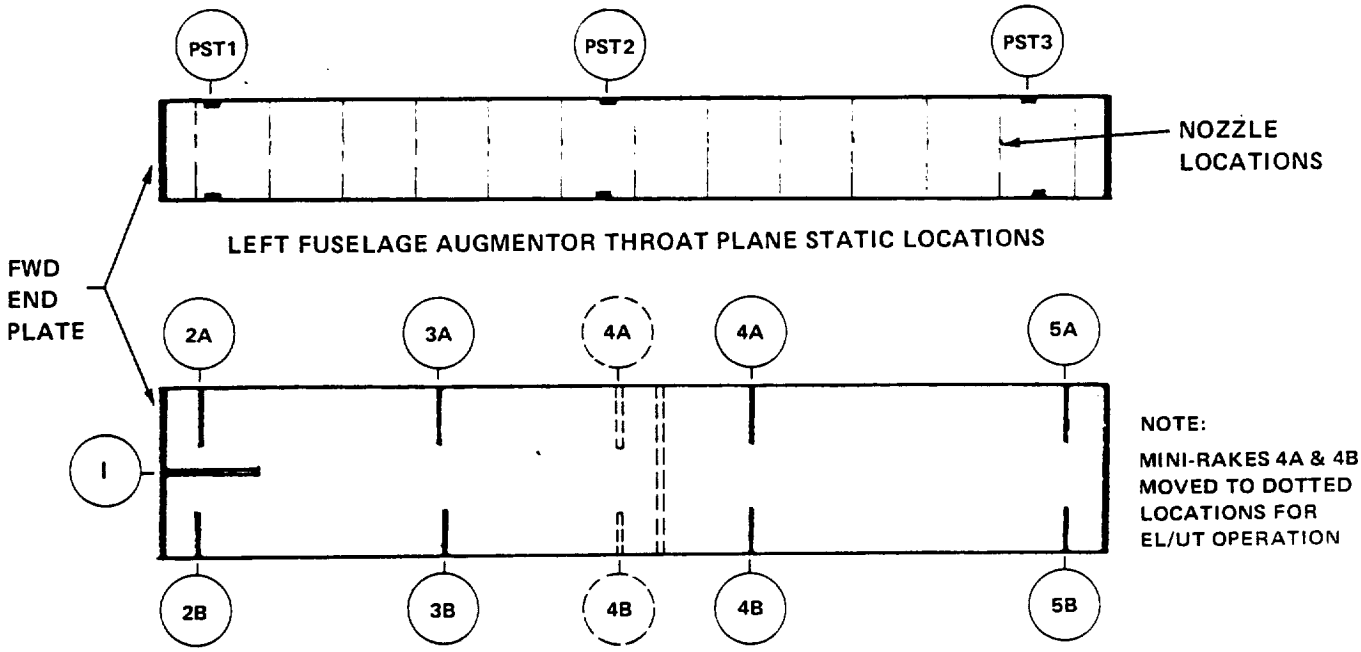

LEFT FUSELAGE AUGMENTOR THROAT PLANE STATIC LOCATIONS

LEFT AUGMENTOR EXIT PLANE – MINI-RAKE LOCATIONS – (PRAKE)

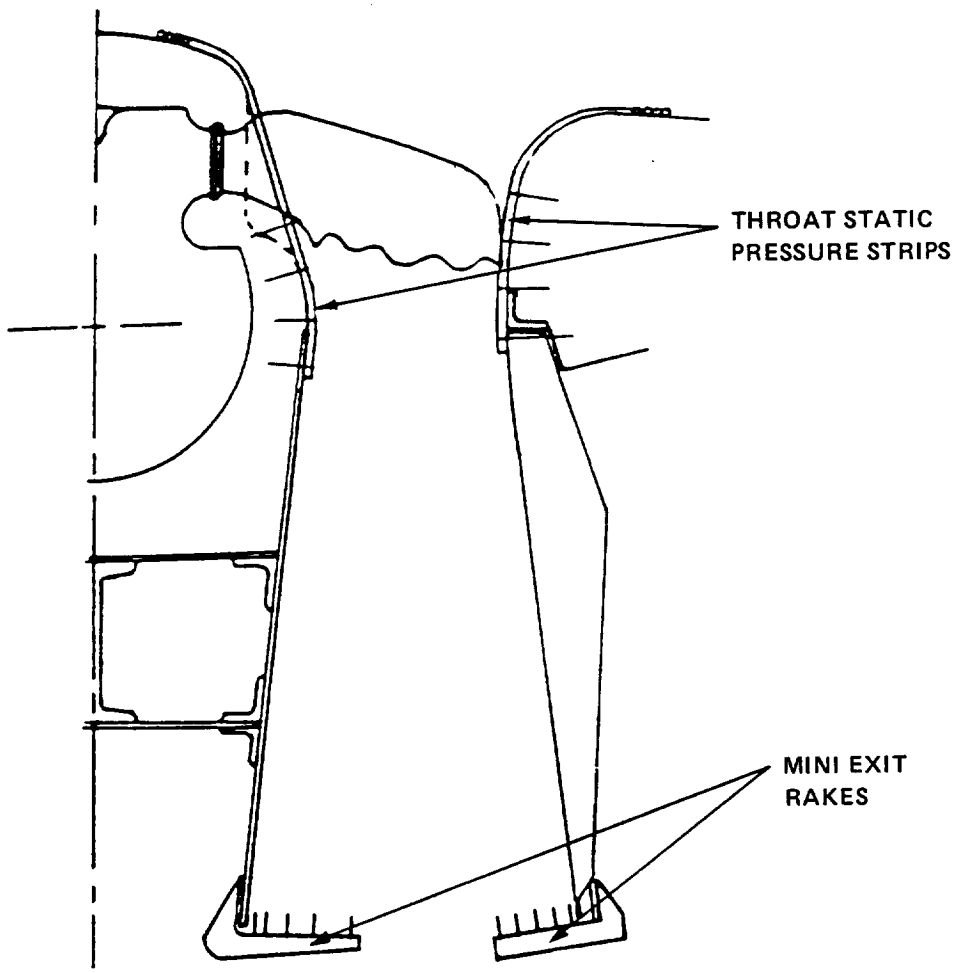

LEFT FUSELAGE AUGMENTOR PRESSURE INSTRUMENTATION

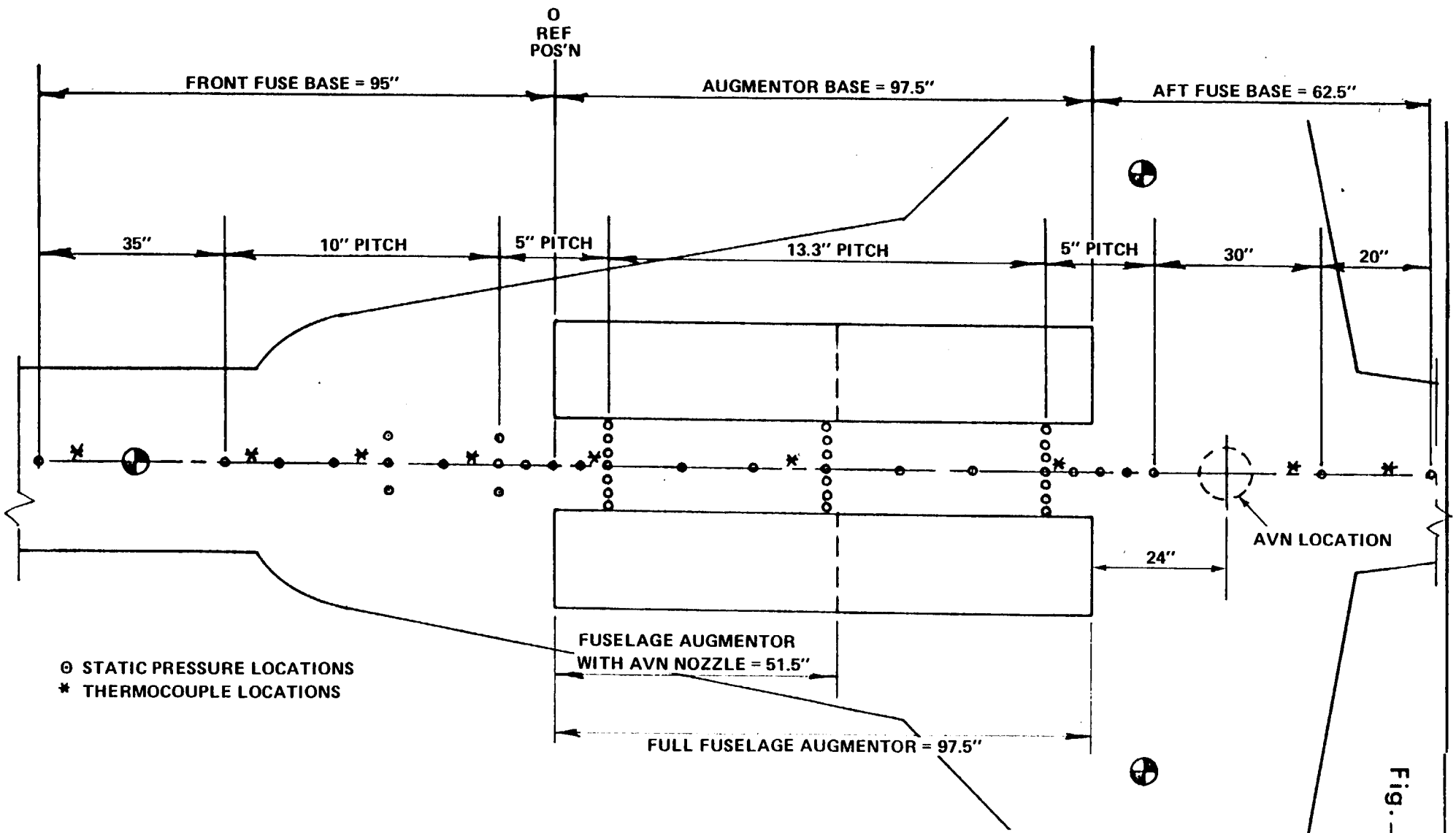

FUSELAGE BASE STATIC PRESSURE TAP AND THERMOCOUPLE LOCATIONS

Fig. 14

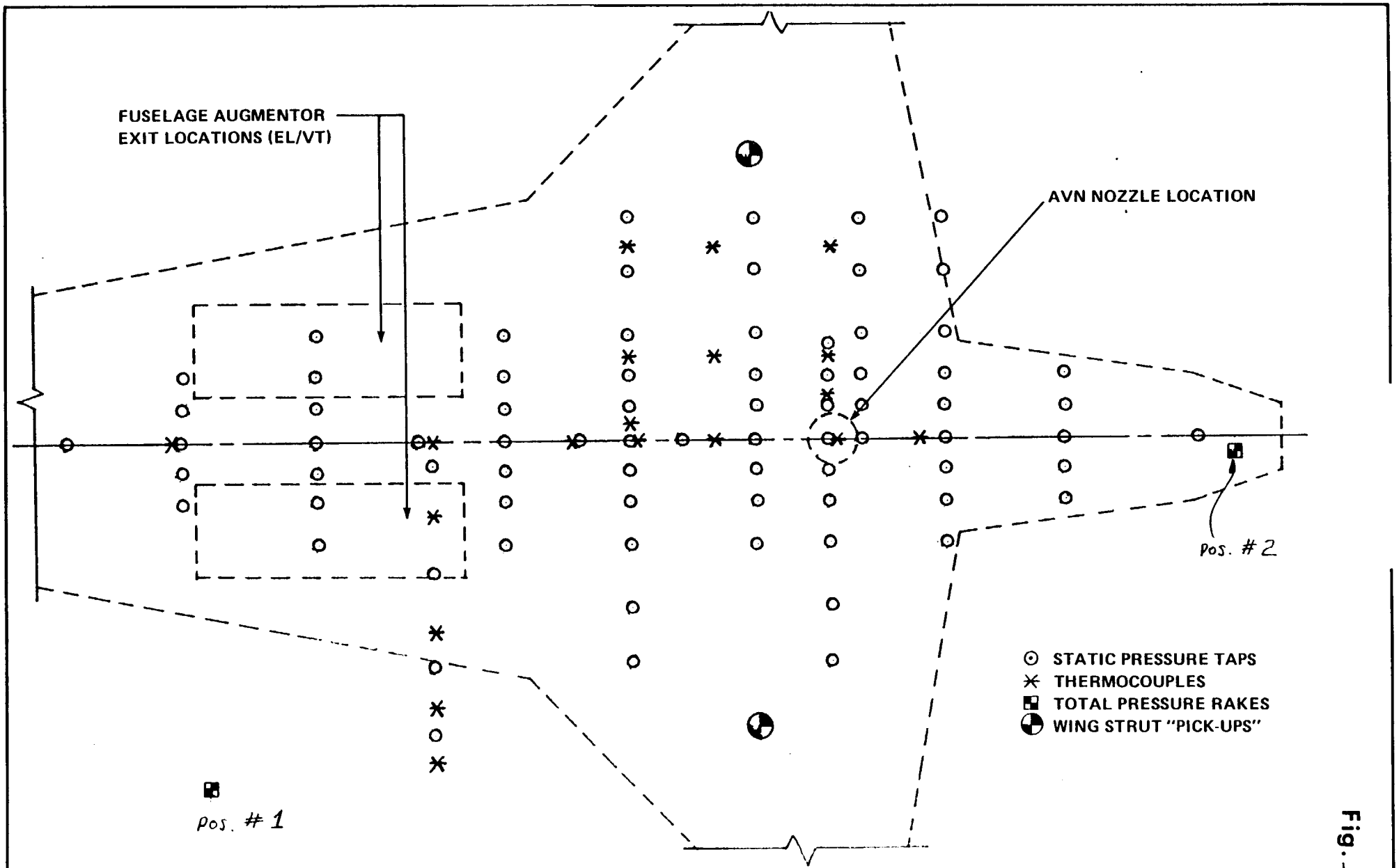

GROUND PLANE INSTRUMENTATION

Fig. 15

Fig. 16

NOTE: PROBES AT W.L. 3.0 & 29.0 ARE THERMOCOUPLES,
REMAINDER ARE TOTAL PRESSURE PROBES.

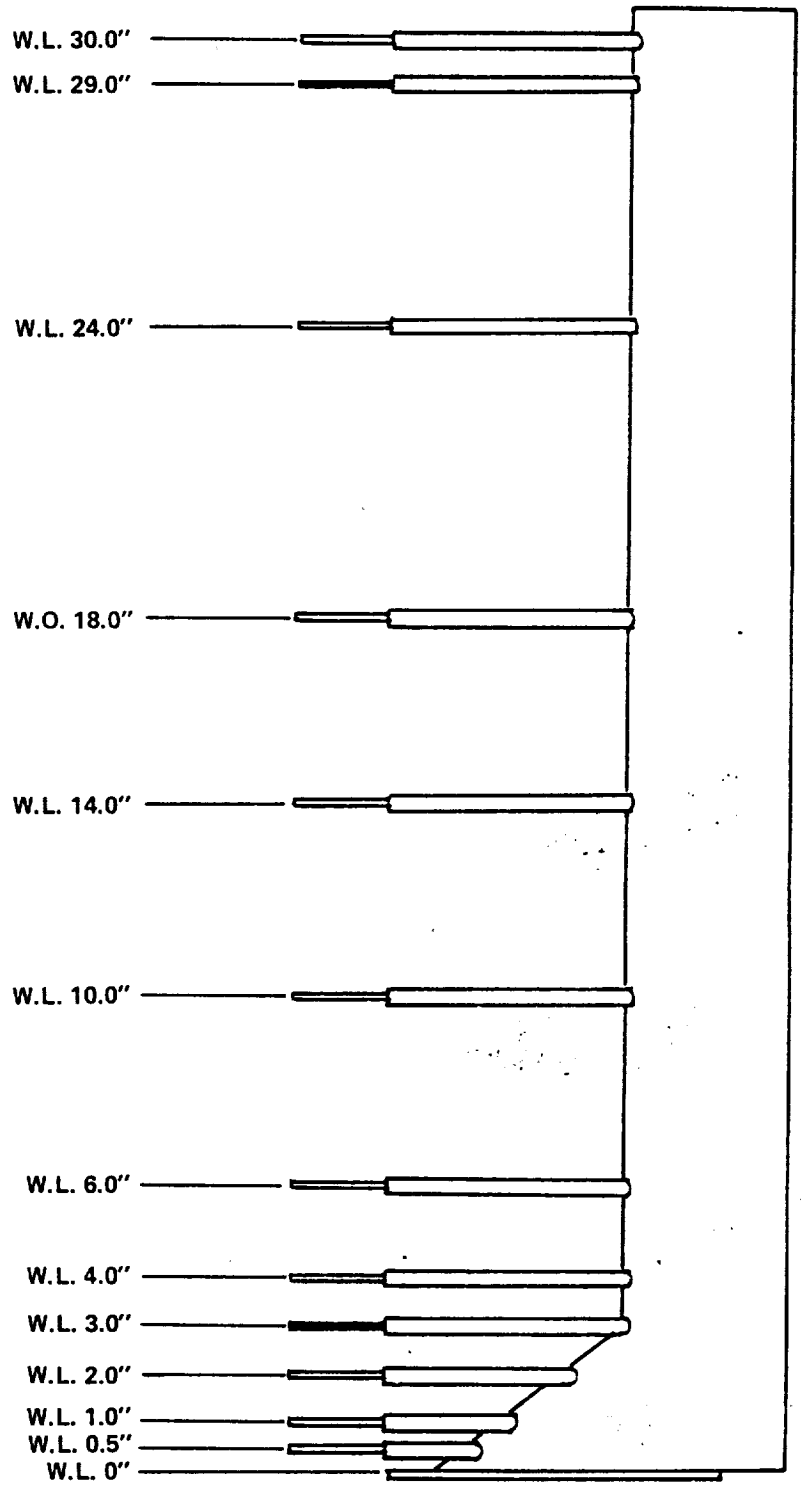

GROUND PLANE RAKE ASSEMBLY (2-OFF)

Fig. 17

VIEW OF J-97 POWERED VTOL MODEL
AT OUTDOOR AERODYNAMICS RESEARCH FACILITY (OARF), AMES RESEARCH CENTER, NASA

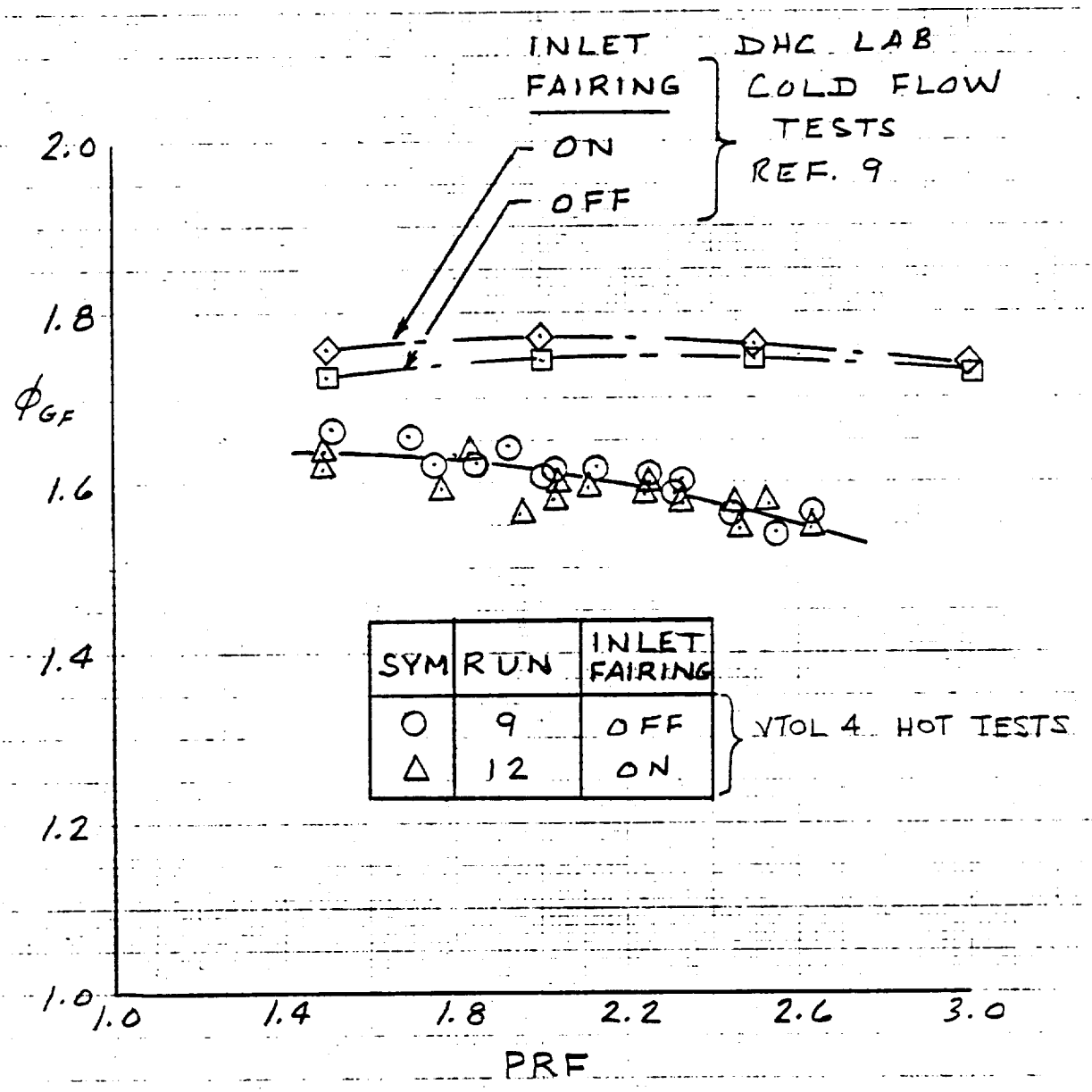

FUSELAGE AUGMENTOR THRUST AUGMENTATION RATIO,
COMPARISON WITH COLD FLOW TESTS; DAR = 1.7; H = 227, RAKE 'ON'

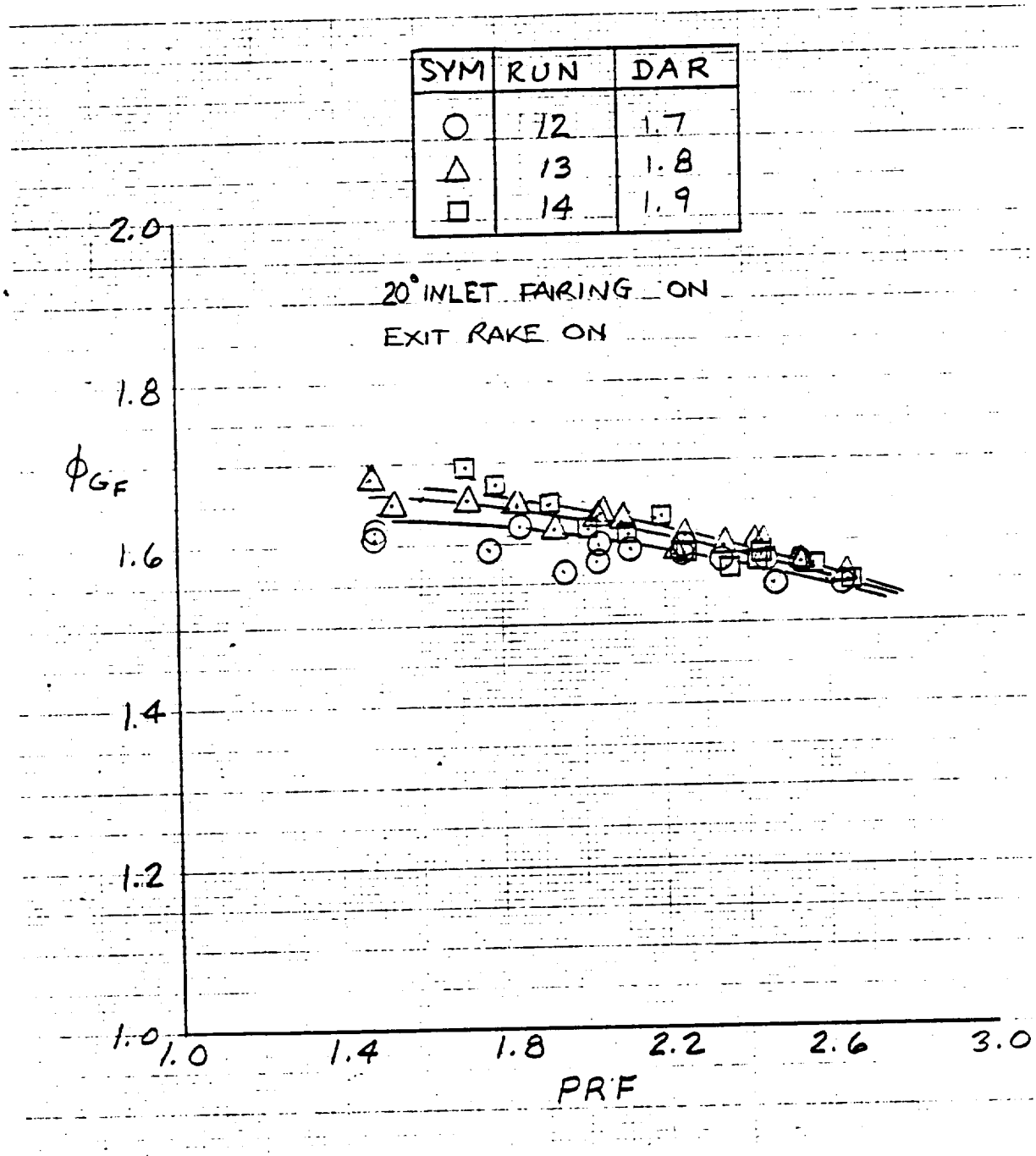

EFFECT OF DAR ON FUSELAGE AUGMENTOR THRUST AUGMENTATION RATIO;
EXIT RAKE ON; H = 227"

Fig. 20

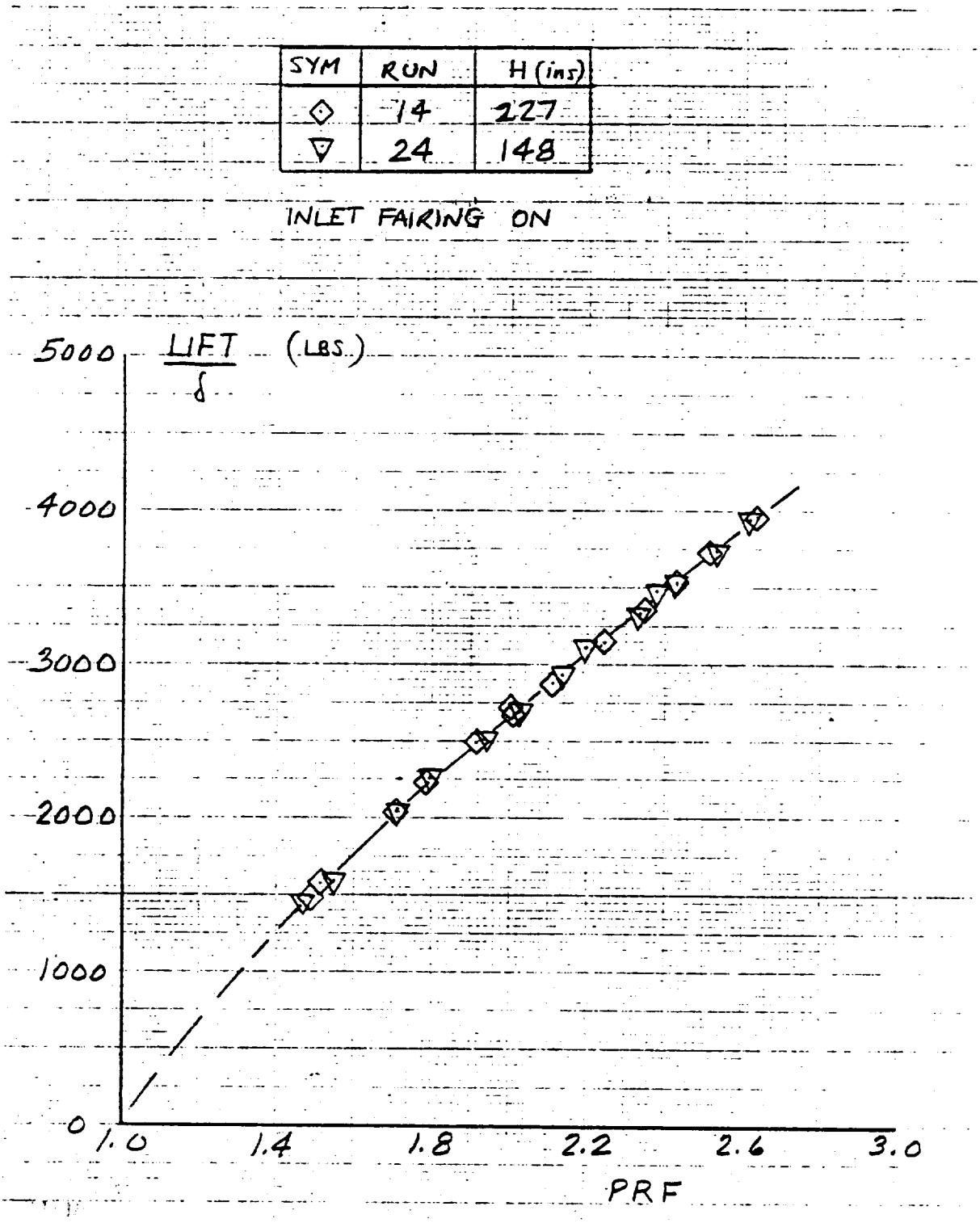

EFFECT OF HEIGHT REDUCTION vs FREE AIR ON LIFT FORCE; DAR = 1.9; EXIT RAKE 'ON'

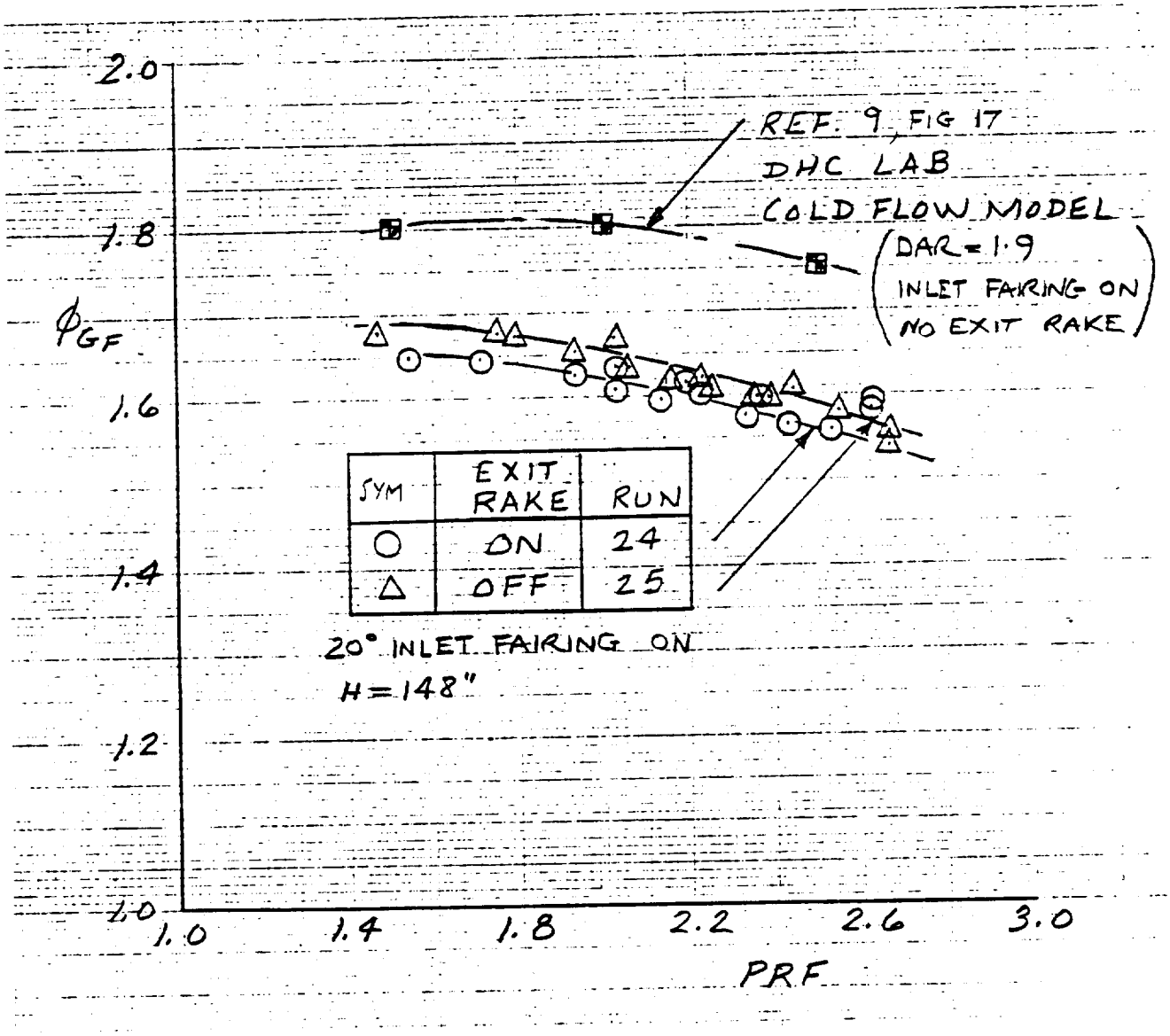

FUSELAGE AUGMENTOR THRUST AUGMENTATION RATIO,
COMPARISON WITH COLD FLOW TESTS; DAR = 1.9

Fig. 22

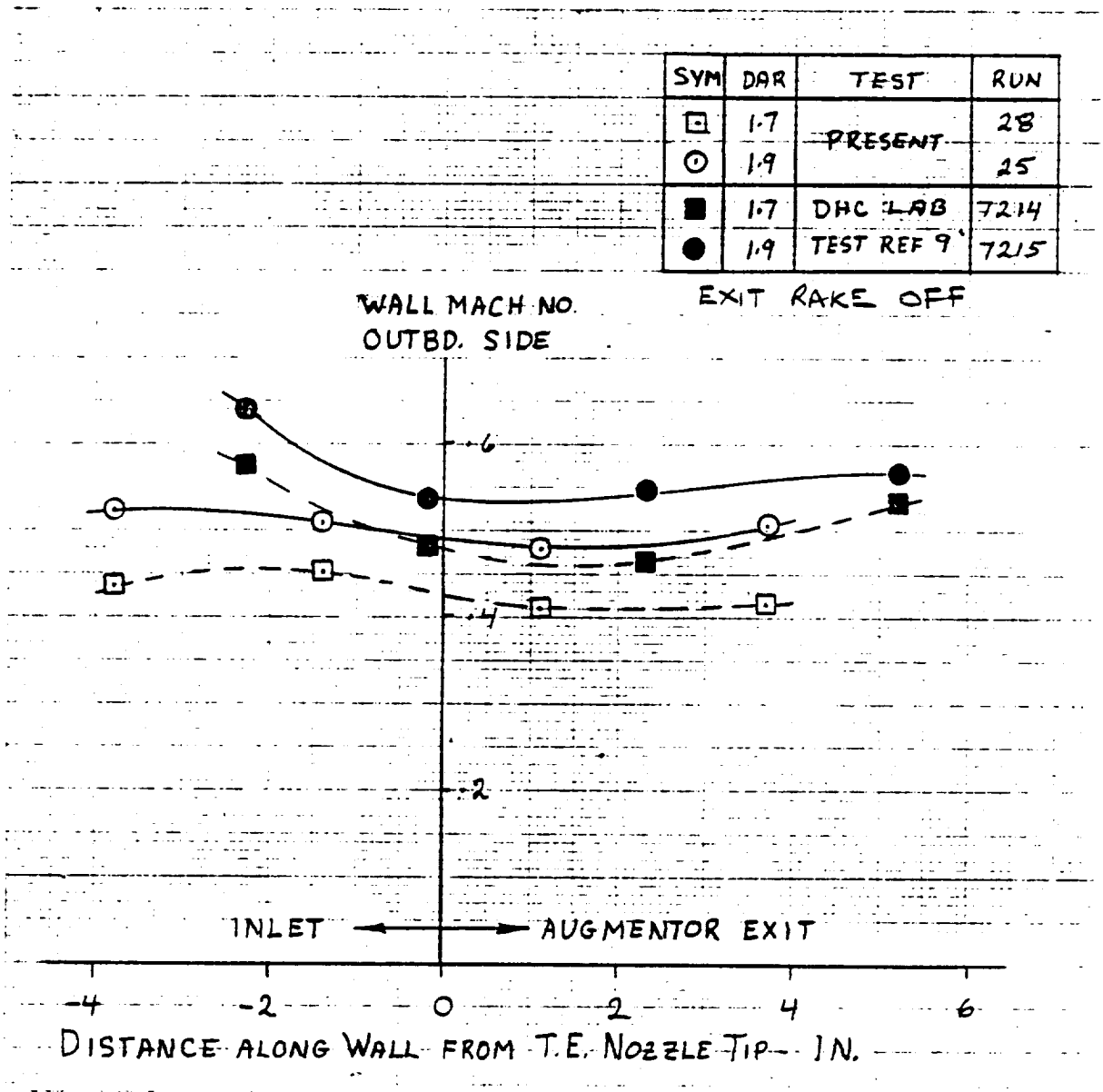

EFFECT OF DAR ON FUSELAGE AUGMENTOR THROAT MACH NO;
PRF = 2.5; INLET FAIRING ON

Fig. 23

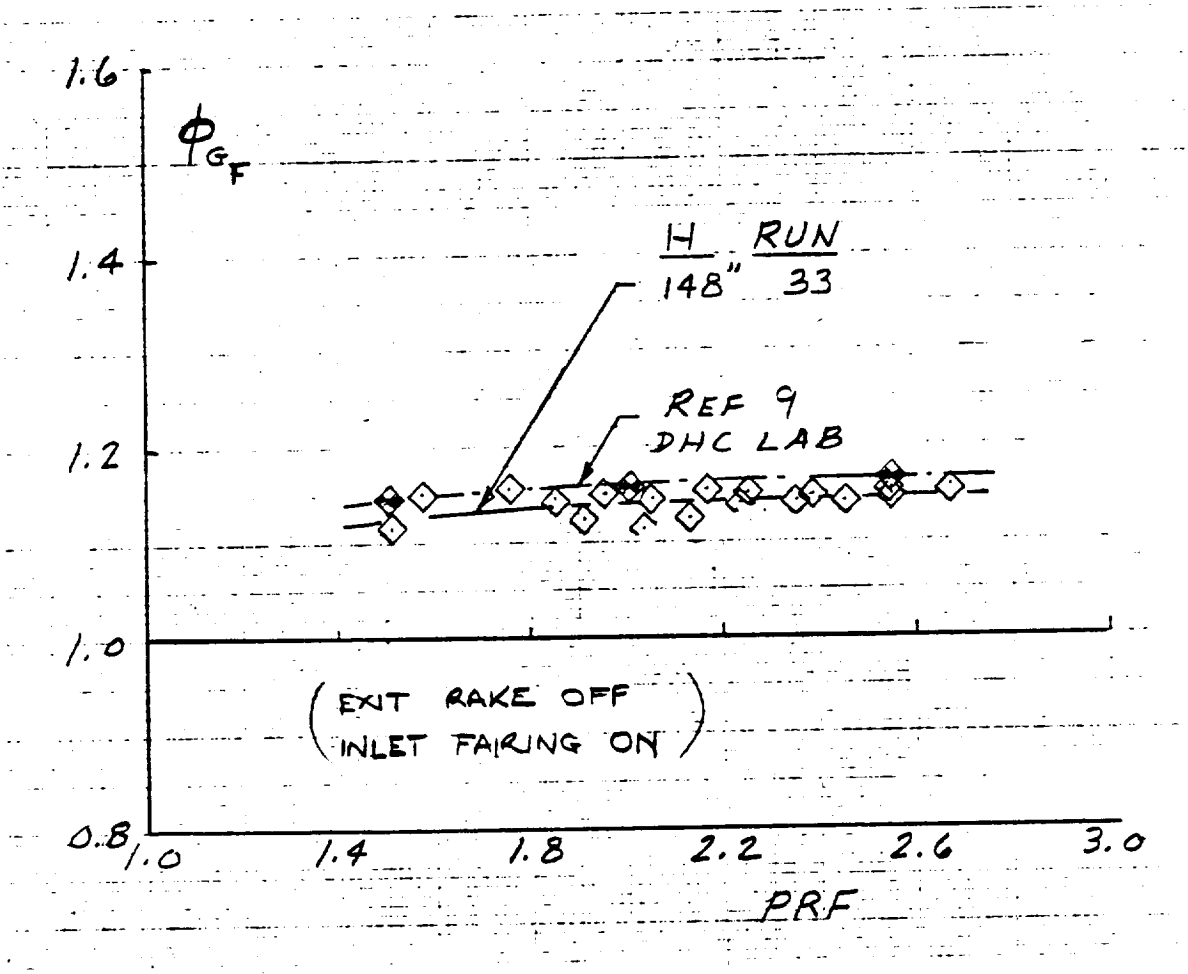

AUGMENTOR PERFORMANCE WITH DOORS OFF,
COMPARISON WITH COLD FLOW TEST RESULT

Fig. 24

ORIGINAL PAGE IS
OF POOR QUALITY

SYM	FAUG	TRIM NOZZLE	WING BLOWING	VENTRAL NOZZLE	TOTAL A_{EFF} (in^2) PRF=2.5
○	1.0	4.8"	ON	OFF	124
△	1.0	2.8"	ON	OFF	115
□	0.538	9.46"	OFF	OFF	116
◇	0.538	2.8"	OFF	ON	120

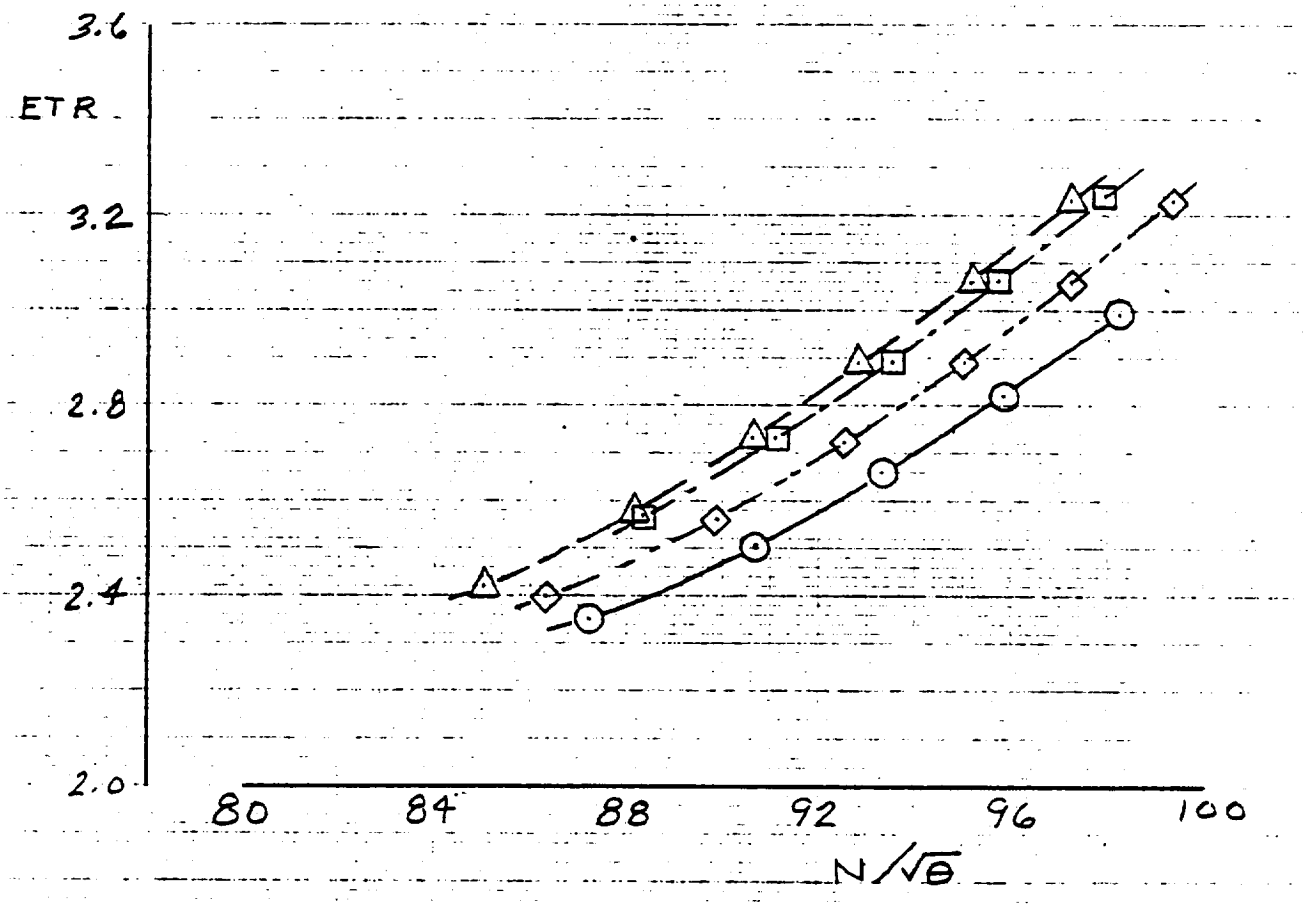

EFFECT OF TOTAL NOZZLE AREA ON J97 RUNNING LINE

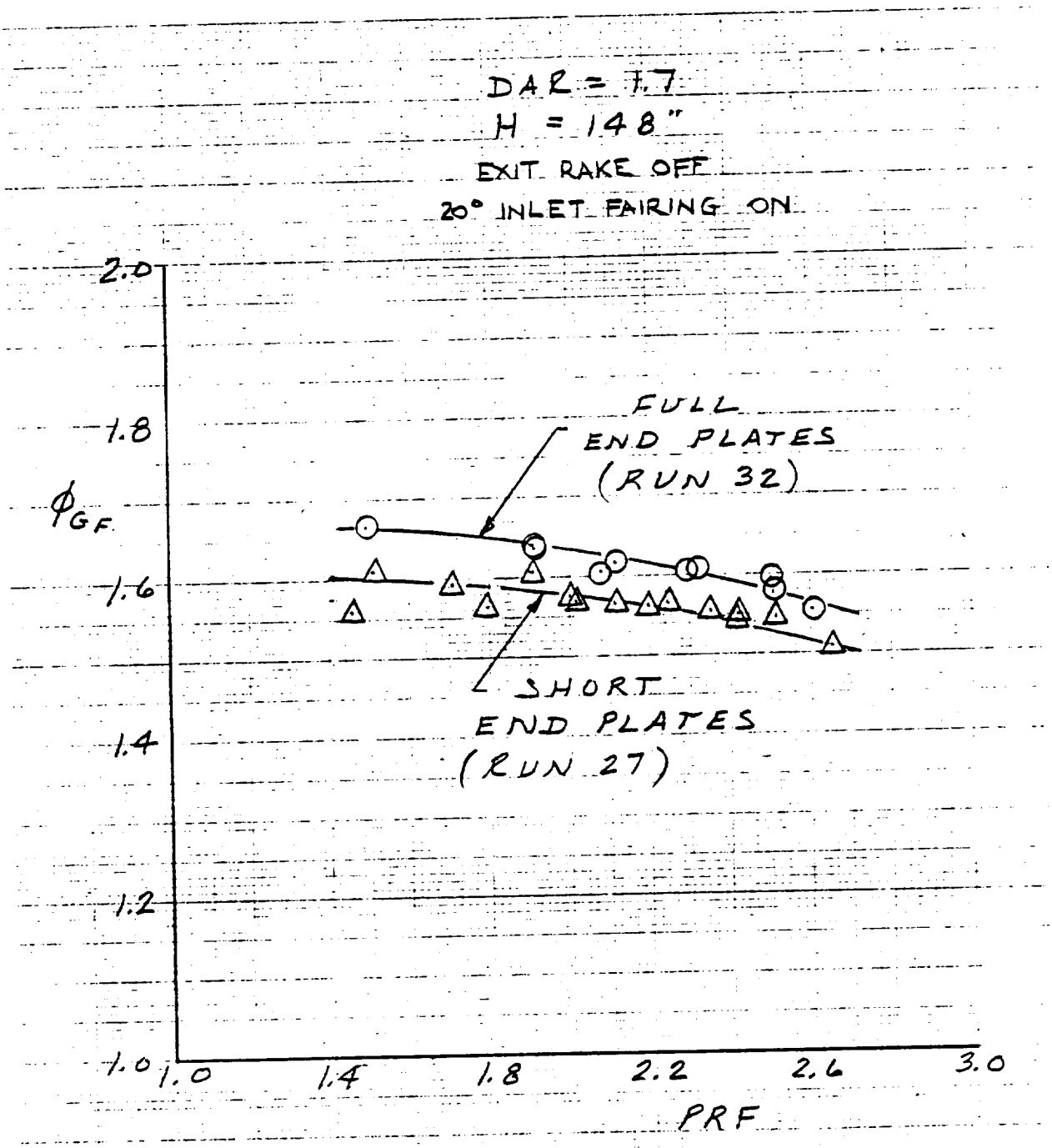

EFFECT OF FUSELAGE AUGMENTOR END PLATE LENGTH ON THRUST AUGMENTATION

Fig. 26

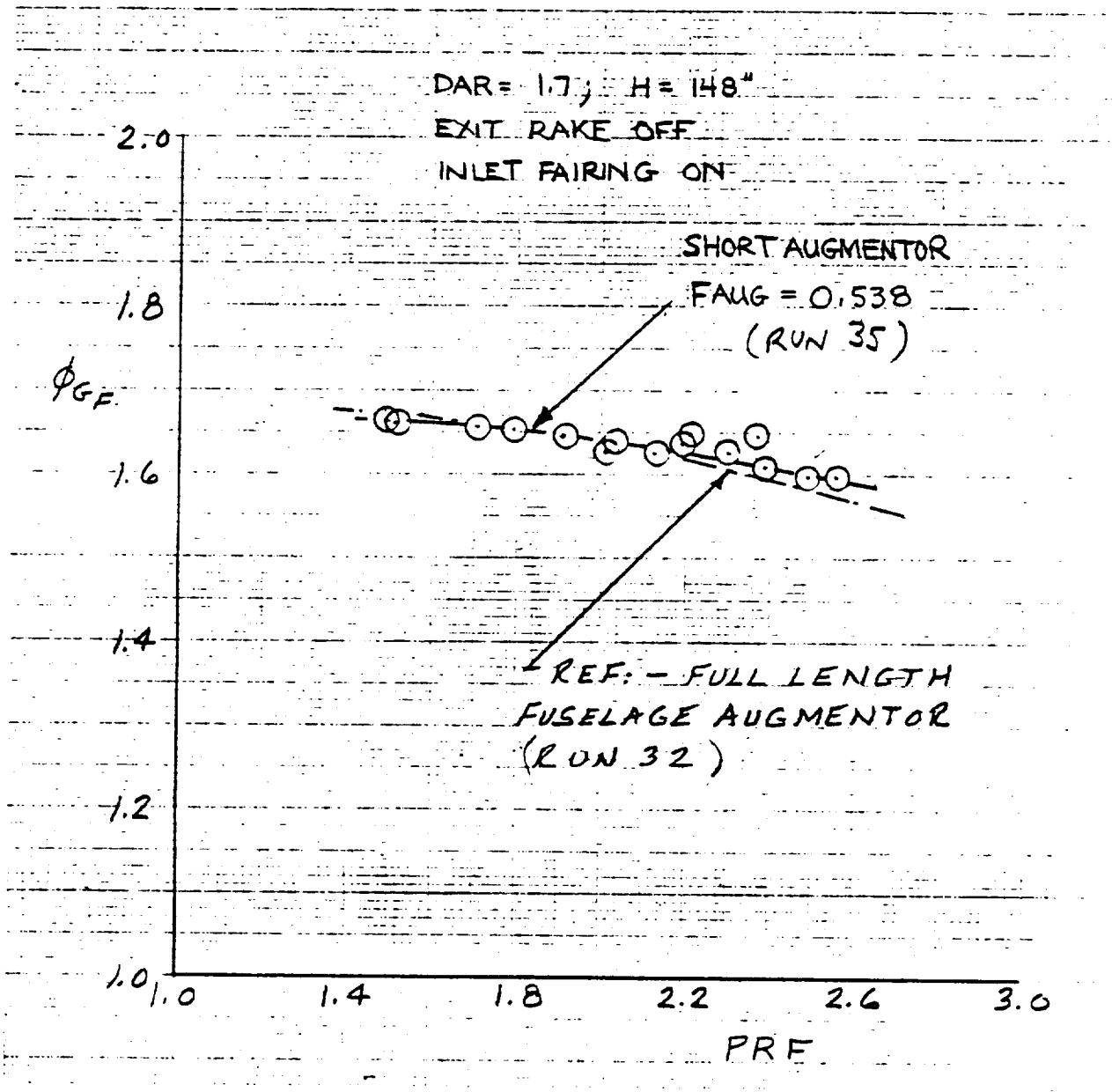

EFFECT OF CHORDWISE LENGTH ON AUGMENTOR PERFORMANCE

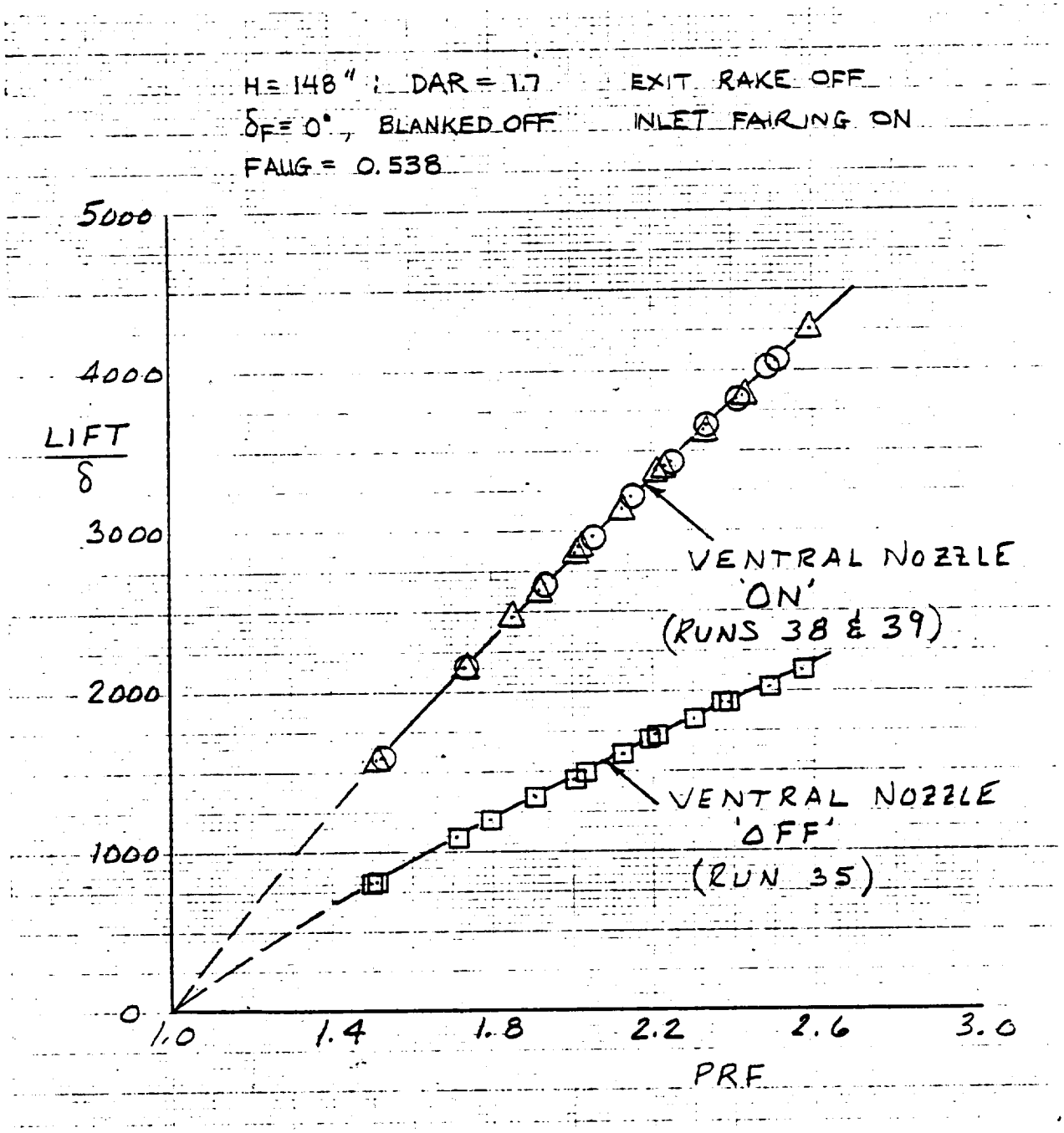

EFFECT OF AFT VENTRAL NOZZLE ON TOTAL LIFT FORCE

Fig. 28

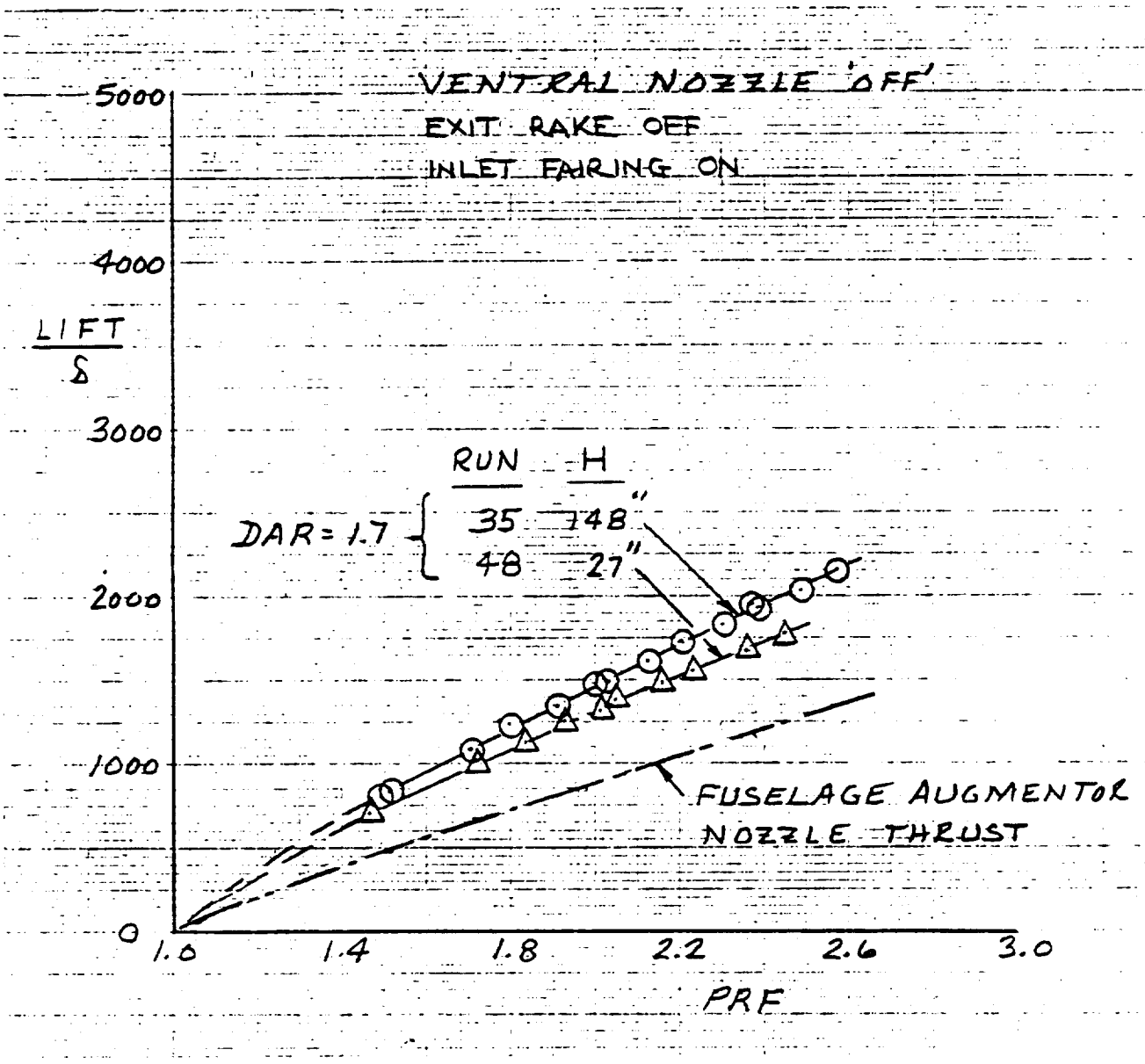

ORIGINAL PAGE IS
OF POOR QUALITY

EFFECT OF HEIGHT ABOVE GROUND ON TOTAL LIFT FORCE;
REDUCED LENGTH FUSELAGE AUGMENTOR (FAUG = .538)

Fig. 29

ORIGINAL PAGE IS
OF POOR QUALITY

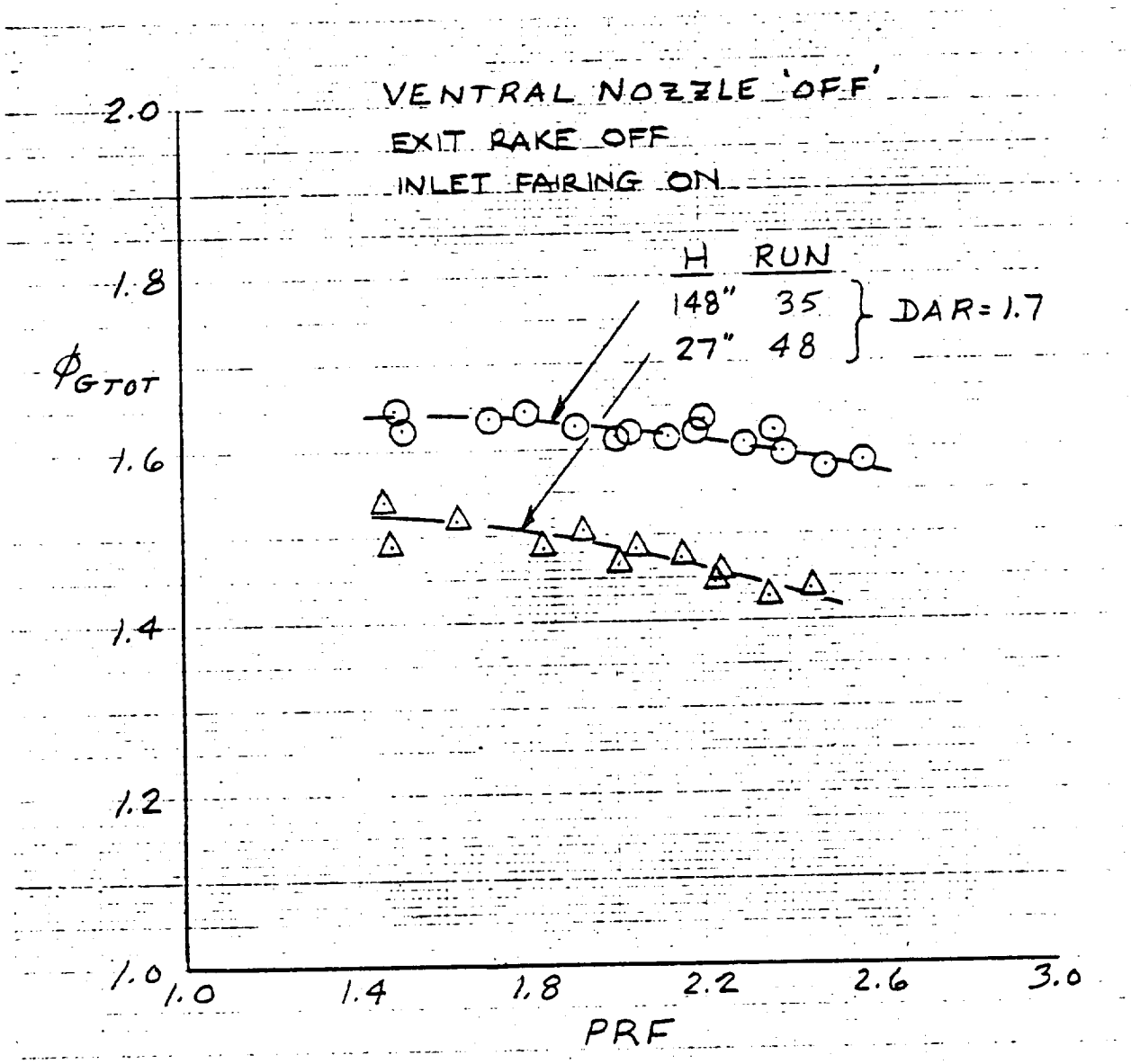

EFFECT OF HEIGHT ABOVE GROUND ON TOTAL THRUST AUGMENTATION RATIO;
REDUCED LENGTH FUSELAGE (FAUG = .538)

Fig. 30

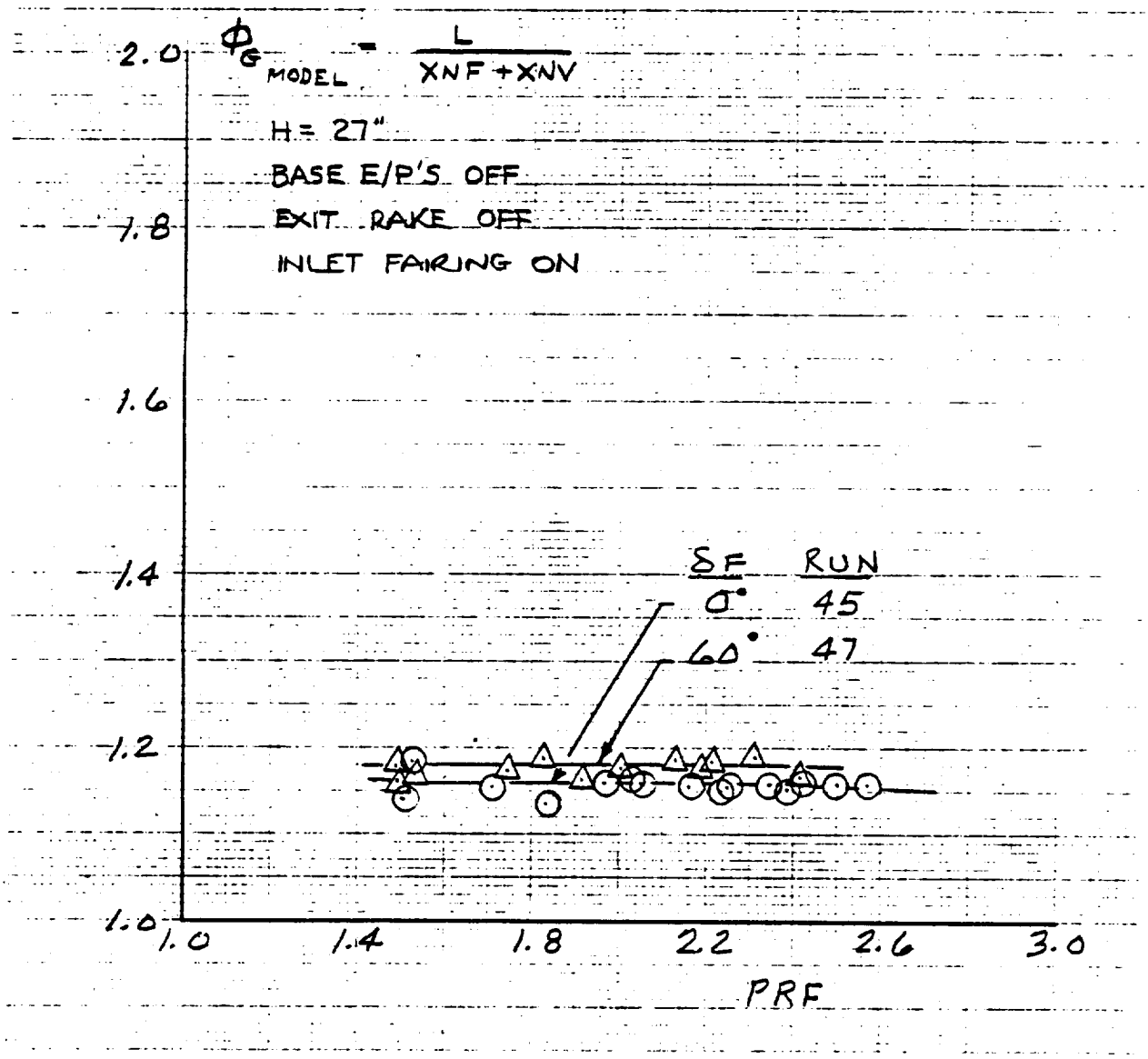

EFFECT OF FLAP DEFLECTION (UNBLOWN) ON TOTAL THRUST AUGMENTATION; REDUCED LENGTH FUSELAGE AUGMENTOR (FAUG = .538); VENTRAL NOZZLE 'ON'

ORIGINAL PAGE IS
OF POOR QUALITY

Fig. 31

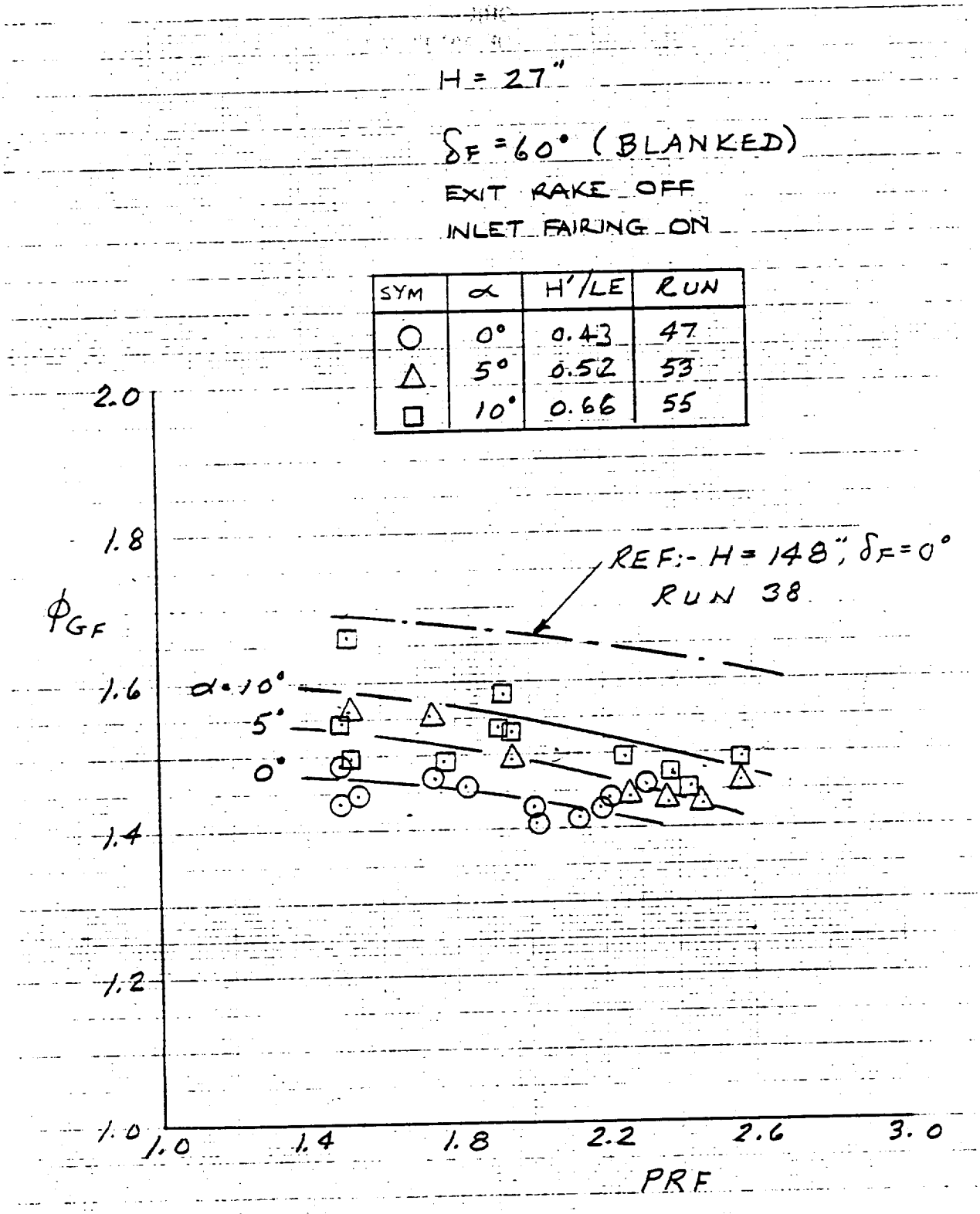

EFFECT OF PITCH ANGLE ON FUSELAGE AUGMENTOR THRUST AUGMENTATION RATIO; REDUCED LENGTH FUSELAGE AUGMENTOR (FAUG = .538), VENTRAL NOZZLE 'ON'; H = 27", δ_F = 60° (UNBLOWN)

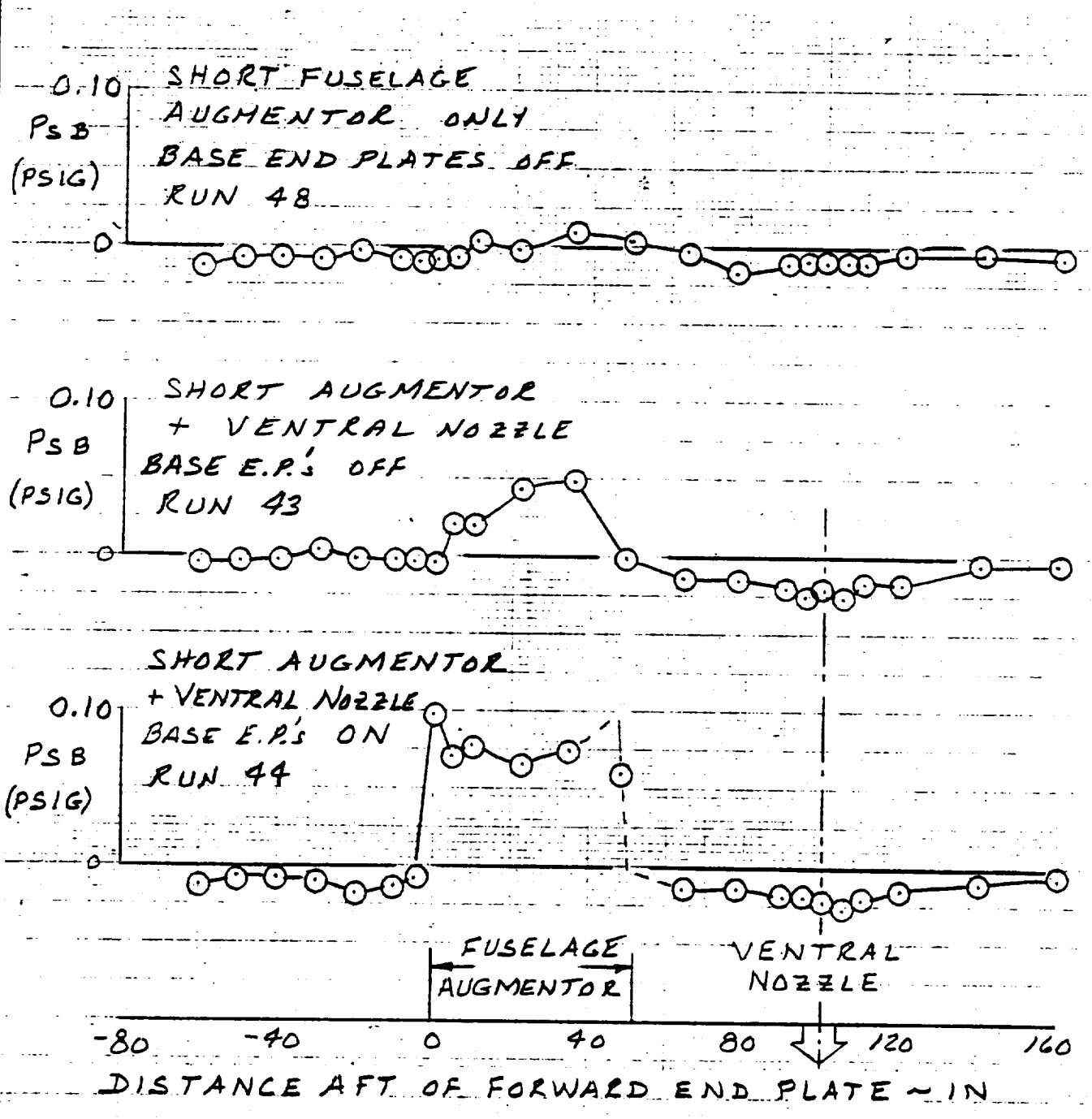

EFFECT OF VENTRAL NOZZLE AND BASE END PLATES ON FUSELAGE C_L BASE PRESSURE;
H = 27", PRF = 2.0, $\delta_F = 0^o$ (UNBLOWN)

Fig. 33

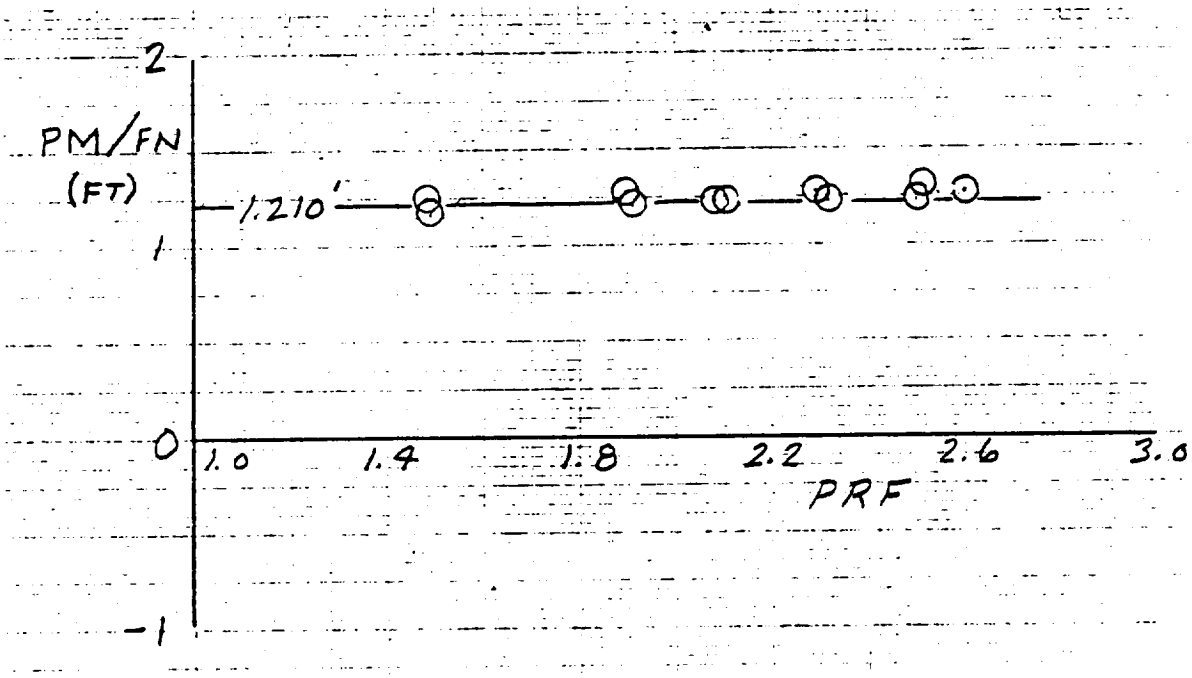

PITCHING MOMENT vs PRF; FULL LENGTH FUSELAGE AUGMENTOR; DAR = 1.7;
H = 148"; $\delta_F = 0^o$; RUN 32

Fig. 34

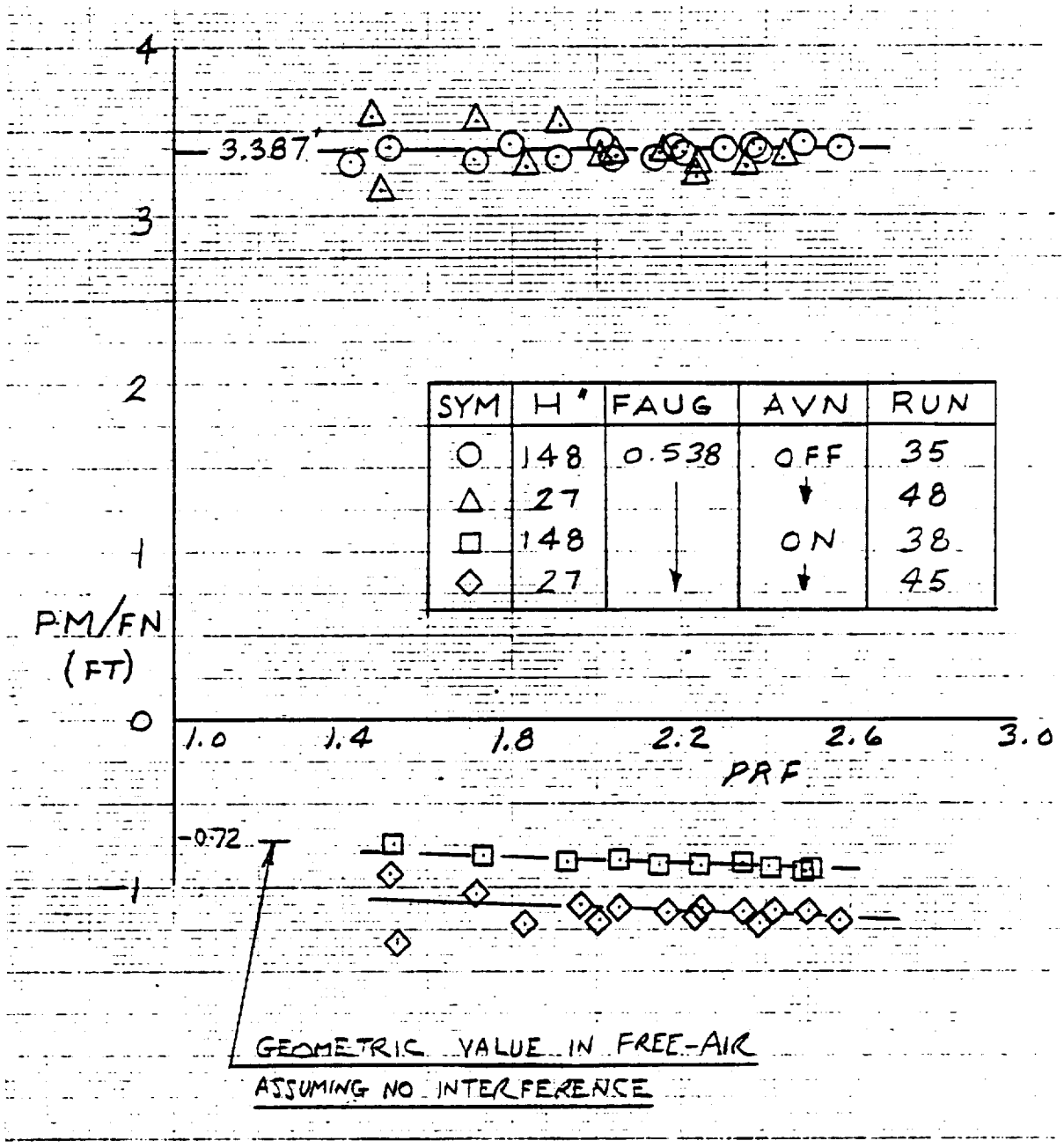

EFFECT OF HEIGHT ABOVE GROUND ON PITCHING MOMENT, REDUCED FUSELAGE AUGMENTOR LENGTH (FAUG = .538), WITH AND WITHOUT VENTRAL NOZZLE; DAR = 1.7; $\delta_F = 0^o$ (UNBLOWN)

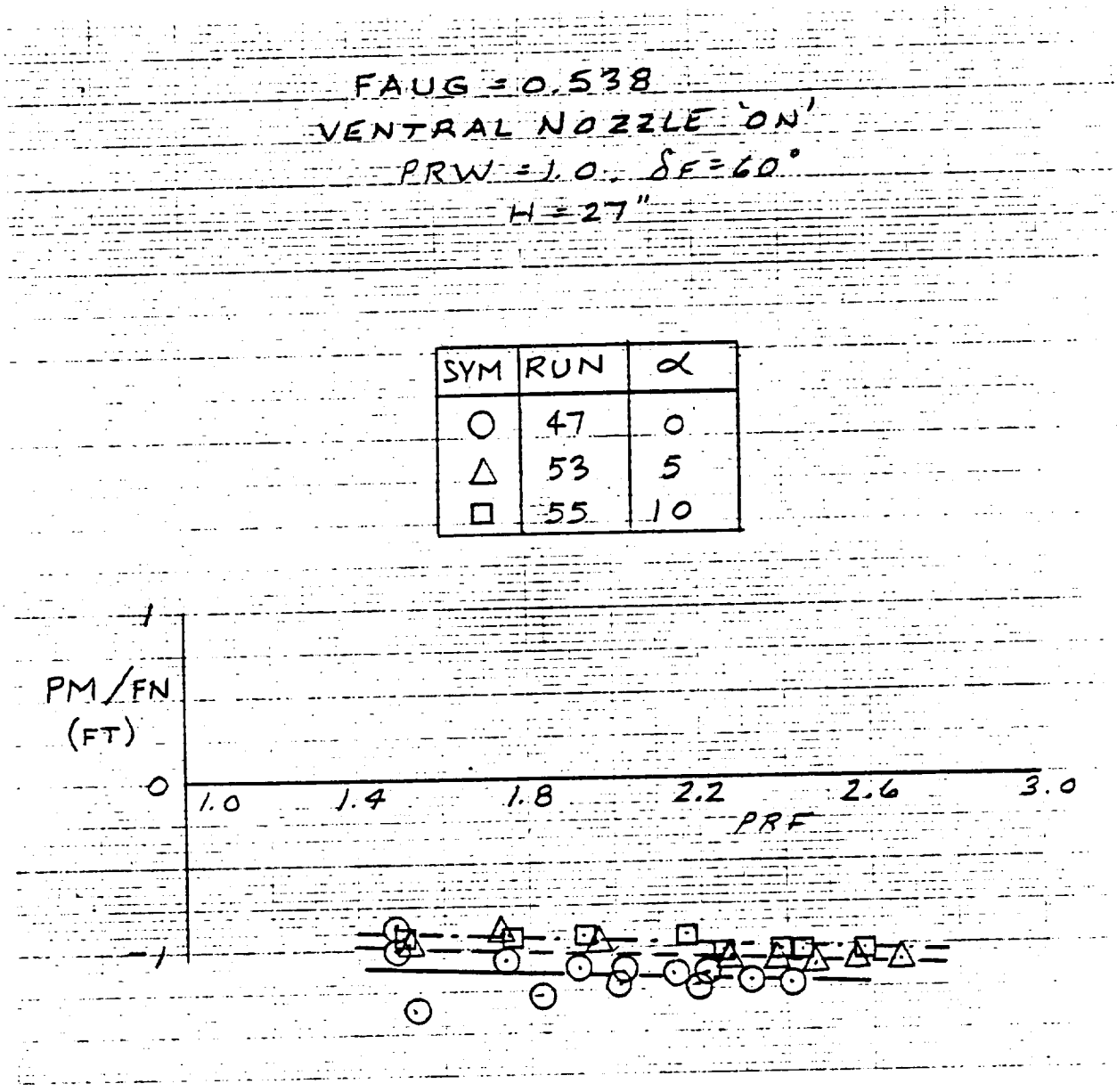

EFFECT OF PITCH ANGLE ON PITCHING MOMENT, REDUCED FUSELAGE AUGMENTOR LENGTH (FAUG = .538), VENTRAL NOZZLE 'ON'; H = 27"; δ_F = 60° (UNBLOWN)

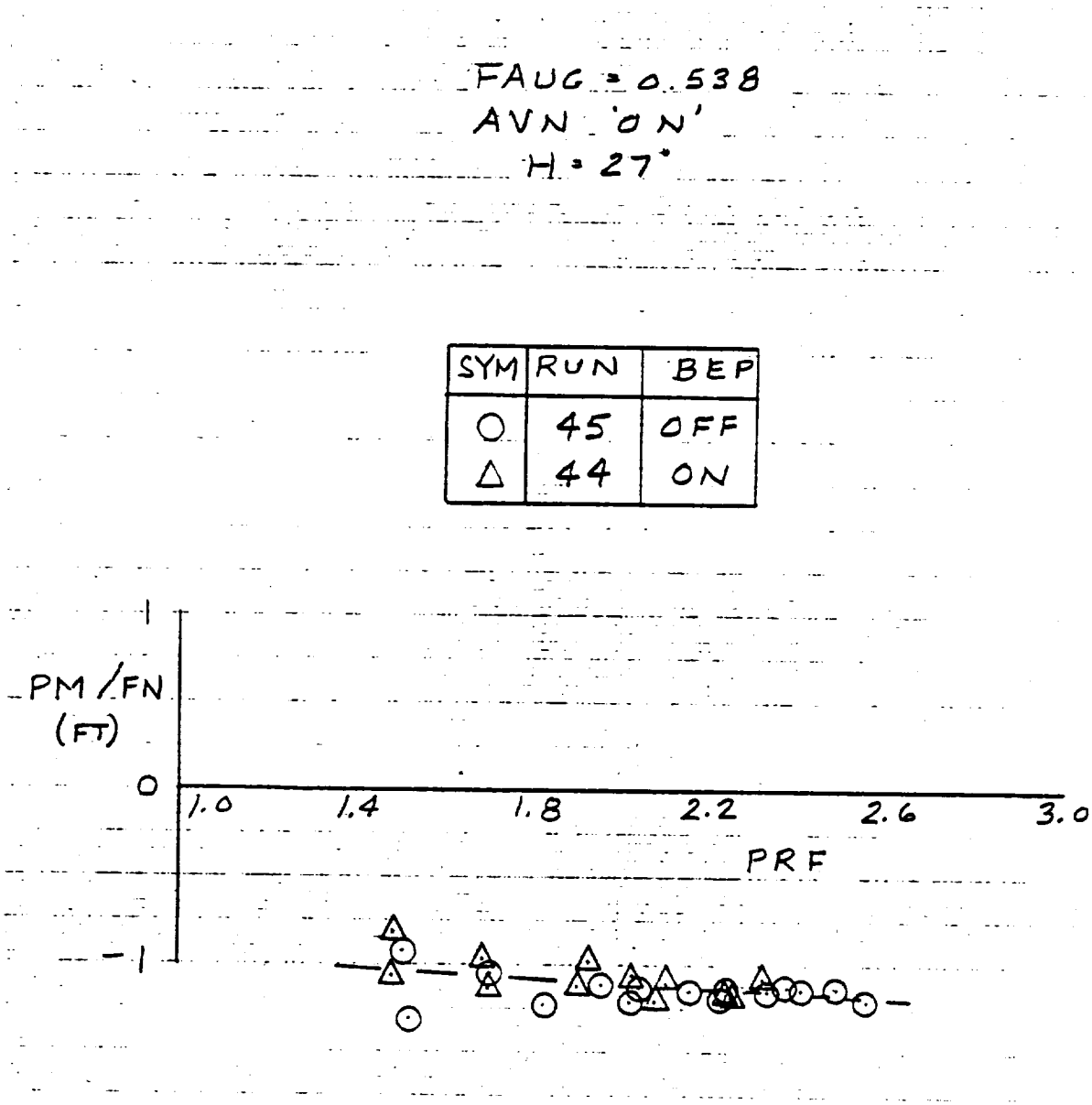

EFFECT OF BASE END PLATES ON PITCHING MOMENT; REDUCED FUSELAGE AUGMENTOR LENGTH (FAUG = .538); VENTRAL NOZZLE 'ON'; H = 27"; $\delta_F = 0^o$ (UNBLOWN)

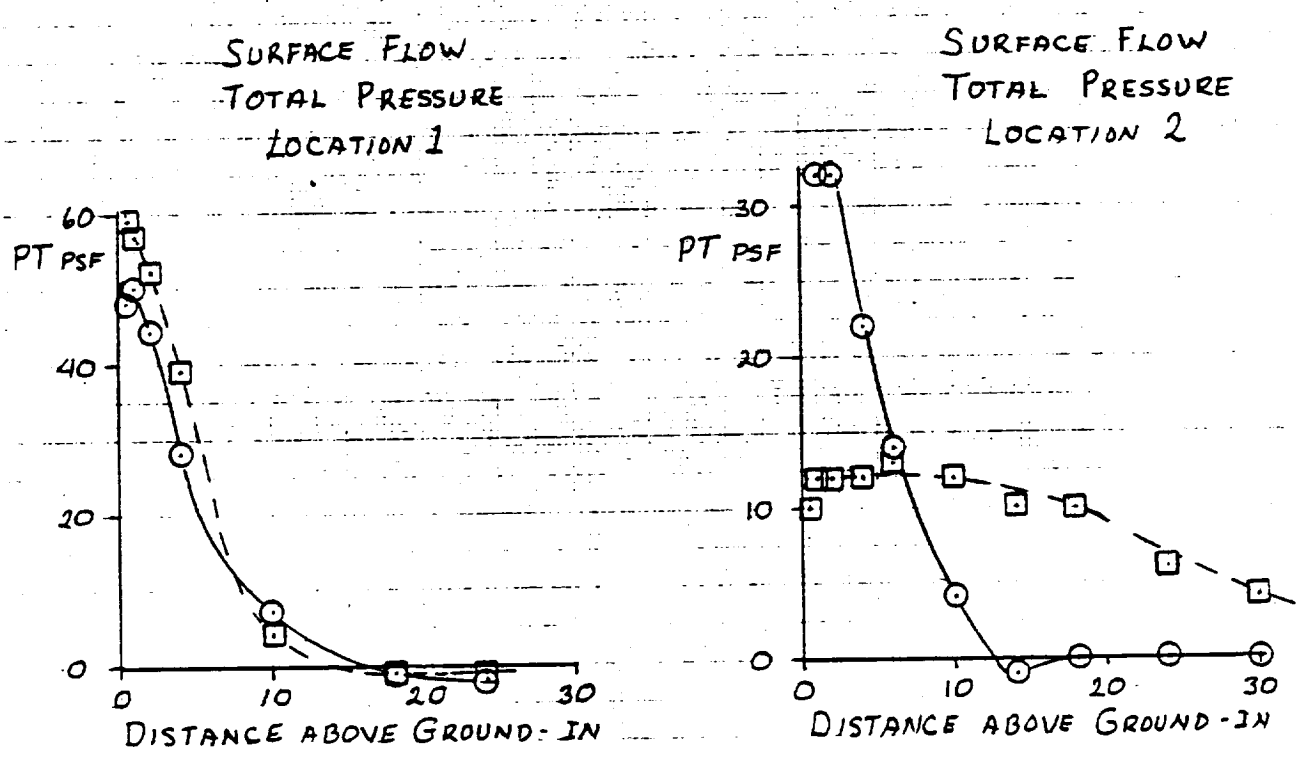

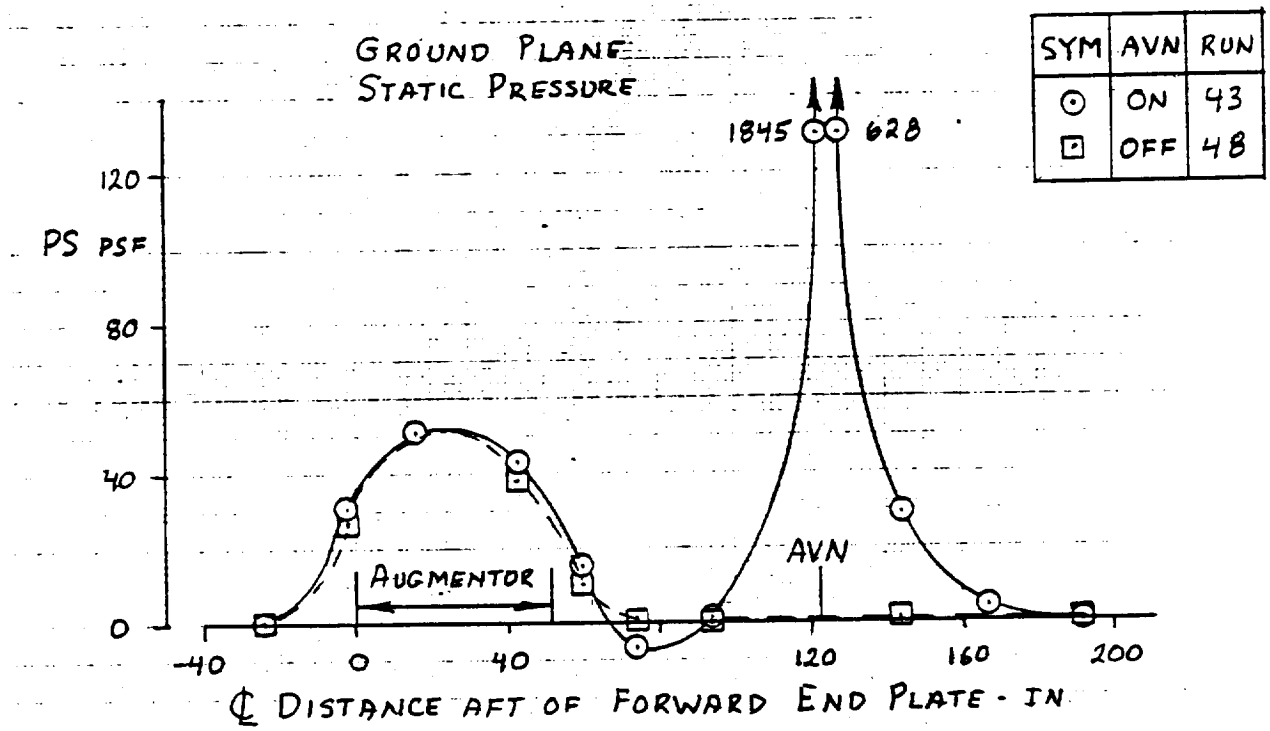

EFFECT OF VENTRAL NOZZLE ON GROUND PLANE FLOW; REDUCED FUSELAGE AUGMENTOR LENGTH (FAUG = .538); H = 27"; PRF = 2.0; $\delta_F = 0^o$ (UNBLOWN)

Fig. 37(b)

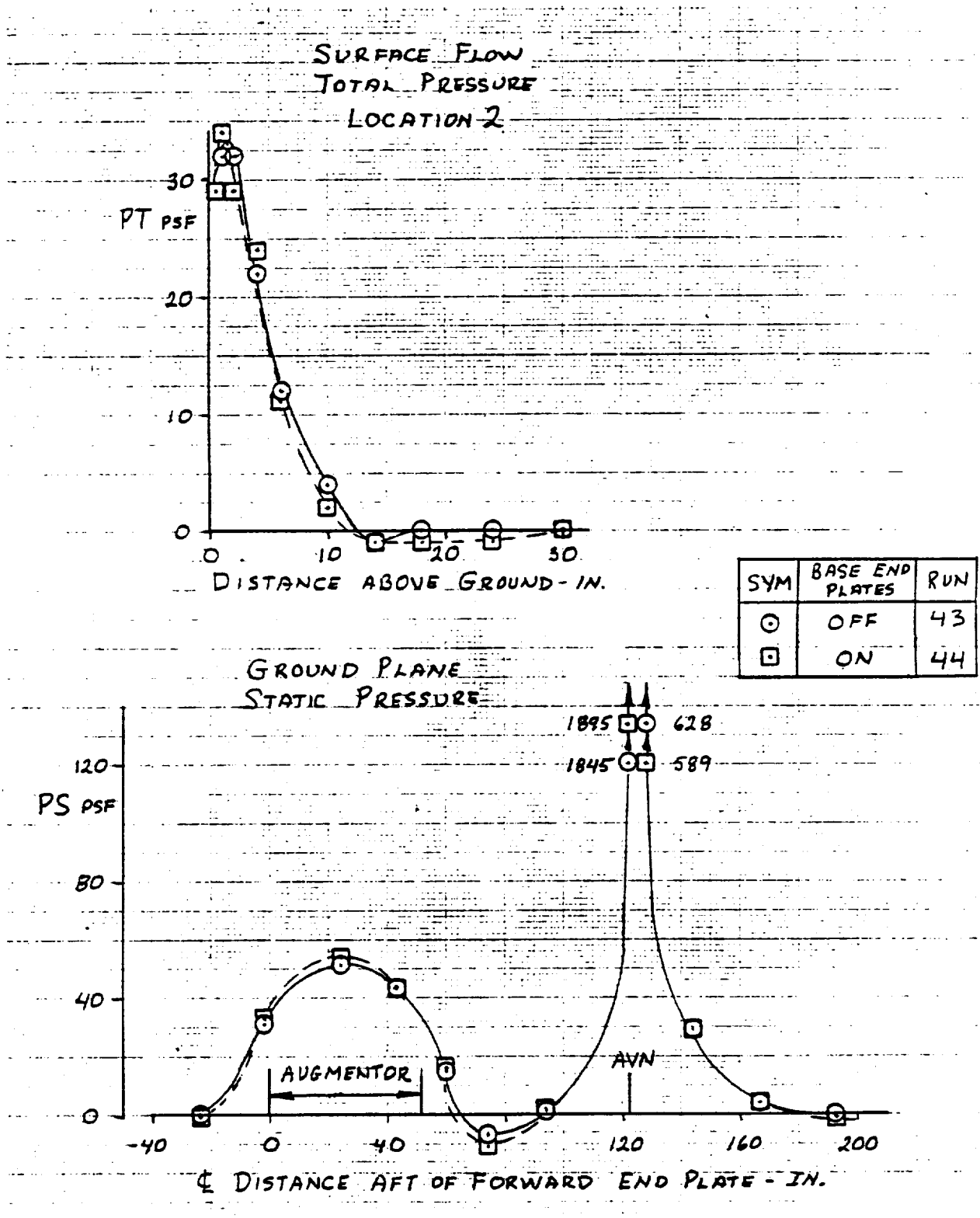

EFFECT OF BASE END PLATES ON GROUND PLANE FLOW; REDUCED FUSELAGE AUGMENTOR LENGTH (FAUG = .538); VENTRAL NOZZLE 'ON'; H = 27"; PRF = 2.0; $\delta_F = 0^o$ (UNBLOWN)

Fig. 37(c)

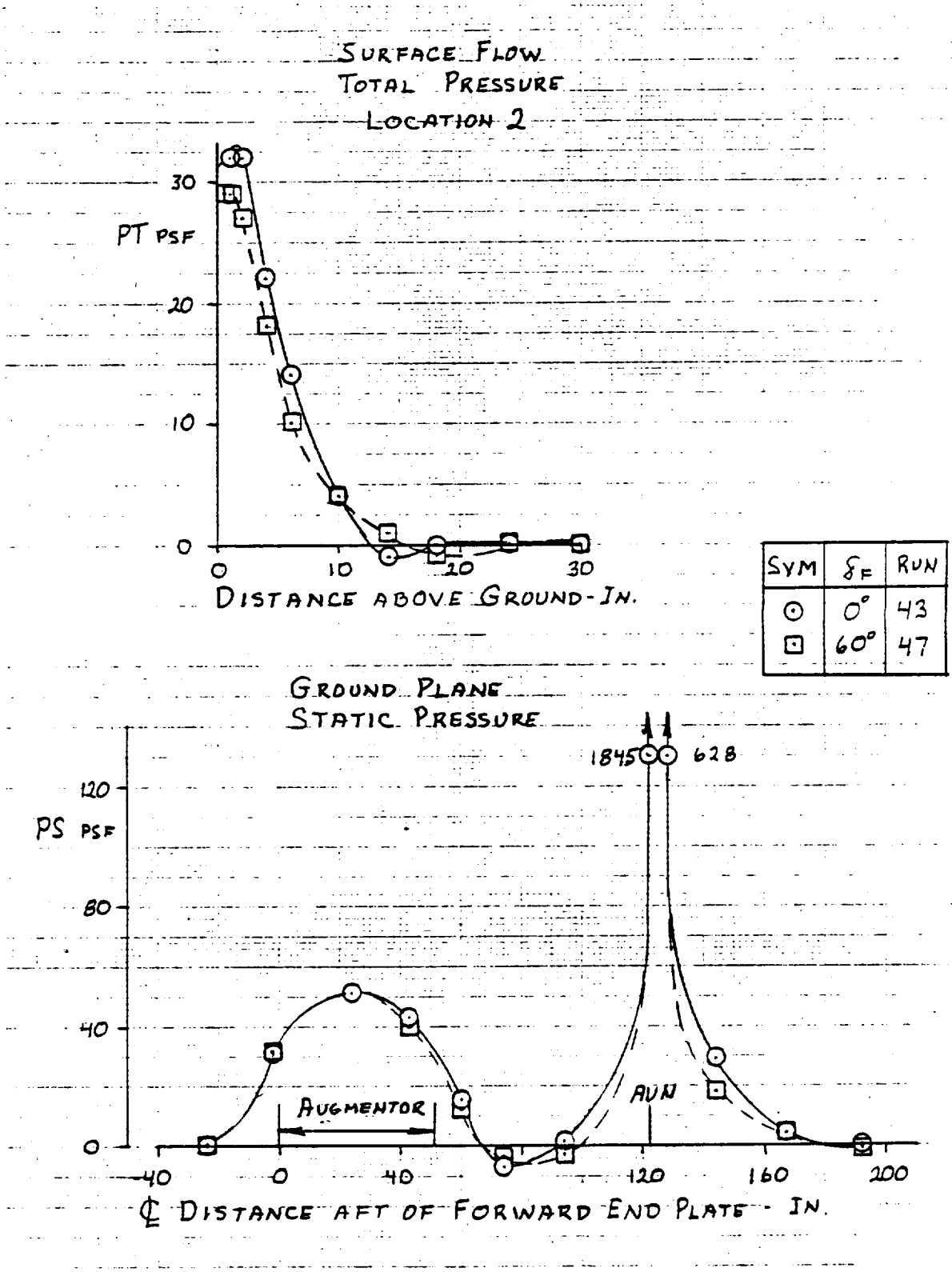

EFFECT OF FLAP ANGLE ON GROUND PLANE FLOW;
REDUCED FUSELAGE AUGMENTOR LENGTH (FAUG = .538);
VENTRAL NOZZLE 'ON'; H = 27"; PRF = 2.0; FLAP UNBLOWN

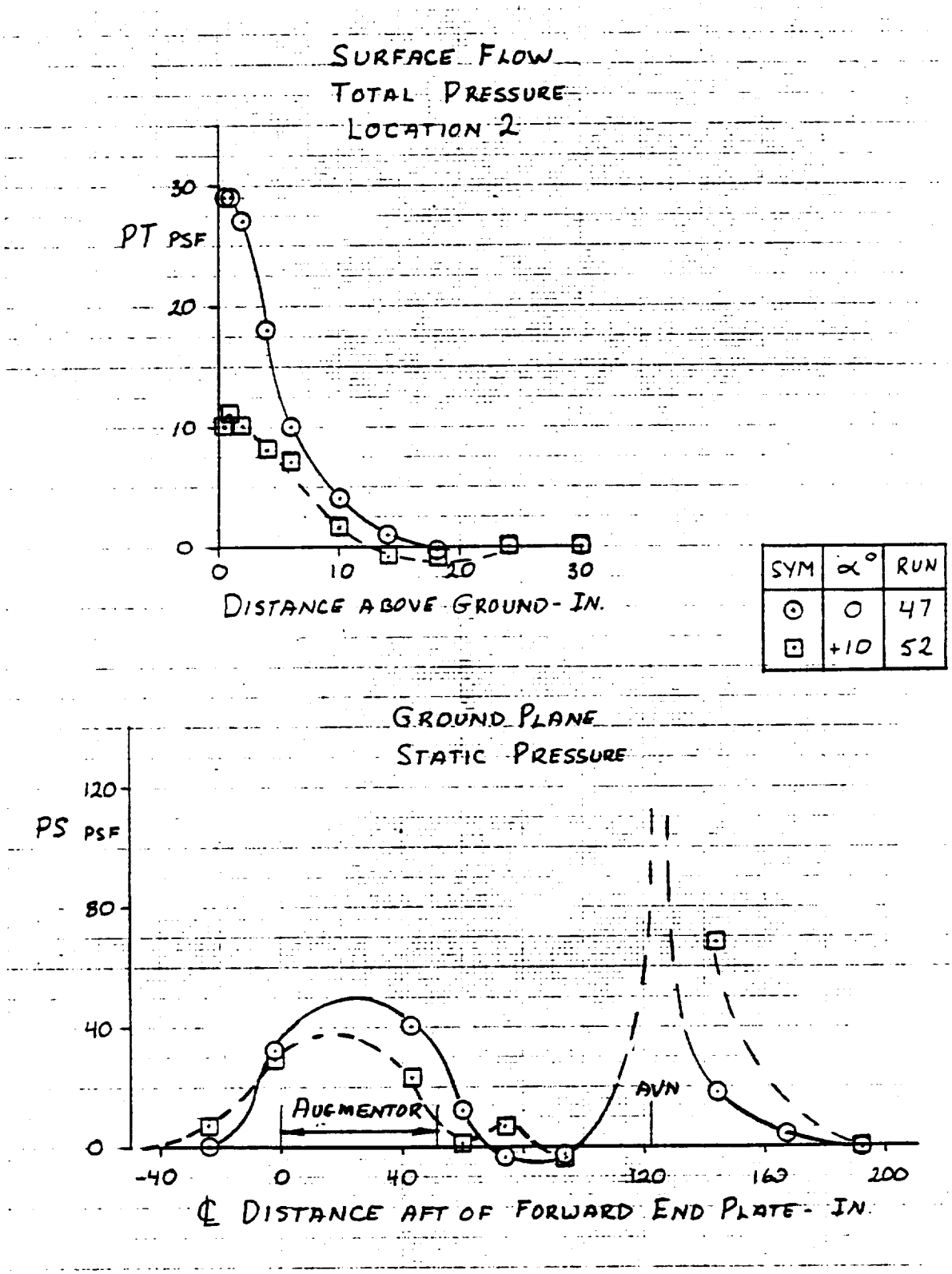

**EFFECT OF PITCH ANGLE ON GROUND PLANE FLOW;
REDUCED FUSELAGE AUGMENTOR LENGTH (FAUG = .538);
VENTRAL NOZZLE 'ON'; H = 27"; PRF = 2.0; $\delta_F = 60^o$ (UNBLOWN)**

Fig. 38

ORIGINAL PAGE IS
OF POOR QUALITY

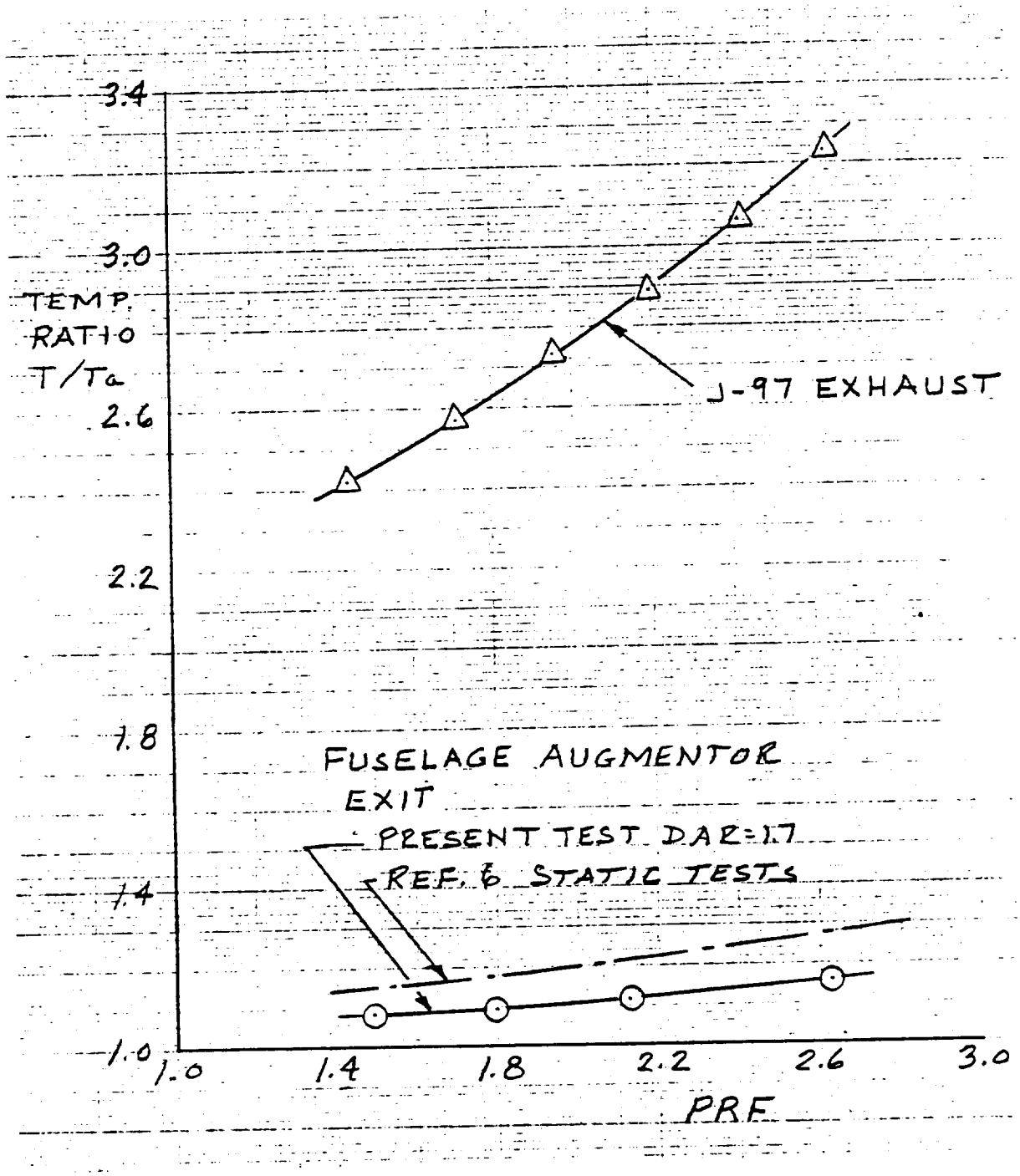

FUSELAGE AUGMENTOR EXIT TEMPERATURE
COMPARED WITH ENGINE EXHAUST TEMPERATURE

Fig. 39

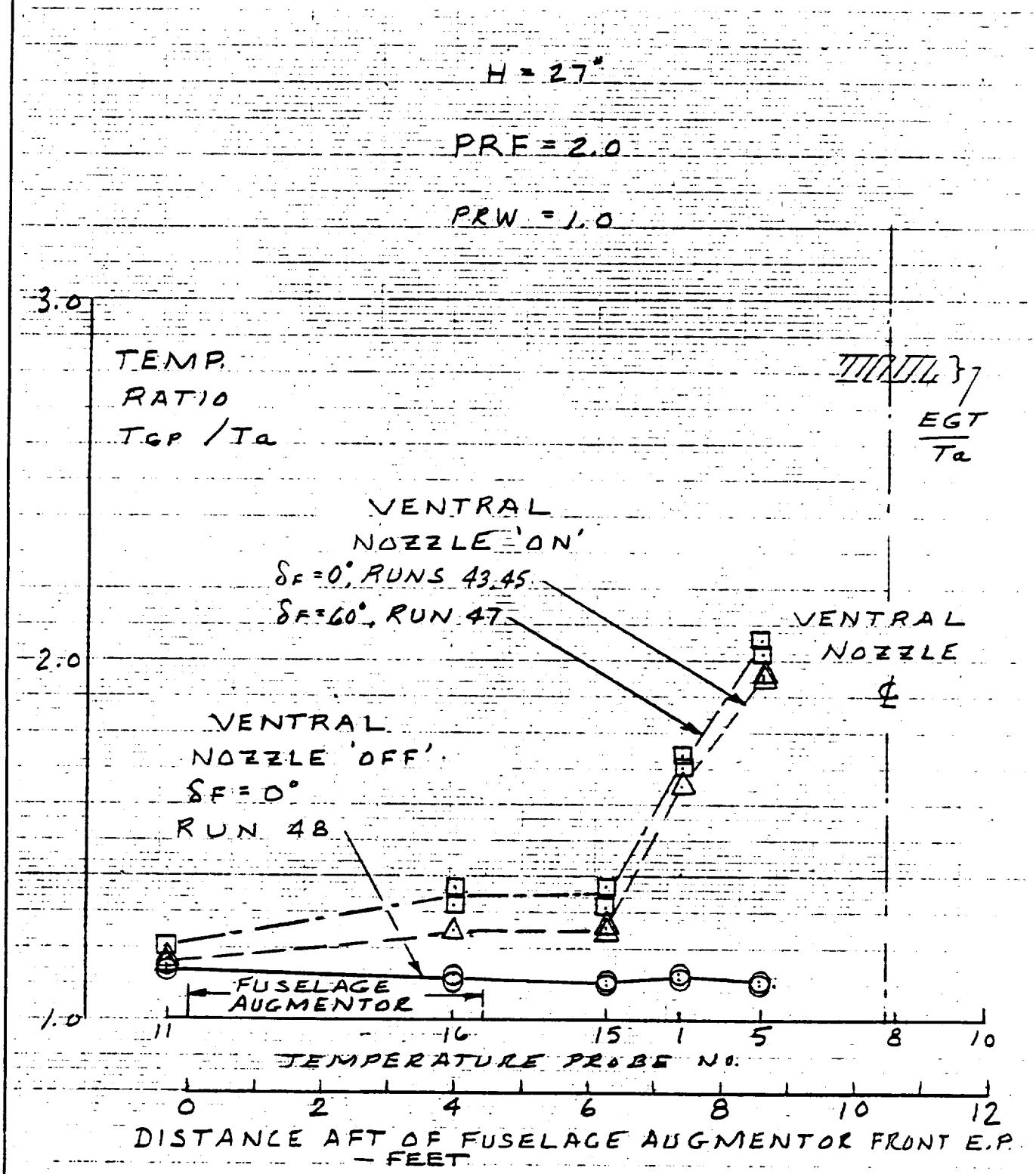

MAXIMUM GROUND PLANE TEMPERATURE ALONG MODEL CENTRELINE; H = 27"; PRF = 2.0; FLAP UNBLOWN

APPENDIX "A"

LABORATORY CALIBRATIONS OF FUSELAGE AUGMENTOR NOZZLES WITH COLD AIR

All of the 26 nozzles used in the present tests of the augmentors of the J-97 powered model were calibrated prior to test with a cold air supply in the DHC Aerodynamics Research Laboratory. Each nozzle was tested individually, (on the rig shown in Figure A-1), to determine its effective area and its thrust efficiency as functions of the nozzle reference pressure ratio.

$$PRF = \frac{PSN + p_a}{p_a}$$

At PRF = 2.50, the 26 nozzles installed in the model had a total effective area of 82.2 in^2. This includes an estimated 1% increment to allow for thrust expansion when operating hot.

The average nozzle thrust efficiency at PRF = 2.5 was 0.925. The variation of η_N and A_{eff} with PRF was as shown in Figure A-2, typical results for a notched nozzle.

The lower curves of Figure A-2 give the calculated (hot) flow and thrust functions.

$$\frac{W\sqrt{T}}{\delta} = \left(\frac{W\sqrt{T}}{AP_T}\right)_I \cdot A_e \cdot PRF \cdot p_a$$

$$\frac{X_{NF}}{\delta} = \eta_N \left(\frac{X}{W\sqrt{T}}\right)_I \cdot \frac{W\sqrt{T}}{\delta}$$

where

$$\left(\frac{W\sqrt{T}}{AP_T}\right)_I = g\sqrt{\frac{2\gamma}{R(\gamma-1)}}\sqrt{\left(\frac{1}{PRF}\right)^{2/\gamma} - \left(\frac{1}{PRF}\right)^{\frac{\gamma+1}{\gamma}}}$$

when PRF $\leq$ 1.853 (i.e. below choking)

and $\left(\frac{W\sqrt{T}}{AP_T}\right)_I$ = 0.3888 above choking.

Also $$\left(\frac{X}{W\sqrt{T}}\right)_I = \frac{1}{g}\sqrt{\frac{2\gamma R}{\gamma-1}\left[1-\left(\frac{1}{PRF}\right)^{\frac{\gamma-1}{\gamma}}\right]}$$

when PRF $\leq$ 1.853

and $$\left(\frac{X}{W\sqrt{T}}\right)_I = \frac{(\gamma+1)-\frac{1.853}{PRF}}{g\sqrt{2\gamma(\gamma+1)/R}}$$ above choking.

Note that these expressions are for isentropic flow from a convergent nozzle (not convergent-divergent). For hot gas (products of combustion) the following values have been used.

γ = 1.3333; R = 3104.4 $(ft/_{sec})^2/°K$; g = 32.177 ft/sec^2

Fig. A-1

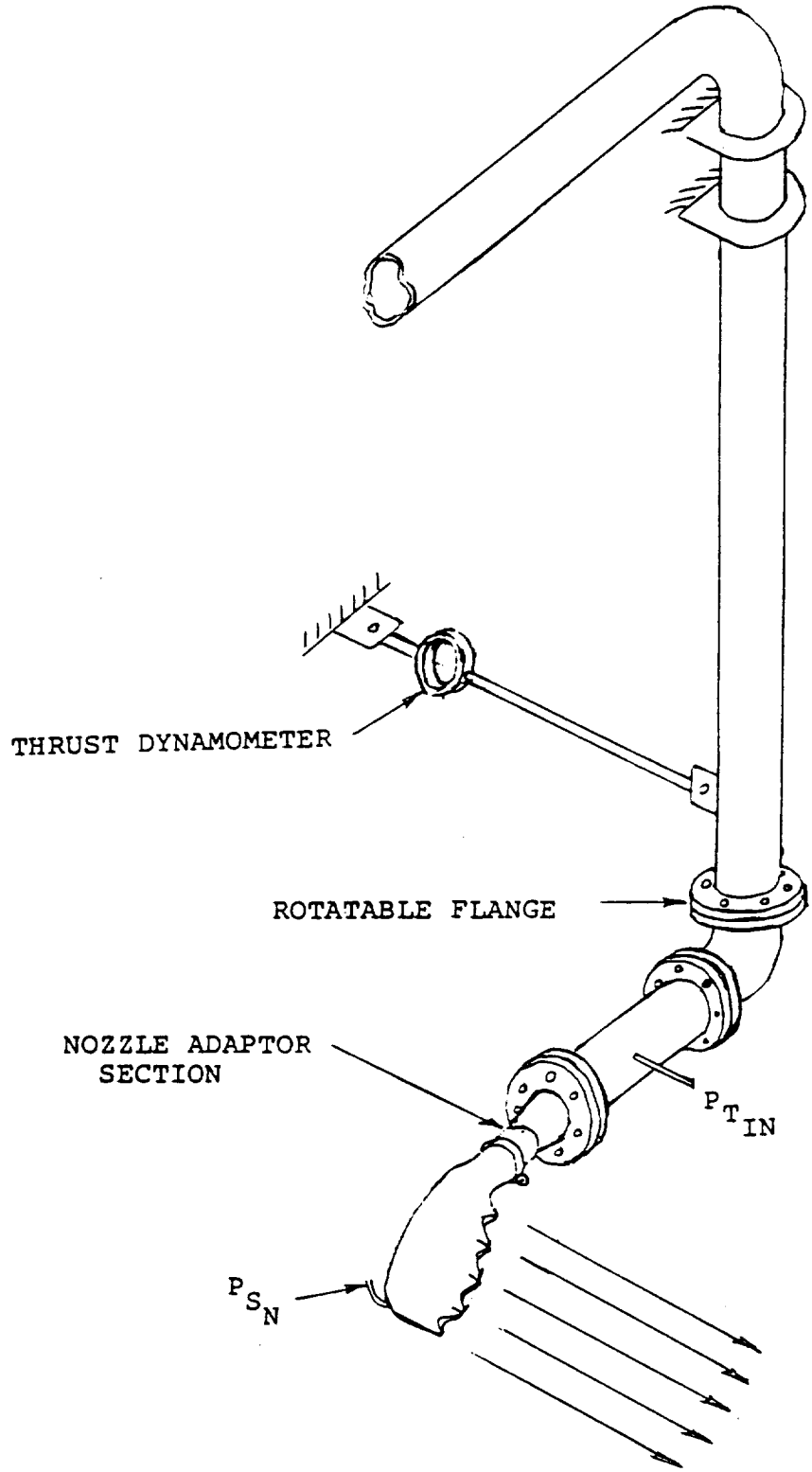

SINGLE NOZZLE TEST RIG

Fig. A-2

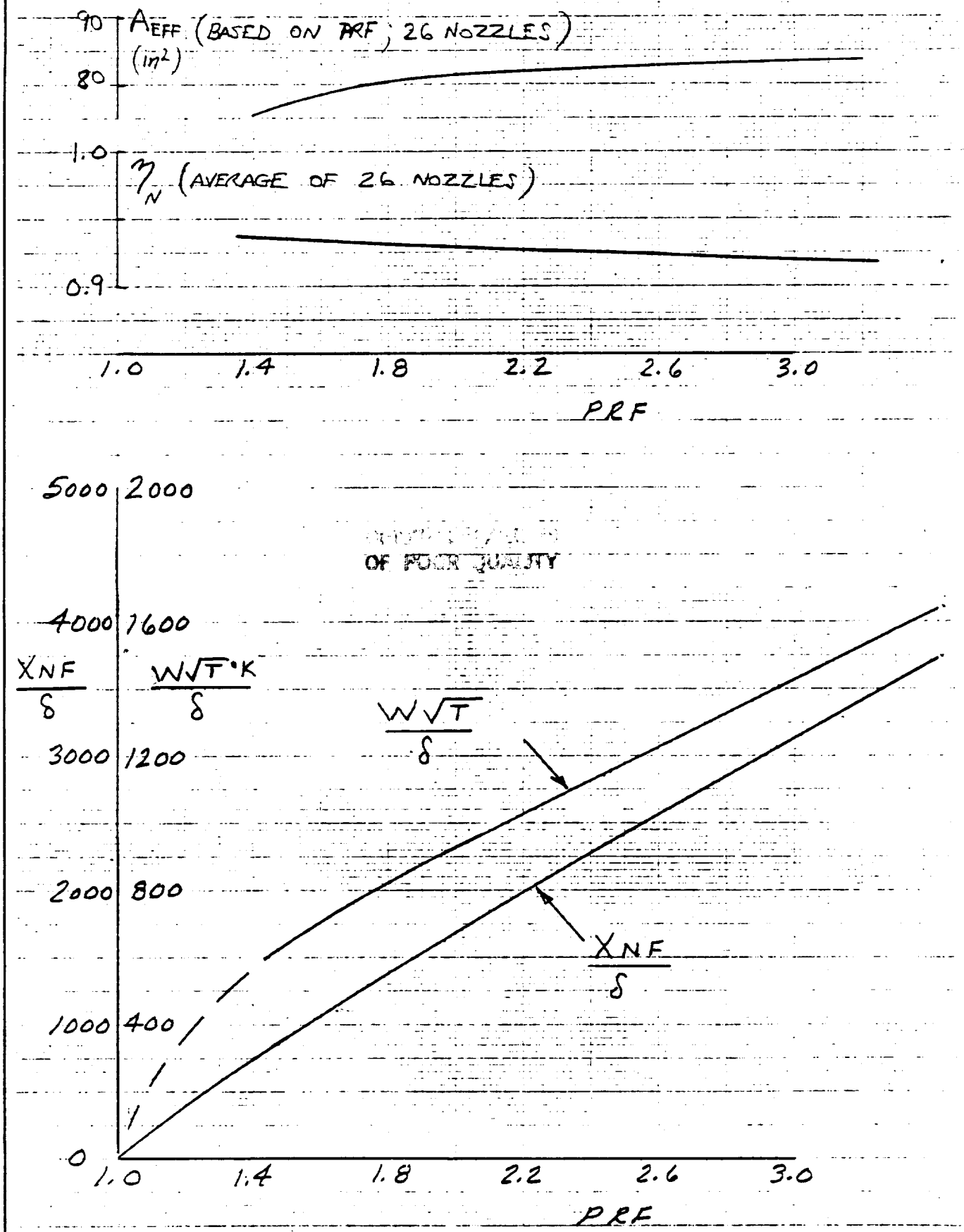

NOTCHED NOZZLE PERFORMANCE (MEASURED SINGLY, X26)

APPENDIX "B"

WING AUGMENTOR NOZZLE PERFORMANCE CHARACTERISTICS

Left and right hand wing augmentor nozzle assemblies were tested statically in the DHC Aerodynamics Research Lab with cold air prior to hot tests at Ames. The assemblies were individually mounted to measure thrust, X_{N_W}, and mass flow, $W\sqrt{T}$. Duct static taps existed to measure PSWL and PSWR and performance characteristics were related to PRW = $\frac{PSW + P_a}{P_a}$ and applied to the J-97 powered model. Both assemblies had essentially equal effective exit area and thrust. The total effective exit area was 24.66 in². (cold) and nozzle efficiency was .955, at PRW = 2.5. Allowing 1% for expansion with hot exhaust flow A_e was 24.92 in². at PRW = 2.5.

Applying A_e and nozzle efficiency to gas flow equations as in Appendix "A", mass flow $\frac{W\sqrt{T}}{\delta}$, and nozzle thrust, XNW/δ, were determined for the J-97 powered model static tests and are shown in Figure B-1. The revised wing augmentor nozzle thrust is 2 - 6% greater than the program value used for previous wind tunnel and static tests.

Fig. B-1

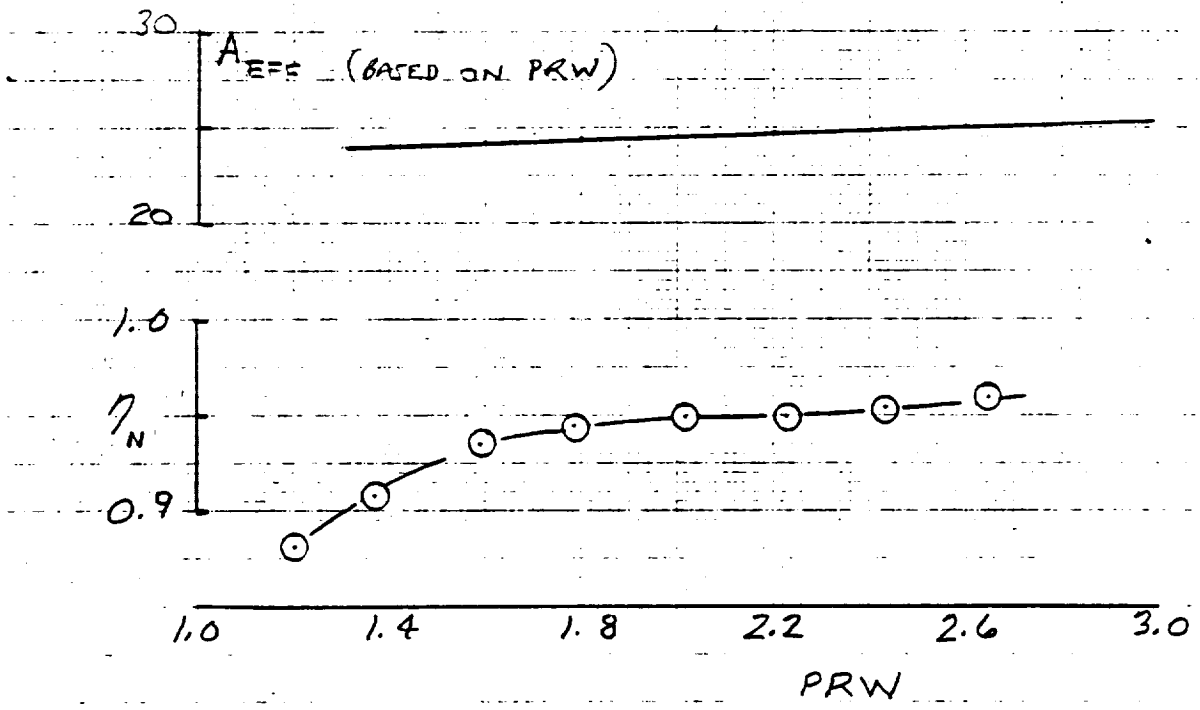

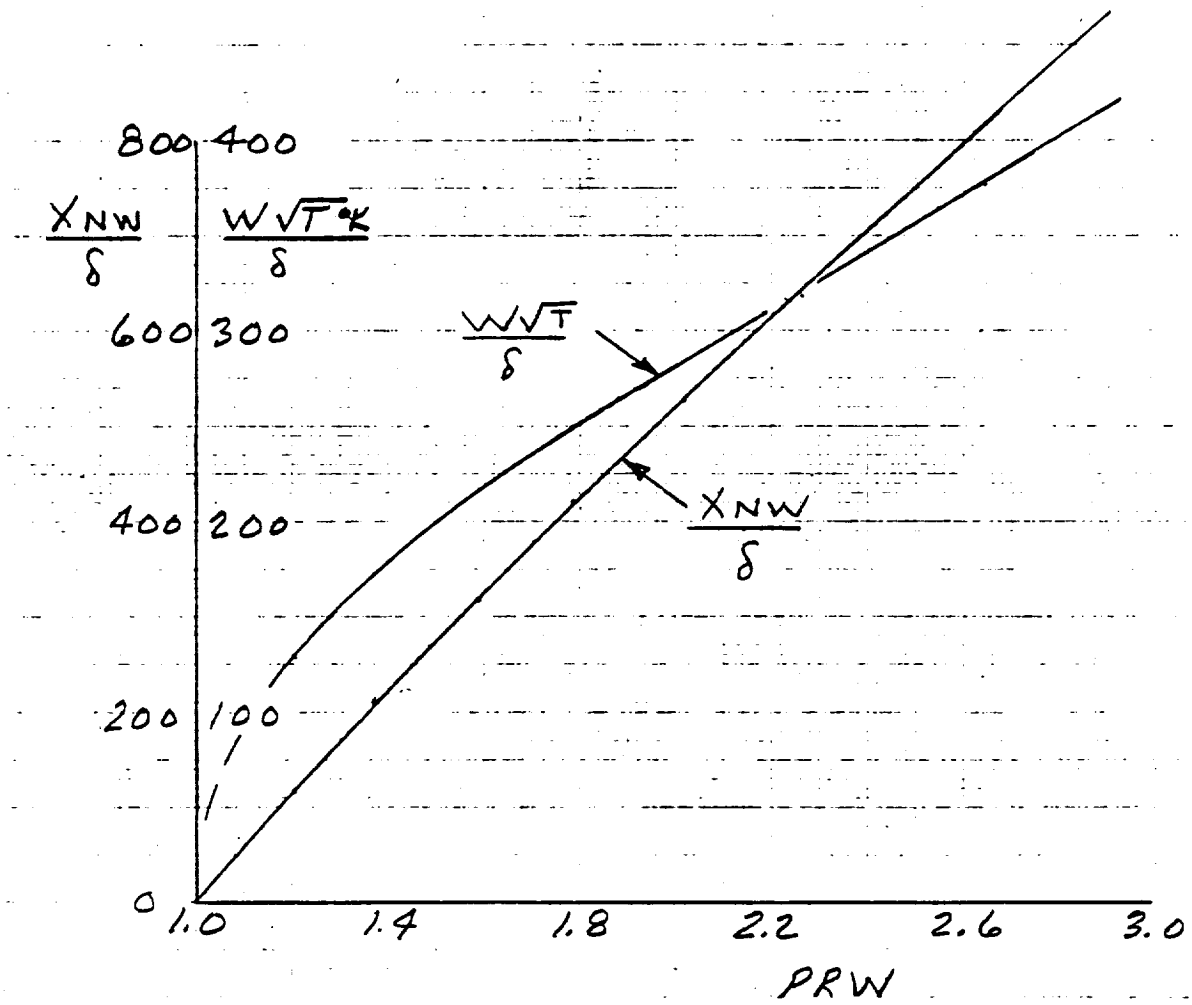

WING AUGMENTOR DUCT/NOZZLE PERFORMANCE – DHC LAB TESTS